

ELUCIDATING ROLES OF PNEUMOCOCCAL SURFACE GLYCANS AND THEIR HOST
INTERACTIONS

by

DUSTIN REED MIDDLETON

(Under the Direction of Fikri Avci)

ABSTRACT

Although *S. pneumoniae* (Spn) has been investigated for over a century, it is still a major human pathogen that causes a variety of invasive pneumococcal diseases (IPDs) such as pneumonia, otitis media, bacteremia, and meningitis. Spn can be divided into over 100 serotypes based on the structural differences of their capsular polysaccharides (CPSs). Since the introduction of the 13-valent (PCV13) glycoconjugate vaccines, effective against the most prevalent serotypes, the incidence rates of IPDs in children have been greatly reduced, with limited effects on morbidity in elderly and immunocompromised populations. Despite a global vaccination program and the use of antibiotics, Spn remains among the deadliest infectious agents worldwide. Widespread use of antibiotics as therapeutics has led to the spread of drug-resistant pneumococcal strains. We hypothesized that previously-characterized and novel pneumococcal surface glycans play important roles in bacterial virulence and its interactions with the host. We also hypothesized that exploiting these surface molecules for immune recognition may address the shortcomings of the incumbent vaccination and antibiotic regimen and offer potent prophylactic and therapeutic approaches to reduce the burden of IPDs. In this dissertation, we provide evidence for the functional roles of Spn serotype 3 CPS-specific CD4+

T cells. We also identified and characterized a serotype 3 CPS degrading enzyme (Pn3Pase) that proves to be protective against serotype 3 Spn in colonization and infection models. Additionally, we show that several glycosyltransferases that modify pneumococcal serine rich protein (PsrP) are critical for Spn virulence. Finally, We characterized the glycosylation of pneumococcal surface protein A (PspA) and demonstrated how this glycan modification contributes to immunogenicity and antigenicity of the protein. These studies increase our understanding of the interactions of pneumococcal surface glycans with the host and may lead to new treatments and vaccines against this highly virulent human pathogen to reduce the burden of IPDs.

INDEX WORDS: *Streptococcus pneumoniae*, Capsular Polysaccharides, Bacterial Protein Glycosylation, Glycoconjugate vaccines, Glycoside Hydrolase

ELUCIDATING ROLES OF PNEUMOCOCCAL SURFACE GLYCANS AND THEIR HOST
INTERACTIONS

by

DUSTIN REED MIDDLETON

B.S., Kennesaw State University, 2012

A Dissertation Submitted to the Graduate Faculty of The University of Georgia in Partial
Fulfillment of the Requirements for the Degree

DOCTOR OF PHILOSOPHY

ATHENS, GEORGIA

2019

© 2019

Dustin Reed Middleton

All Rights Reserved

ELUCIDATING ROLES OF PNEUMOCOCCAL SURFACE GLYCANS AND THEIR HOST
INTERACTIONS

by

DUSTIN REED MIDDLETON

Major Professor:	Fikri Avci
Committee:	Michael Pierce
	Lance Wells
	Fred Quinn

Electronic Version Approved:

Suzanne Barbour
Dean of the Graduate School
The University of Georgia
August 2019

DEDICATION

This dissertation is dedicated to my wife, Caitlin. I will be forever grateful for her love and support throughout the completion of this work.

ACKNOWLEDGEMENTS

I would like to thank my advisor, Fikri Avci for his excellent mentorship. His constant guidance and passion for science has been a tremendous source of encouragement and motivation. I would like to thank Dr. Lina Sun and Dr. Amy Paschall for being exceptional role models for me in the lab. A special thanks to the fellow graduate students, Paeton Wantuch, Ahmet Ozdilek, Jeremy Duke, and Javid Aceil and all members of the Avci lab being incredible teammates, for the help and conversations, and for maintaining a collegial lab environment making the past 6 years truly enjoyable. I would like to thank all of the colleagues and faculty at the CCRC and CMM, my committee members, and the department of Biochemistry and Molecular Biology for making my graduate school years a fun and interactive learning experience.

TABLE OF CONTENTS

	Page
ACKNOWLEDGEMENTS	v
CHAPTER	
1 INTRODUCTION AND LITERATURE REVIEW	1
Invasive Pneumococcal Diseases.....	4
Capsular Polysaccharides.....	4
Protein Virulence Factors	6
Pneumococcal Vaccines.....	10
References.....	17
Figures.....	39
2 T CELL-MEDIATED HUMORAL IMMUNE RESPONSES TO TYPE 3 CAPSULAR POLYSACCHARIDE OF <i>STREPTOCOCCUS PNEUMONIAE</i>	45
Abstract.....	46
Introduction.....	46
Materials and Methods.....	48
Results.....	52
Discussion.....	56
References.....	58
Figures.....	62

3	IDENTIFICATION AND CHARACTERIZATION OF <i>STREPTOCOCCUS PNEUMONIAE</i> TYPE 3 CAPSULE-SPECIFIC GLYCOSIDE HYDROLASE OF <i>PAENIBACILLUS SPECIES</i> 32352.....	71
	Abstract.....	72
	Introduction.....	73
	Results.....	74
	Discussion.....	78
	Materials and Methods.....	81
	References.....	87
	Figures.....	94
4	ENZYMATIC HYDROLYSIS OF PNEUMOCOCCAL CAPSULAR POLYSACCHARIDE RENDERS THE BACTERIUM VULNERABLE TO HOST DEFENSE.....	101
	Abstract.....	102
	Introduction.....	102
	Results.....	104
	Discussion.....	109
	Materials and Methods.....	112
	References.....	119
	Figures.....	132
5	GLYCOSYLATION OF PNEUMOCOCCAL SERINE-RICH PROTEIN (PSRP) ENHANCES VIRULENCE AND HOST INFLAMMATORY RESPONSE.....	136
	Abstract.....	137

Introduction.....	137
Results.....	139
Discussion.....	142
Methods and Materials.....	144
References.....	150
Figures.....	154
6 IMMUNOLOGICAL CHARACTERIZATION OF PNEUMOCOCCAL SURFACE PROTEIN A (PSPA) GLYCOSYLATION	163
Abstract.....	164
Introduction.....	164
Results.....	166
Discussion.....	168
Materials and Methods.....	170
References.....	177
Figures.....	184
7 Conclusions and future directions.....	190
References.....	196
APPENDICES	
A. COMPLETE GENOME SEQUENCE OF THE BACTERIUM <i>BACILLUS</i> <i>CIRCULANS</i> JORDAN STRAIN	
32352.....	201

CHAPTER 1

INTRODUCTION AND LITERATURE REVIEW

The goal of this dissertation has been to elucidate critical molecular and cellular mechanisms operated through the interaction of pneumococcal surface glycans and the host immune system. We will utilize this mechanistic information to address the shortcomings of the incumbent vaccination and antibiotic regimen and offer alternative prophylactic and therapeutic approaches for invasive pneumococcal diseases.

Chapter 1 discusses the pneumococcus, the burden of invasive pneumococcal diseases (IPDs), and virulence mechanisms that contribute to its pathogenesis. Additionally, this chapter discusses the current status of glycoconjugate vaccines employed for pneumococcal disease prevention as well as newly described conjugation technologies.

Chapter 2 uses a model glycoconjugate vaccine of type 3 *Streptococcus pneumoniae* CPS (Pn3P) to assess whether carbohydrate-specific adaptive immune response can be applied to these conjugates. I provide evidence for the functional roles of Pn3P-specific CD4⁺ T cells utilizing mouse immunization schemes that induce Pn3P-specific immunoglobulin G (IgG) responses in a Tcarb (i.e., carbohydrate-specific T cell)-dependent manner.

Chapter 3 discusses the identification of the gene and characterization of the type 3 *Streptococcus pneumoniae* CPS (Pn3P) degrading enzyme (Pn3Pase) that is produced by *Paenibacillus sp.* 32352. We identified the putative amino acid sequence of Pn3Pase through mass spectrometry-based proteomics and cloned the gene for recombinant expression. We then

characterized the oligosaccharide products generated upon the enzymatic depolymerization of Pn3P.

Chapter 4 evaluates the protective role of the glycoside hydrolase, Pn3Pase, which targets the CPS of type 3 *Streptococcus pneumoniae*, one of the most virulent pneumococcal serotypes. We first assessed the ability of Pn3Pase to degrade the capsule on a live type 3 strain. Through *in vitro* assays we observe that Pn3Pase treatment increases the bacterium's susceptibility to phagocytosis by macrophages and complement-mediated killing by neutrophils. We further demonstrate that *in vivo* Pn3Pase treatment reduces nasopharyngeal colonization, and protects mice from sepsis caused by type 3 *Streptococcus pneumoniae*.

Chapter 5 examines the effects of deletion of glycosyltransferases, which modify the pneumococcal serine rich protein (PsrP), on virulence of the TIGR4 strain of *Streptococcus pneumoniae*. Through single gene knockouts, we determined which glycosyltransferases were critical virulence determinants in *in vitro* assays and *in vivo* infection models.

Chapter 6 investigates and characterizes the glycosylation of pneumococcal surface protein A (PspA) and how this glycan modification contributes to immunogenicity and antigenicity of the native protein.

Chapter 7 summarizes the major conclusions from the work and offers future directions and implications of the research.

Literature Review

Streptococcus pneumoniae (Spn) is a Gram-positive opportunistic bacterial pathogen that colonizes the host nasopharynx and upper respiratory tract. Although colonization in healthy individuals is typically asymptomatic, dissemination of the bacterium to otherwise sterile sites can prompt invasive pneumococcal diseases (IPDs) such as pneumonia (lungs), otitis media (middle ear), bacteremia (bloodstream), or meningitis (meninges)(1, 2). Currently, Spn is responsible for the majority of all community-acquired pneumonia cases(3). The pneumococcus is an historically notorious bacterium determined as the causative agent of significant mortality during the Flu pandemic of 1918(4). Although over 100 years have been devoted to the investigation of pathogenesis, prophylactics, and treatments for IPDs, these diseases account for one million deaths in children less than 5 years of age each year(5).

Spn can be divided into nearly 100 serotypes based on the structural differences of their capsular polysaccharides (CPSs)(6). Since the introduction of the 23-valent polysaccharide-based vaccine (PPV-23) followed by 7-valent (PCV7) and 13-valent (PCV13) glycoconjugate vaccines (prepared by covalent-conjugation of the polysaccharide with a carrier protein), effective against the most prevalent serotypes of Spn, the incidence rates of IPD in children have been reduced significantly, with limited reduction in morbidity in elderly and immunocompromised individuals (7, 8) A serotype distribution shift after conjugate vaccine introduction highlights the importance of generating improved pneumococcal vaccines to include a wider range of serotypes(9). Additionally, widespread use of antibiotics as therapeutics has led to the spread of drug-resistant pneumococcal strains(10-12). Despite a global vaccination program and the use of antibiotics, Spn remains among the deadliest infectious agents worldwide.

This chapter describes the burden of IPDs, and virulence mechanisms that contribute to

Spn pathogenesis. I also discuss the current status of glycoconjugate vaccines and new conjugation technologies.

Invasive Pneumococcal Diseases

Due to a variety of bacterial and host factors, *Streptococcus pneumoniae* can adhere to host cells, and evade innate and adaptive immunity to stably colonize the human nasopharynx. Colonization by Spn is typically a benign and harmless event under normal circumstances(13, 14). However, in cases of viral infection or induction of inflammatory responses in the upper respiratory tract, Spn can proliferate and migrate to adjacent tissues to cause invasive disease (**Figure 1.1**)(15-17). IPDs occur most frequently in young children, elderly, and immunocompromised patients. These infections include pneumonia, otitis media, bacteremia and meningitis(18). There are approximately half a million cases of pneumonia, 7 million cases of otitis media, 12,000 cases of bacteremia, and 4,000 cases of meningitis caused by Spn each year in the United States(8, 19-21). Even in developed countries with antibiotic therapies, the mortality rate for pneumococcal pneumonia is as high as 40%(6, 22).

Capsular polysaccharides

The pneumococcus is decorated with a capsular polysaccharide on its outermost surface. These polysaccharide structures are the major virulence factors of the bacterium, providing it with a charged (with the exceptions of types 7A, 7F, 14, 33F, 33A, and 37 which are neutral) shield to evade complement deposition and engulfment by host phagocytic cells(23-26). To date, nearly 100 distinct polysaccharide structures have been identified(6). Capsule types have been classically defined by reactivity with type-specific antisera, leading specific pneumococcal capsules to be referred to as “serotypes”(27, 28). Tremendous efforts have been made to define the biochemical structures of these serotypes, with major advances in the field to determine

repeating unit compositions, linkages, configurations, and substitutions that contribute to the massive diversity of these polysaccharides(29, 30).

Genetics and synthesis

All genes essential for CPS biosynthesis are arranged in a cassette termed the *cps* locus that are transcribed together. A given strain has a single *cps* locus in its genome and therefore expresses one capsule type(31-33). Many capsule cassettes have a set of conserved genes (*cpsA-D*) involved in regulation of the capsule. These genes are followed by additional glycosyltransferases, modification, and export machinery that distinguish each serotype from the next(34-36). Two uncommon *cps* loci that have been revealed by sequencing are serotype 3 and 37. Serotype 3 utilizes synthase-dependent assembly and has disrupted *cpsA,B*, and *D* regulatory genes(37-39). The single gene required for serotype 37 synthesis resides completely outside of the normal chromosomal cassette for the *cps* locus(40, 41). Capsule locus sequencing has allowed for quick and easy serotyping of clinical isolates by polymerase chain reaction, which may prove critical for future serotype-specific IPD therapies.

Most capsular polysaccharide synthesis mechanisms occur in what is considered the Wzy-dependent mechanism. In this mechanism, the oligosaccharide-repeating unit is built on an undecaprenyl phosphate acceptor on the inside of the cell. Once a single unit is complete, a flippase will flip the oligosaccharide to the outside of the cell where the Wzy polymerase will synthesize the polymer. If there are additional substituents on the polymer, such as acetylation, this will typically occur on the outer leaflet of the membrane during polymerization(42-44).

The second, less-common mechanism for CPS synthesis is the synthase-dependent mechanism. This mechanism occurs in serotype 3 and 37 synthesis using a single enzyme to initiate and extend the polymer. The mechanism for type 3 synthesis initiates with a glucose

addition to a phosphatidyl glycerol acceptor from a UDP-glucose donor, followed by alternating addition of glucuronic acid and glucose to build the β -D-GlcA(1-4) β -D-Glc(1- linear type 3 polysaccharide. Serotype 3 will be a major focus of this thesis, and type 3 cps locus and synthetic mechanism is shown in **figure 1.2**(37, 39, 45, 46).

Serotypes and diseases

The virulence of Spn is most commonly affected by the capsular serotype. The capsule is critical for colonization and invasiveness for the majority of pneumococcal strains(47, 48). Most CPS are thick and negatively charged structures that shield the bacterium from host phagocytes and complement components that may target underlying proteins on the bacterial surface (**Figure 1.3**)(49). Additionally, the capsule greatly reduces trapping and antimicrobial effects of neutrophil extracellular traps and allows for bacterial escape(50). There is substantial variability in invasiveness for certain serotypes, with only about 30 serotypes showing significant invasive potential(6, 51). Furthermore, a smaller subset of serotypes presents marked increases in mortality rates, i.e. serotype 3. Numerous animal models and epidemiology studies have associated serotype 3 strains with increased virulence and mortality (52-54). A recent report has highlighted increased phenotypic variation and antibiotic resistance cassette incorporation associated with this serotype(55). Serotypes 3, 6B, 9N, 11A, 16F, 19F, and 19A have been emphasized recently with high invasive potential and mortality rates(53, 56, 57).

Protein virulence factors

In recent years, Spn surface proteins have been explored as virulence factors and vaccine targets largely due to their reduced sequence variability among pneumococcal strains. These proteins have been viewed as conserved immunogens that may offer broadly protective immune

responses as a universal pneumococcal vaccine(58). Major protein virulence factors and the mechanisms that contribute to disease establishment and progression are discussed below and diagramed in **Figure 1.3**.

Neuraminidase

Pneumococcal sialidases hydrolyze sialic acid residues off of host glycoconjugates that reside on the cell surface as well as soluble proteins(59). Spn encodes at least two neuraminidases, *nanA*, *nanB*, and, in 50% of strains, *nanC*(60, 61). The distinct function of each neuraminidase remains unclear, but *nanA* and *nanB* are essential for pneumococcal survival in the bloodstream and respiratory tract(62). Additional work has shown that NanA is dispensable for colonization of the nasopharynx(59). A recent report has shown that underlying galactose, exposed by NanA mediated terminal sialic acid removal, can promote biofilm formation by Spn during colonization(63). Vaccination studies with NanA indicate that anti-NanA antibodies can protect against otitis media by blocking sialidase mediated exposure of host receptors with limited efficacy against pneumococcal pneumonia(64).

Pneumolysin

Pneumolysin (Ply) is a conserved, cholesterol-dependent pore forming cytolysin. Pneumolysin has been shown to oligomerize in the membrane of target cells to form a large ring-shaped 260 angstrom pore consisting of approximately 40 monomer units(65). This pore formation leads to cytolytic or other modulatory activities of the host cells such as induction of complement depletion, inhibition of respiratory ciliary beating, and inhibition of respiratory phagocytic bursts(66, 67). In a recent report, Ply has been identified as a ligand for the mannose receptor on dendritic cells and alveolar macrophages. This allows Spn to invade these host cells and establish an intracellular population that avoid clearance and dampen inflammatory cytokine

responses(68). Pneumolysin has been reported as essential for establishment and persistence of pneumococcal pneumonia(69, 70). Many groups have begun testing Ply and its detoxified derivatives as pneumococcal vaccines in animal models. Native Ply vaccines have been protective in mice after systemic intraperitoneal challenge. Immunization with detoxified derivatives, termed pneumolysoids, was protective in a pneumococcal pneumonia mouse model(71).

Pneumococcal surface protein A

Pneumococcal surface protein A, or PspA, is a member of the choline binding protein family and it has critical roles in Spn virulence with high immunogenicity(72, 73). Choline binding proteins have C-terminal domains that mediate non-covalent binding to choline moieties on pneumococcal surface teichoic and lipoteichoic acid(74). PspA is present in essentially all clinical isolates, but has variable primary amino acid sequence among strains (75, 76). Based on its sequence, PspA can be organized into three families, or 6 clades. It has been reported that up to 99% of pneumococcal isolates belong to families 1 and 2 (clades 1-5)(77, 78). PspA has been shown to inhibit complement-mediated opsonization by interfering with the C3 complement component(79, 80). PspA helps to protect Spn from bactericidal activity by binding lactoferrin (2, 81). This surface-exposed virulence determinant is antigenic and is therefore an attractive vaccine target. PspA has been characterized as a protective antigen in multiple reports(82-86). Monoclonal antibodies to PspA protect mice from fatal pneumococcal sepsis(87, 88). It was demonstrated that mice immunized with native PspA isolated from Spn were protected from fatal sepsis in challenge experiments, whereas PspA expressed in *E. coli* recombinantly was significantly less immunogenic and protective in comparison to native PspA (86). Although PspA is divided into distinct families and clades, it is exceptionally cross-reactive with anti-sera

and monoclonal antibodies(73, 89). Immunization with a single PspA can offer variable protection to mice against strains expressing other PspA clades(75). PspA is a promising protein vaccine candidate and fragments have been included in two phase I clinical vaccine trials conducted by Sanofi-Pasteur(58).

Choline binding protein A

Choline binding protein A, or CbpA, is another member of the choline binding protein family, as its name suggests. CbpA is a major virulence determinant that binds to the complement regulator factor H and secretory IgA molecules(90-92). This IgA binding largely mediates the invasion of the bacterium from its nasopharyngeal niche to establish pneumonia in the lungs or during transition to bacteremia(91). CbpA is extremely polymorphic with high sequence variability, which may limit the scope of protection against IPDs if used as a vaccine. However, CbpA mucosal immunization has been shown to offer protection in a murine colonization model(93).

Pneumococcal serine rich protein

The Pneumococcal serine-rich protein, or PsrP, is an adhesin protein that mediates bacterial attachment to host as well as other bacterial cells(94). This large glycoprotein is encoded in a 37-kb genomic island, *psrP-secY2A2*. This island is present and conserved in many globally distributed invasive clones, particularly in 51.2% of 547 clinical isolates collected in Barcelona, Spain, from 2004-2010 (95). The *psrP* locus carries all of the genes necessary to glycosylate and export the PsrP to the bacterial surface(96). PsrP consists of a signal peptide, a short serine rich repeat region, followed by a basic region full of lysine residues, a very long serine rich repeat region, and a domain to anchor the protein to the cell wall peptidoglycan as depicted in **figure 1.4**. Multiple reports have implicated PsrP in establishment of lung infection

in murine models. These studies have implicated this locus and products of this locus in invasive pneumococcal disease through genetic characterization of isolates and mutagenesis studies (94-98). One proposed mechanism is that Spn adhesion to lung epithelium is mediated through PsrP basic region binding to Keratin 10(99). As of yet, the specific roles of the PsrP glycans in disease progression or bacterial physiology have not been completely elucidated. Moreover, enzymatic properties and specificities of these glycosyltransferases along with their potential role in bacterial virulence mechanisms have yet to be fully characterized. Additionally, PsrP glycans may be a promising vaccine target as the immense size of the protein allows these epitopes to extend past the capsule.

Pneumococcal vaccines

In the early 20th century, attenuated whole-cell vaccines were tested and proven efficacious(100). It was soon realized that immune protection elicited in these vaccine preparations was serotype specific. It became apparent that any pneumococcal vaccine formulation would need to offer protection against the most prevalent serotypes that are encountered in the clinic that cause IPDs(6).

Polysaccharide vaccines

Pneumovax, or PPV23, was introduced in the US in 1983. This vaccine is composed of 25 ug of each of the 23 included serotypes(101, 102). This vaccine has been effective at preventing IPDs in adults(22). However, there are major limitations with the polysaccharide-based vaccine, most of which stem from the inability of pure polysaccharides to elicit T-cell dependent adaptive immune responses(103). PPV23 is poorly immunogenic in infants and the elderly(104, 105). It has shown poor efficacy in protection from pneumonia. Additionally, secondary vaccination with PPV23 fails to induce boosted serum antibody titers, in

fact serum titers are much lower than those elicited after primary vaccination(106).

Glycoconjugate vaccines (adapted from Sun, Middleton *et al. Glycobiology* 2016(107))

A major breakthrough in vaccine development has been in glycoconjugate vaccines in which the carbohydrates are conjugated to carrier proteins to evoke strong protective antibody responses against the pathogens associated with the carbohydrate. Most carbohydrate-based vaccines focus on eliciting humoral immunity to produce protective antibodies, which are addressed elsewhere (108-110). The glycoconjugates that induce T cell responses to help B cell produce protective antibodies are discussed in the following section, starting with the impact of pneumococcal conjugate vaccines.

The first pneumococcal conjugate vaccine, PCV7 was introduced in 2000. This vaccine consisted of 7 pneumococcal serotypes covalently conjugated to a carrier protein CRM197 (111). This vaccine had a dramatic herd effect on the general population and offered significant protection against community acquired pneumonia in children(112). In 2010, a new conjugate vaccine, Pfizer's Prevnar PCV13 was released in the United States to cover 6 additional serotypes. PCV13 resulted in a significant reduction of IPD in infants and the elderly(113). The impact of glycoconjugate vaccines on pneumococcal disease has been a tremendous success. Introduction of PCV7 accounted for a 77% reduction in pneumonia in the U.S.(114). Furthermore, PCV13 has reduced the cases of infant IPD by 36% (112, 115). However, there are still a few vaccine-included serotypes that persist. Incidence of serotypes 3, 7F, and 19A have remained significant post-PCV13 introduction, although 7F and 19A have started a downward trend as shown in **figure 1.5** (116).

Glycoconjugate vaccines elicit T cell dependent immune protection

The CPSs of major human pathogens, including *Streptococcus pneumoniae*, *Neisseria*

meningitidis, and *Haemophilus influenzae*, significantly contribute to their virulence mechanisms. CPSs support immune evasion through increasing bacterial attachment to the host, thus inhibiting complement activation and preventing phagocytosis (117, 118). The surface localization and unique structures of CPSs make them ideal candidates for vaccines designed to elicit a carbohydrate specific immune response to protect against these bacteria.

Most microbial polysaccharides, however, are poorly immunogenic. Pure, non-zwitterionic CPSs are T cell-independent antigens and cannot trigger T cell help to induce antibody class switching, affinity maturation, or create memory B and T cells (119-121). Pure polysaccharide vaccines are used today and have been somewhat effective against a few serotypes of *S. pneumoniae*, *S. typhi*, and *N. meningitides*. These vaccines, while having some success in adults, have been unsuccessful in providing protection in infants, the elderly, and immunocompromised individuals (122-124).

Eliciting a T cell dependent immune response against CPSs can be accomplished by coupling CPSs to a carrier protein to create a glycoconjugate vaccine (125, 126). Immunizations with glycoconjugate vaccines such as Prevnar 13®, Menhibrix®, and Pentacel® have been effective at inducing a long-lasting protective capability against encapsulated pathogens. Glycoconjugate vaccines induce a CPS specific adaptive immune response, IgM to IgG class switching, B and T cell memory, and significantly higher protection compared to pure polysaccharide vaccines (127, 128). Glycoconjugates containing CPSs from *S. pneumoniae*, *H. influenzae*, and *N. meningitidis* have been highly successful in preventing these infections (121, 122, 124, 129). Although success has been observed, problems with current glycoconjugate vaccines still persist. Glycoconjugates have been poorly immunogenic in individuals with HIV and the elderly (130, 131). These problems illustrate the need for efforts to enhance vaccine

efficacy by developing structurally defined glycoconjugate vaccines based on the mechanisms of their activation of the immune system.

Glycoconjugate vaccine induces carbohydrate-specific T cell response

The traditional hypothesis for glycoconjugate vaccine activation of an adaptive immune response proposes that helper CD4⁺ T cells recognize a carrier protein derived peptide (132). According to this hypothesis, the glycoconjugate binds to the surface of a B cell that stimulates the production of antibodies to the CPS portion of the glycoconjugate. The B cell processes the protein portion of the glycoconjugate and presents a peptide from the carrier protein in the context of MHCII to the T cell receptor (TCR) of CD4⁺ T cells. Activation of the T cell results in production of cytokine IL-4, which induces maturation of the B cell and consequent production of antibodies specific for CPS, immunoglobulin class switching from IgM to high affinity IgG, and production of memory B and T cells (123, 127). This hypothesis was originally based on the assumption that only protein antigens can be presented to and recognized by T cells. The traditional mechanism assumes the strong covalent link between the CPS and carrier proteins is broken during endosomal degradation of the glycoconjugate and does not consider whether T cells can recognize non-zwitterionic carbohydrates linked to a peptide whose binding to MHCII allows presentation of the carbohydrate by the APC to T cells (124, 129, 131, 133).

The mechanisms of glycoconjugate vaccine activation of an adaptive immune response have recently been uncovered that shifts the paradigm of peptide-centric T cell recognition (134). In the most comprehensive study of glycoconjugate vaccine activation mechanisms to date, Avci *et al.* demonstrated that, upon uptake by APCs, glycoconjugate vaccines are involved in a depolymerization reaction that processes the glycoconjugate into a smaller molecular weight

processed glycan-peptide conjugate (glycan_p-peptide) (134). This glycan_p-peptide is then displayed on the surface of the APC in association with MHCII. MHCII-deficient APCs showed no processed glycan_p-peptide presentation. These findings suggest that the carrier protein-derived peptide portion of the glycoconjugate binds to MHCII, leaving the hydrophilic glycan exposed on the APC surface to be recognized by the TCR of CD4⁺ T cells (Figure 2). This study also shows that glycoconjugate immunization induces a subset of CD4⁺ T cells, termed Tcarbs, which recognize the carbohydrate portion of the glycoconjugate. A series of immunization experiments revealed that stimulation of Tcarbs by their carbohydrate epitopes recruits T cell help for B cell IgM to IgG class switching (134). The proposed mechanism is depicted in **Figure 1.6**.

The carbohydrate specific T cells (i.e. Tcarbs) were isolated from mice immunized with a GBSIII-OVA (Group B streptococcus serotype III conjugated to Ovalbumin) glycoconjugate and enriched by stimulating the lymphocytes for 10–14 days with APCs in the presence of carbohydrate with alternate carrier proteins. By performing limiting dilutions, two Tcarb clones were isolated. One clone recognized GBSIII epitope in the context of the I-E^d and the other with the I-A^d. The CD4⁺ T-cell clones secreted both IL-2 and IL-4, but not IFN- γ , in the presence of glycoconjugates other than the proteins alone (134, 135). The knowledge gained from these mechanistic studies was used to synthesize a new glycoconjugate vaccine enriching the glycan epitope to create a much more robust carbohydrate specific IgG response and protein from GBS challenge (134, 135).

Additional reports, along with this mechanistic study on GBSIII glycoconjugates suggest the generalizability of Tcarb mediated immune responses induced by glycoconjugate vaccines. We have employed glycoconjugates of type 3 *Streptococcus pneumoniae* CPS (Pn3P) and

provided evidence for the functional roles of Pn3P-specific CD4⁺ T cells utilizing mouse immunization schemes that induce Pn3P-specific immunoglobulin G (IgG) responses in a Tcarb-dependent manner(136). More recently, work out of the Kasper lab has demonstrated the Tcarb-mediated mechanism induce adaptive immune responses for Vi antigen from *Salmonella typhi*, Group B *streptococcus* type 1b, as well as *H. influenza* type b(137). Importantly, this work showed that group C polysaccharide from *Neisseria meningitidis* failed to induce humoral immunity through the Tcarb mechanism due to rapid depolymerization of the polysialic acid structure during antigen processing. An additional study showed, based on confocal microscopy images, the carbohydrate component of a pneumococcal type 14 glycoconjugate vaccine was localized on the APC surface, suggesting possible MHCII presentation of carbohydrate epitopes to CD4⁺ T cells (138). Furthermore, immunization with meningococcal polysaccharide-tetanus toxoid conjugate was shown to induce carbohydrate reactive T cells (139).

Conjugation technologies

Current conjugation techniques involve the activation of proteins or polysaccharides to create reactive functional groups such as aldehydes, esters, thiols or hydrazides (131, 135, 140). These strategies often lead to heterogeneous structures of various molecular weights and linkages that form matrix-like structures (141). A current strategy-protein glycan coupling technology (PGCT) utilizes the oligosyltransferase enzyme pglB of *Campylobacter jejuni* to enzymatically transfer a polysaccharide to a recombinantly expressed carrier protein. With this technology, glycans, coupling enzymes and proteins are synthesized in the *E. coli* glycoconjugate factory (142, 143). Studies are underway that could extend the usefulness of this method to generate O-linked glycoconjugates through an enzymatic coupling process using PglS (144-148). The major drawbacks to this method are the limited oligosaccharides that can be used as a substrate for

pgIB and the inability to conjugate the polysaccharide to peptides or polypeptides (131, 149, 150). Recently, researchers have demonstrated the conjugation of polysaccharide to protein via copper-free click chemistry reactions, conferring the ability to perform site-selective conjugation of the oligosaccharides (151-154). This method provides a structurally defined glycoconjugate that can be easily characterized by analytical methods. A few drawbacks to this approach are multiple steps, low yield, and potential unwanted immunological responses (152). Novel approaches for glyconjugation are necessary for creating well-defined glycoconjugate vaccines that lack heterogeneity and batch-to-batch variability. These strategies, along with the mechanistic insights of glycoconjugate vaccine activation of adaptive immunity, provide an outline for the development of highly immunogenic vaccines against pathogenic bacterial, parasitic, and viral surface glycans.

References

1. Bogaert, D., R. De Groot, and P. W. Hermans. 2004. Streptococcus pneumoniae colonisation: the key to pneumococcal disease. *Lancet Infect Dis* 4: 144-154.
2. Kadioglu, A., J. N. Weiser, J. C. Paton, and P. W. Andrew. 2008. The role of Streptococcus pneumoniae virulence factors in host respiratory colonization and disease. *Nature Reviews Microbiology* 6: 288-301.
3. Verma, R., and P. Khanna. 2012. Pneumococcal conjugate vaccine: a newer vaccine available in India. *Hum Vaccin Immunother* 8: 1317-1320.
4. Morens, D. M., J. K. Taubenberger, and A. S. Fauci. 2008. Predominant role of bacterial pneumonia as a cause of death in pandemic influenza: implications for pandemic influenza preparedness. *J Infect Dis* 198: 962-970.
5. O'Brien, K. L., L. J. Wolfson, J. P. Watt, E. Henkle, M. Deloria-Knoll, N. McCall, E. Lee, K. Mulholland, O. S. Levine, T. Cherian, Hib, and T. Pneumococcal Global Burden of Disease Study. 2009. Burden of disease caused by Streptococcus pneumoniae in children younger than 5 years: global estimates. *Lancet* 374: 893-902.
6. Geno, K. A., G. L. Gilbert, J. Y. Song, I. C. Skovsted, K. P. Klugman, C. Jones, H. B. Konradsen, and M. H. Nahm. 2015. Pneumococcal Capsules and Their Types: Past, Present, and Future. *Clin Microbiol Rev* 28: 871-899.
7. Torres, A., P. Bonanni, W. Hryniewicz, M. Moutschen, R. R. Reinert, and T. Welte. 2015. Pneumococcal vaccination: what have we learnt so far and what can we expect in the future? *Eur J Clin Microbiol Infect Dis* 34: 19-31.

8. Wantuch, P. L., and F. Y. Avci. 2018. Current status and future directions of invasive pneumococcal diseases and prophylactic approaches to control them. *Hum Vaccin Immunother*: 1-19.
9. Wyres, K. L., L. M. Lambertsen, N. J. Croucher, L. McGee, A. von Gottberg, J. Linares, M. R. Jacobs, K. G. Kristinsson, B. W. Beall, K. P. Klugman, J. Parkhill, R. Hakenbeck, S. D. Bentley, and A. B. Brueggemann. 2013. Pneumococcal capsular switching: a historical perspective. *J Infect Dis* 207: 439-449.
10. Kim, L., L. McGee, S. Tomczyk, and B. Beall. 2016. Biological and Epidemiological Features of Antibiotic-Resistant *Streptococcus pneumoniae* in Pre- and Post-Conjugate Vaccine Eras: a United States Perspective. *Clin Microbiol Rev* 29: 525-552.
11. Li, Y., B. J. Metcalf, S. Chochua, Z. Li, R. E. Gertz, H. Walker, P. A. Hawkins, T. Tran, C. G. Whitney, L. McGee, and B. W. Beall. 2016. Penicillin-Binding Protein Transpeptidase Signatures for Tracking and Predicting β -Lactam Resistance Levels in *Streptococcus pneumoniae*. *MBio* 7.
12. Metcalf, B. J., R. E. Gertz, R. A. Gladstone, H. Walker, L. K. Sherwood, D. Jackson, Z. Li, C. Law, P. A. Hawkins, S. Chochua, M. Sheth, N. Rayamajhi, S. D. Bentley, L. Kim, C. G. Whitney, L. McGee, B. Beall, and A. B. C. s. team. 2016. Strain features and distributions in pneumococci from children with invasive disease before and after 13-valent conjugate vaccine implementation in the USA. *Clin Microbiol Infect* 22: 60.e69-60.e29.
13. Abdullahi, O., A. Karani, C. C. Tigo, D. Mugo, S. Kungu, E. Wanjiru, J. Jomo, R. Musyimi, M. Lipsitch, and J. A. Scott. 2012. The prevalence and risk factors for

- pneumococcal colonization of the nasopharynx among children in Kilifi District, Kenya. *PLoS One* 7: e30787.
14. Tigo, C. C., H. Gatakaa, A. Karani, D. Mugo, S. Kungu, E. Wanjiru, J. Jomo, R. Musyimi, J. Ojal, N. E. Glass, O. Abdullahi, and J. A. Scott. 2012. Rates of acquisition of pneumococcal colonization and transmission probabilities, by serotype, among newborn infants in Kilifi District, Kenya. *Clin Infect Dis* 55: 180-188.
 15. Gwaltney, J. M., Jr., M. A. Sande, R. Austrian, and J. O. Hendley. 1975. Spread of *Streptococcus pneumoniae* in families. II. Relation of transfer of *S. pneumoniae* to incidence of colds and serum antibody. *J Infect Dis* 132: 62-68.
 16. McCullers, J. A., J. L. McAuley, S. Browall, A. R. Iverson, K. L. Boyd, and B. Henriques Normark. 2010. Influenza enhances susceptibility to natural acquisition of and disease due to *Streptococcus pneumoniae* in ferrets. *J Infect Dis* 202: 1287-1295.
 17. Diavatopoulos, D. A., K. R. Short, J. T. Price, J. J. Wilksch, L. E. Brown, D. E. Briles, R. A. Strugnell, and O. L. Wijburg. 2010. Influenza A virus facilitates *Streptococcus pneumoniae* transmission and disease. *FASEB J* 24: 1789-1798.
 18. Weiser, J. N., D. M. Ferreira, and J. C. Paton. 2018. *Streptococcus pneumoniae*: transmission, colonization and invasion. *Nat Rev Microbiol* 16: 355-367.
 19. Thigpen, M. C., C. G. Whitney, N. E. Messonnier, E. R. Zell, R. Lynfield, J. L. Hadler, L. H. Harrison, M. M. Farley, A. Reingold, N. M. Bennett, A. S. Craig, W. Schaffner, A. Thomas, M. M. Lewis, E. Scallan, A. Schuchat, and N. Emerging Infections Programs. 2011. Bacterial Meningitis in the United States, 1998-2007. *New England Journal of Medicine* 364: 2016-2025.

20. Hausdorff, W. P., J. Bryant, C. Kloek, P. R. Paradiso, and G. R. Siber. 2000. The contribution of specific pneumococcal serogroups to different disease manifestations: implications for conjugate vaccine formulation and use, part II. *Clin Infect Dis* 30: 122-140.
21. Hausdorff, W. P., R. Dagan, F. Beckers, and L. Schuerman. 2009. Estimating the direct impact of new conjugate vaccines against invasive pneumococcal disease. *Vaccine* 27: 7257-7269.
22. Daniels, C. C., P. D. Rogers, and C. M. Shelton. 2016. A Review of Pneumococcal Vaccines: Current Polysaccharide Vaccine Recommendations and Future Protein Antigens. *J Pediatr Pharmacol Ther* 21: 27-35.
23. Magee, A. D., and J. Yother. 2001. Requirement for capsule in colonization by *Streptococcus pneumoniae*. *Infect Immun* 69: 3755-3761.
24. Bruyn, G. A., B. J. Zegers, and R. van Furth. 1992. Mechanisms of host defense against infection with *Streptococcus pneumoniae*. *Clin Infect Dis* 14: 251-262.
25. Winkelstein, J. A. 1984. Complement and the host's defense against the pneumococcus. *Crit Rev Microbiol* 11: 187-208.
26. Winkelstein, J. A. 1981. The role of complement in the host's defense against *Streptococcus pneumoniae*. *Rev Infect Dis* 3: 289-298.
27. Dochez, A. R., and L. J. Gillespie. 1913. A biological classification of pneumococci by means of immunity reactions. *J Amer Med Assoc* 61: 727-730.
28. Griffith, F. 1928. The Significance of Pneumococcal Types. *J Hyg-Cambridge* 27: 113-159.

29. Camilli, R., B. L. Spencer, M. Moschioni, V. Pinto, F. Berti, M. H. Nahm, and A. Pantosti. 2014. Identification of *Streptococcus pneumoniae* serotype 11E, serovariant 11Av and mixed populations by high-resolution magic angle spinning nuclear magnetic resonance (HR-MAS NMR) spectroscopy and flow cytometric serotyping assay (FCSA). *PLoS One* 9: e100722.
30. Abeygunawardana, C., T. C. Williams, J. S. Sumner, and J. P. Hennessey, Jr. 2000. Development and validation of an NMR-based identity assay for bacterial polysaccharides. *Anal Biochem* 279: 226-240.
31. Garcia, E., C. Arrecubieta, R. Munoz, M. Mollerach, and R. Lopez. 1997. A functional analysis of the *Streptococcus pneumoniae* genes involved in the synthesis of type 1 and type 3 capsular polysaccharides. *Microb Drug Resist* 3: 73-88.
32. Garcia, E., and R. Lopez. 1997. Molecular biology of the capsular genes of *Streptococcus pneumoniae*. *FEMS Microbiol Lett* 149: 1-10.
33. Guidolin, A., J. K. Morona, R. Morona, D. Hansman, and J. C. Paton. 1994. Nucleotide sequence analysis of genes essential for capsular polysaccharide biosynthesis in *Streptococcus pneumoniae* type 19F. *Infect Immun* 62: 5384-5396.
34. Varvio, S. L., K. Auranen, E. Arjas, and P. H. Makela. 2009. Evolution of the capsular regulatory genes in *Streptococcus pneumoniae*. *J Infect Dis* 200: 1144-1151.
35. Kolkman, M. A., B. A. van der Zeijst, and P. J. Nuijten. 1998. Diversity of capsular polysaccharide synthesis gene clusters in *Streptococcus pneumoniae*. *J Biochem* 123: 937-945.

36. Jiang, S. M., L. Wang, and P. R. Reeves. 2001. Molecular characterization of *Streptococcus pneumoniae* type 4, 6B, 8, and 18C capsular polysaccharide gene clusters. *Infect Immun* 69: 1244-1255.
37. Cartee, R. T., W. T. Forsee, J. S. Schutzbach, and J. Yother. 2000. Mechanism of type 3 capsular polysaccharide synthesis in *Streptococcus pneumoniae*. *J Biol Chem* 275: 3907-3914.
38. Dillard, J. P., M. W. Vandersea, and J. Yother. 1995. Characterization of the cassette containing genes for type 3 capsular polysaccharide biosynthesis in *Streptococcus pneumoniae*. *J Exp Med* 181: 973-983.
39. Dillard, J. P., and J. Yother. 1994. Genetic and molecular characterization of capsular polysaccharide biosynthesis in *Streptococcus pneumoniae* type 3. *Mol Microbiol* 12: 959-972.
40. Llull, D., E. Garcia, and R. Lopez. 2001. Tts, a processive beta-glucosyltransferase of *Streptococcus pneumoniae*, directs the synthesis of the branched type 37 capsular polysaccharide in *Pneumococcus* and other gram-positive species. *J Biol Chem* 276: 21053-21061.
41. Llull, D., R. Munoz, R. Lopez, and E. Garcia. 1999. A single gene (tts) located outside the cap locus directs the formation of *Streptococcus pneumoniae* type 37 capsular polysaccharide. Type 37 pneumococci are natural, genetically binary strains. *J Exp Med* 190: 241-251.
42. Whitfield, C. 2006. Biosynthesis and assembly of capsular polysaccharides in *Escherichia coli*. *Annu Rev Biochem* 75: 39-68.

43. James, D. B., K. Gupta, J. R. Hauser, and J. Yother. 2013. Biochemical activities of *Streptococcus pneumoniae* serotype 2 capsular glycosyltransferases and significance of suppressor mutations affecting the initiating glycosyltransferase Cps2E. *J Bacteriol* 195: 5469-5478.
44. Xayarath, B., and J. Yother. 2007. Mutations blocking side chain assembly, polymerization, or transport of a Wzy-dependent *Streptococcus pneumoniae* capsule are lethal in the absence of suppressor mutations and can affect polymer transfer to the cell wall. *J Bacteriol* 189: 3369-3381.
45. Forsee, W. T., R. T. Cartee, and J. Yother. 2009. Characterization of the lipid linkage region and chain length of the cellubionic acid capsule of *Streptococcus pneumoniae*. *J Biol Chem* 284: 11826-11835.
46. Forsee, W. T., R. T. Cartee, and J. Yother. 2006. Role of the carbohydrate binding site of the *Streptococcus pneumoniae* capsular polysaccharide type 3 synthase in the transition from oligosaccharide to polysaccharide synthesis. *J Biol Chem* 281: 6283-6289.
47. Mac, L. C., and M. R. Kraus. 1950. Relation of virulence of pneumococcal strains for mice to the quantity of capsular polysaccharide formed in vitro. *J Exp Med* 92: 1-9.
48. Hostetter, M. K. 1986. Serotypic variations among virulent pneumococci in deposition and degradation of covalently bound C3b: implications for phagocytosis and antibody production. *J Infect Dis* 153: 682-693.
49. Hyams, C., E. Camberlein, J. M. Cohen, K. Bax, and J. S. Brown. 2010. The *Streptococcus pneumoniae* capsule inhibits complement activity and neutrophil phagocytosis by multiple mechanisms. *Infect Immun* 78: 704-715.

50. Wartha, F., K. Beiter, B. Albiger, J. Fernebro, A. Zychlinsky, S. Normark, and B. Henriques-Normark. 2007. Capsule and D-alanylated lipoteichoic acids protect *Streptococcus pneumoniae* against neutrophil extracellular traps. *Cell Microbiol* 9: 1162-1171.
51. Brady, A. M., J. J. Calix, J. Yu, K. A. Geno, G. R. Cutter, and M. H. Nahm. 2014. Low invasiveness of pneumococcal serotype 11A is linked to ficolin-2 recognition of O-acetylated capsule epitopes and lectin complement pathway activation. *J Infect Dis* 210: 1155-1165.
52. Briles, D. E., M. J. Crain, B. M. Gray, C. Forman, and J. Yother. 1992. Strong association between capsular type and virulence for mice among human isolates of *Streptococcus pneumoniae*. *Infect Immun* 60: 111-116.
53. Weinberger, D. M., Z. B. Harboe, E. A. Sanders, M. Ndiritu, K. P. Klugman, S. Rückinger, R. Dagan, R. Adegbola, F. Cutts, H. L. Johnson, K. L. O'Brien, J. A. Scott, and M. Lipsitch. 2010. Association of serotype with risk of death due to pneumococcal pneumonia: a meta-analysis. *Clin Infect Dis* 51: 692-699.
54. Martens, P., S. W. Worm, B. Lundgren, H. B. Konradsen, and T. Benfield. 2004. Serotype-specific mortality from invasive *Streptococcus pneumoniae* disease revisited. *BMC Infect Dis* 4: 21.
55. Azarian, T., P. K. Mitchell, M. Georgieva, C. M. Thompson, A. Ghouila, A. J. Pollard, A. von Gottberg, M. du Plessis, M. Antonio, B. A. Kwambana-Adams, S. C. Clarke, D. Everett, J. Cornick, E. Sadowy, W. Hryniewicz, A. Skoczynska, J. C. Moisi, L. McGee, B. Beall, B. J. Metcalf, R. F. Breiman, P. L. Ho, R. Reid, K. L. O'Brien, R. A. Gladstone,

- S. D. Bentley, and W. P. Hanage. 2018. Global emergence and population dynamics of divergent serotype 3 CC180 pneumococci. *PLoS Pathog* 14: e1007438.
56. Harboe, Z. B., R. W. Thomsen, A. Riis, P. Valentiner-Branth, J. J. Christensen, L. Lambertsen, K. A. Krogfelt, H. B. Konradsen, and T. L. Benfield. 2009. Pneumococcal serotypes and mortality following invasive pneumococcal disease: a population-based cohort study. *PLoS Med* 6: e1000081.
57. Grabenstein, J. D., and L. K. Musey. 2014. Differences in serious clinical outcomes of infection caused by specific pneumococcal serotypes among adults. *Vaccine* 32: 2399-2405.
58. Darrieux, M., C. Goulart, D. Briles, and L. C. Leite. 2015. Current status and perspectives on protein-based pneumococcal vaccines. *Crit Rev Microbiol* 41: 190-200.
59. King, S. J., K. R. Hippe, and J. N. Weiser. 2006. Deglycosylation of human glycoconjugates by the sequential activities of exoglycosidases expressed by *Streptococcus pneumoniae*. *Mol Microbiol* 59: 961-974.
60. King, S. J., K. R. Hippe, J. M. Gould, D. Bae, S. Peterson, R. T. Cline, C. Fasching, E. N. Janoff, and J. N. Weiser. 2004. Phase variable desialylation of host proteins that bind to *Streptococcus pneumoniae* in vivo and protect the airway. *Mol Microbiol* 54: 159-171.
61. Pettigrew, M. M., K. P. Fennie, M. P. York, J. Daniels, and F. Ghaffar. 2006. Variation in the presence of neuraminidase genes among *Streptococcus pneumoniae* isolates with identical sequence types. *Infect Immun* 74: 3360-3365.
62. Manco, S., F. Herson, H. Yesilkaya, J. C. Paton, P. W. Andrew, and A. Kadioglu. 2006. Pneumococcal neuraminidases A and B both have essential roles during infection of the respiratory tract and sepsis. *Infect Immun* 74: 4014-4020.

63. Blanchette, K. A., A. T. Shenoy, J. Milner, 2nd, R. P. Gilley, E. McClure, C. A. Hinojosa, N. Kumar, S. C. Daugherty, L. J. Tallon, S. Ott, S. J. King, D. M. Ferreira, S. B. Gordon, H. Tettelin, and C. J. Orihuela. 2016. Neuraminidase A-Exposed Galactose Promotes *Streptococcus pneumoniae* Biofilm Formation during Colonization. *Infect Immun* 84: 2922-2932.
64. Long, J. P., H. H. Tong, and T. F. DeMaria. 2004. Immunization with native or recombinant *Streptococcus pneumoniae* neuraminidase affords protection in the chinchilla otitis media model. *Infect Immun* 72: 4309-4313.
65. Tilley, S. J., E. V. Orlova, R. J. Gilbert, P. W. Andrew, and H. R. Saibil. 2005. Structural basis of pore formation by the bacterial toxin pneumolysin. *Cell* 121: 247-256.
66. Mitchell, T. J., P. W. Andrew, F. K. Saunders, A. N. Smith, and G. J. Boulnois. 1991. Complement activation and antibody binding by pneumolysin via a region of the toxin homologous to a human acute-phase protein. *Mol Microbiol* 5: 1883-1888.
67. Rubins, J. B., D. Charboneau, C. Fasching, A. M. Berry, J. C. Paton, J. E. Alexander, P. W. Andrew, T. J. Mitchell, and E. N. Janoff. 1996. Distinct roles for pneumolysin's cytotoxic and complement activities in the pathogenesis of pneumococcal pneumonia. *Am J Respir Crit Care Med* 153: 1339-1346.
68. Subramanian, K., D. R. Neill, H. A. Malak, L. Spelmink, S. Khandaker, G. Dalla Libera Marchiori, E. Dearing, A. Kirby, M. Yang, A. Achour, J. Nilvebrant, P. A. Nygren, L. Plant, A. Kadioglu, and B. Henriques-Normark. 2019. Pneumolysin binds to the mannose receptor C type 1 (MRC-1) leading to anti-inflammatory responses and enhanced pneumococcal survival. *Nat Microbiol* 4: 62-70.

69. Berry, A. M., J. Yother, D. E. Briles, D. Hansman, and J. C. Paton. 1989. Reduced virulence of a defined pneumolysin-negative mutant of *Streptococcus pneumoniae*. *Infect Immun* 57: 2037-2042.
70. Kadioglu, A., S. Taylor, F. Iannelli, G. Pozzi, T. J. Mitchell, and P. W. Andrew. 2002. Upper and lower respiratory tract infection by *Streptococcus pneumoniae* is affected by pneumolysin deficiency and differences in capsule type. *Infect Immun* 70: 2886-2890.
71. Kirkham, L. A., A. R. Kerr, G. R. Douce, G. K. Paterson, D. A. Dilts, D. F. Liu, and T. J. Mitchell. 2006. Construction and immunological characterization of a novel nontoxic protective pneumolysin mutant for use in future pneumococcal vaccines. *Infect Immun* 74: 586-593.
72. Ogunniyi, A. D., K. S. LeMessurier, R. M. Graham, J. M. Watt, D. E. Briles, U. H. Stroehel, and J. C. Paton. 2007. Contributions of pneumolysin, pneumococcal surface protein A (PspA), and PspC to pathogenicity of *Streptococcus pneumoniae* D39 in a mouse model. *Infect Immun* 75: 1843-1851.
73. McDaniel, L. S., J. S. Sheffield, P. Delucchi, and D. E. Briles. 1991. PspA, a surface protein of *Streptococcus pneumoniae*, is capable of eliciting protection against pneumococci of more than one capsular type. *Infect Immun* 59: 222-228.
74. Yother, J., and J. M. White. 1994. Novel surface attachment mechanism of the *Streptococcus pneumoniae* protein PspA. *J Bacteriol* 176: 2976-2985.
75. Briles, D. E., R. C. Tart, E. Swiatlo, J. P. Dillard, P. Smith, K. A. Benton, B. A. Ralph, A. Brooks-Walter, M. J. Crain, S. K. Hollingshead, and L. S. McDaniel. 1998. Pneumococcal diversity: considerations for new vaccine strategies with emphasis on pneumococcal surface protein A (PspA). *Clin Microbiol Rev* 11: 645-657.

76. Khan, N., R. A. Qadri, and D. Sehgal. 2015. Correlation between in vitro complement deposition and passive mouse protection of anti-pneumococcal surface protein A monoclonal antibodies. *Clin Vaccine Immunol* 22: 99-107.
77. Hotomi, M., A. Togawa, M. Kono, Y. Ikeda, S. Takei, S. K. Hollingshead, D. E. Briles, K. Suzuki, and N. Yamanaka. 2013. PspA family distribution, antimicrobial resistance and serotype of *Streptococcus pneumoniae* isolated from upper respiratory tract infections in Japan. *PLoS One* 8: e58124.
78. Hollingshead, S. K., L. Baril, S. Ferro, J. King, P. Coan, D. E. Briles, and P. P. E. S. Group. 2006. Pneumococcal surface protein A (PspA) family distribution among clinical isolates from adults over 50 years of age collected in seven countries. *J Med Microbiol* 55: 215-221.
79. Ren, B., J. Li, K. Genschmer, S. K. Hollingshead, and D. E. Briles. 2012. The absence of PspA or presence of antibody to PspA facilitates the complement-dependent phagocytosis of pneumococci in vitro. *Clin Vaccine Immunol* 19: 1574-1582.
80. Ren, B., A. J. Szalai, S. K. Hollingshead, and D. E. Briles. 2004. Effects of PspA and antibodies to PspA on activation and deposition of complement on the pneumococcal surface. *Infect Immun* 72: 114-122.
81. Shaper, M., S. K. Hollingshead, W. H. Benjamin, and D. E. Briles. 2004. PspA protects *Streptococcus pneumoniae* from killing by apolactoferrin, and antibody to PspA enhances killing of pneumococci by apolactoferrin [corrected]. *Infect Immun* 72: 5031-5040.
82. Ogunniyi, A. D., M. Grabowicz, D. E. Briles, J. Cook, and J. C. Paton. 2007. Development of a vaccine against invasive pneumococcal disease based on combinations of virulence proteins of *Streptococcus pneumoniae*. *Infect Immun* 75: 350-357.

83. Goulart, C., T. R. da Silva, D. Rodriguez, W. R. Politano, L. C. Leite, and M. Darrieux. 2013. Characterization of protective immune responses induced by pneumococcal surface protein A in fusion with pneumolysin derivatives. *PLoS One* 8: e59605.
84. Briles, D. E., E. Ades, J. C. Paton, J. S. Sampson, G. M. Carlone, R. C. Huebner, A. Virolainen, E. Swiatlo, and S. K. Hollingshead. 2000. Intranasal immunization of mice with a mixture of the pneumococcal proteins PsaA and PspA is highly protective against nasopharyngeal carriage of *Streptococcus pneumoniae*. *Infect Immun* 68: 796-800.
85. Briles, D. E., S. K. Hollingshead, J. C. Paton, E. W. Ades, L. Novak, F. W. van Ginkel, and W. H. Benjamin. 2003. Immunizations with pneumococcal surface protein A and pneumolysin are protective against pneumonia in a murine model of pulmonary infection with *Streptococcus pneumoniae*. *J Infect Dis* 188: 339-348.
86. Briles, D. E., J. D. King, M. A. Gray, L. S. McDaniel, E. Swiatlo, and K. A. Benton. 1996. PspA, a protection-eliciting pneumococcal protein: immunogenicity of isolated native PspA in mice. *Vaccine* 14: 858-867.
87. McDaniel, L. S., G. Scott, J. F. Kearney, and D. E. Briles. 1984. Monoclonal antibodies against protease-sensitive pneumococcal antigens can protect mice from fatal infection with *Streptococcus pneumoniae*. *J Exp Med* 160: 386-397.
88. Briles, D. E., C. Forman, J. C. Horowitz, J. E. Volanakis, W. H. Benjamin, L. S. McDaniel, J. Eldridge, and J. Brooks. 1989. Antipneumococcal effects of C-reactive protein and monoclonal antibodies to pneumococcal cell wall and capsular antigens. *Infect Immun* 57: 1457-1464.
89. Crain, M. J., W. D. Waltman, J. S. Turner, J. Yother, D. F. Talkington, L. S. McDaniel, B. M. Gray, and D. E. Briles. 1990. Pneumococcal surface protein A (PspA) is

- serologically highly variable and is expressed by all clinically important capsular serotypes of *Streptococcus pneumoniae*. *Infect Immun* 58: 3293-3299.
90. Dave, S., A. Brooks-Walter, M. K. Pangburn, and L. S. McDaniel. 2001. PspC, a pneumococcal surface protein, binds human factor H. *Infect Immun* 69: 3435-3437.
 91. Dave, S., S. Carmicle, S. Hammerschmidt, M. K. Pangburn, and L. S. McDaniel. 2004. Dual roles of PspC, a surface protein of *Streptococcus pneumoniae*, in binding human secretory IgA and factor H. *J Immunol* 173: 471-477.
 92. Dave, S., M. K. Pangburn, C. Pruitt, and L. S. McDaniel. 2004. Interaction of human factor H with PspC of *Streptococcus pneumoniae*. *Indian J Med Res* 119 Suppl: 66-73.
 93. Balachandran, P., A. Brooks-Walter, A. Virolainen-Julkunen, S. K. Hollingshead, and D. E. Briles. 2002. Role of pneumococcal surface protein C in nasopharyngeal carriage and pneumonia and its ability to elicit protection against carriage of *Streptococcus pneumoniae*. *Infect Immun* 70: 2526-2534.
 94. Sanchez, C., P. Shivshankar, K. Stol, S. Trakhtenbroit, and C. Orihuela. 2010. The Pneumococcal Serine-Rich Repeat Protein Is an IntraSpecies Bacterial Adhesin That Promotes Bacterial Aggregation In Vivo and in Biofilms. *PLOS Pathogens*.
 95. Selva, L., P. Ciruela, K. Blanchette, E. del Amo, R. Pallares, C. J. Orihuela, and C. Muñoz-Almagro. 2012. Prevalence and clonal distribution of pcpA, psrP and Pilus-1 among pediatric isolates of *Streptococcus pneumoniae*. *PLoS One* 7: e41587.
 96. Lizcano, A., R. Akula Suresh Babu, A. T. Shenoy, A. M. Saville, N. Kumar, A. D'Mello, C. A. Hinojosa, R. P. Gilley, J. Segovia, T. J. Mitchell, H. Tettelin, and C. J. Orihuela. 2017. Transcriptional organization of pneumococcal psrP-secY2A2 and impact of GtfA and GtfB deletion on PsrP-associated virulence properties. *Microbes Infect* 19: 323-333.

97. Obert, C., J. Sublett, D. Kaushal, E. Hinojosa, T. Barton, E. I. Tuomanen, and C. J. Orihuela. 2006. Identification of a Candidate *Streptococcus pneumoniae* core genome and regions of diversity correlated with invasive pneumococcal disease. *Infect Immun* 74: 4766-4777.
98. Hava, D. L., and A. Camilli. 2002. Large-scale identification of serotype 4 *Streptococcus pneumoniae* virulence factors. *Mol Microbiol* 45: 1389-1406.
99. Shivshankar, P., C. Sanchez, L. F. Rose, and C. J. Orihuela. 2009. The *Streptococcus pneumoniae* adhesin PsrP binds to Keratin 10 on lung cells. *Mol Microbiol* 73: 663-679.
100. Grabenstein, J. D., and K. P. Klugman. 2012. A century of pneumococcal vaccination research in humans. *Clin Microbiol Infect* 18 Suppl 5: 15-24.
101. Robbins, J. B., R. Austrian, C. J. Lee, S. C. Rastogi, G. Schiffman, J. Henrichsen, P. H. Makela, C. V. Broome, R. R. Facklam, R. H. Tiesjema, and et al. 1983. Considerations for formulating the second-generation pneumococcal capsular polysaccharide vaccine with emphasis on the cross-reactive types within groups. *J Infect Dis* 148: 1136-1159.
102. Robbins, J. B., and R. Schneerson. 1983. Planning for a second (23 valent) generation pneumococcal vaccine. With special reference to new developments in our understanding of the structure and biology of polysaccharides. *Bull Eur Physiopathol Respir* 19: 215-226.
103. Weintraub, A. 2003. Immunology of bacterial polysaccharide antigens. *Carbohydr. Res.* 338: 2539-2547.
104. Song, J. Y., M. A. Moseley, R. L. Burton, and M. H. Nahm. 2013. Pneumococcal vaccine and opsonic pneumococcal antibody. *J Infect Chemother* 19: 412-425.

105. Andrews, N. J., P. A. Waight, R. C. George, M. P. Slack, and E. Miller. 2012. Impact and effectiveness of 23-valent pneumococcal polysaccharide vaccine against invasive pneumococcal disease in the elderly in England and Wales. *Vaccine* 30: 6802-6808.
106. O'Brien, K. L., M. Hochman, and D. Goldblatt. 2007. Combined schedules of pneumococcal conjugate and polysaccharide vaccines: is hyporesponsiveness an issue? *Lancet Infect Dis* 7: 597-606.
107. Sun, L., D. R. Middleton, P. L. Wantuch, A. Ozdilek, and F. Y. Avci. 2016. Carbohydrates as T-cell antigens with implications in health and disease. *Glycobiology*.
108. Li, P., and F. Wang. 2015. Polysaccharides: Candidates of promising vaccine adjuvants. *Drug Discov Ther* 9: 88-93.
109. Vella, M., and D. Pace. 2015. Glycoconjugate vaccines: an update. *Expert Opin Biol Ther* 15: 529-546.
110. Zimmermann, S., and B. Lepenies. 2015. Glycans as Vaccine Antigens and Adjuvants: Immunological Considerations. *Methods Mol Biol* 1331: 11-26.
111. Croucher, N. J., J. A. Finkelstein, S. I. Pelton, P. K. Mitchell, G. M. Lee, J. Parkhill, S. D. Bentley, W. P. Hanage, and M. Lipsitch. 2013. Population genomics of post-vaccine changes in pneumococcal epidemiology. *Nature genetics* 45: 656-663.
112. Aliberti, S., M. Mantero, M. Mirsaeidi, and F. Blasi. 2014. The role of vaccination in preventing pneumococcal disease in adults. *Clin Microbiol Infect* 20 Suppl 5: 52-58.
113. Bonten, M. J., S. M. Huijts, M. Bolkenbaas, C. Webber, S. Patterson, S. Gault, C. H. van Werkhoven, A. M. van Deursen, E. A. Sanders, T. J. Verheij, M. Patton, A. McDonough, A. Moradoghli-Haftvani, H. Smith, T. Mellelieu, M. W. Pride, G. Crowther, B. Schmoele-Thoma, D. A. Scott, K. U. Jansen, R. Lobatto, B. Oosterman, N. Visser, E.

- Caspers, A. Smorenburg, E. A. Emini, W. C. Gruber, and D. E. Grobbee. 2015. Polysaccharide conjugate vaccine against pneumococcal pneumonia in adults. *N Engl J Med* 372: 1114-1125.
114. Rodenburg, G. D., S. C. de Greeff, A. G. Jansen, H. E. de Melker, L. M. Schouls, E. Hak, L. Spanjaard, E. A. Sanders, and A. van der Ende. 2010. Effects of pneumococcal conjugate vaccine 2 years after its introduction, the Netherlands. *Emerg Infect Dis* 16: 816-823.
115. 2016. Trends by Serotype Group, 1998-2015. In *Active Bacterial Core surveillance*. D. o. B. D. National Center for Immunization and Respiratory Diseases, ed. Centers for Disease Control and Prevention
116. Moore, M. R., R. Link-Gelles, W. Schaffner, R. Lynfield, C. Lexau, N. M. Bennett, S. Petit, S. M. Zansky, L. H. Harrison, A. Reingold, L. Miller, K. Scherzinger, A. Thomas, M. M. Farley, E. R. Zell, T. H. Taylor, Jr., T. Pondo, L. Rodgers, L. McGee, B. Beall, J. H. Jorgensen, and C. G. Whitney. 2015. Effect of use of 13-valent pneumococcal conjugate vaccine in children on invasive pneumococcal disease in children and adults in the USA: analysis of multisite, population-based surveillance. *Lancet Infect Dis* 15: 301-309.
117. AlonsoDeVelasco, E., A. F. Verheul, J. Verhoef, and H. Snippe. 1995. Streptococcus pneumoniae: virulence factors, pathogenesis, and vaccines. *Microbiol Rev* 59: 591-603.
118. Casadevall, A., and L. A. Pirofski. 2009. Virulence factors and their mechanisms of action: the view from a damage-response framework. *J Water Health* 7 Suppl 1: S2-S18.
119. Coutinho, A., and G. Möller. 1973. B cell mitogenic properties of thymus-independent antigens. *Nat New Biol* 245: 12-14.

120. Barrett, D. J. 1985. Human immune responses to polysaccharide antigens: an analysis of bacterial polysaccharide vaccines in infants. *Advances in Pediatrics*. 139-158.
121. Weintraub, A. 2003. Immunology of bacterial polysaccharide antigens. *Carbohydr Res* 338: 2539-2547.
122. Jones, C. 2005. Vaccines based on the cell surface carbohydrates of pathogenic bacteria. *An Acad Bras Cienc* 77: 293-324.
123. Avci, F., D. Kasper, W. Paul, D. Littman, and W. Yokoyama. 2010. How Bacterial Carbohydrates Influence the Adaptive Immune System. *Annual Review of Immunology, Vol 28* 28: 107-130.
124. Avci, F. Y., X. Li, M. Tsuji, and D. L. Kasper. 2013. Carbohydrates and T cells: a sweet twosome. *Semin Immunol* 25: 146-151.
125. Schneerson, R., O. Barrera, A. Sutton, and J. B. Robbins. 1980. Preparation, characterization, and immunogenicity of Haemophilus influenzae type b polysaccharide-protein conjugates. *J Exp Med* 152: 361-376.
126. Beuvery, E., F. Vanrossum, and J. Nagel. 1982. Comparison of the induction of immunoglobulin M and G antibodies in mice with purified pneumococcal type 3 and meningococcal group C polysaccharides and their protein conjugates. *Infection and Immunity* 37: 15-22.
127. Guttormsen, H., L. Wetzler, R. Finberg, and D. Kasper. 1998. Immunologic memory induced by a glycoconjugate vaccine in a murine adoptive lymphocyte transfer model. *Infection and Immunity* 66: 2026-2032.
128. Wessels, M., L. Paoletti, A. Rodewald, F. Michon, J. Difabio, H. Jennings, and D. Kasper. 1993. Stimulation of protective antibodies against type Ia and Ib group B

- streptococci by a type Ia polysaccharide-tetanus toxoid conjugate vaccine. *Infection and Immunity* 61: 4760-4766.
129. Trotter, C., J. McVernon, M. Ramsay, C. Whitney, E. Mulholland, D. Goldblatt, J. Hombach, M. Kieny, and S. Subgrp. 2008. Optimising the use of conjugate vaccines to prevent disease caused by Haemophilus influenzae type b, Neisseria meningitidis and Streptococcus pneumoniae. *Vaccine* 26: 4434-4445.
130. Pirofski, L. 2001. Polysaccharides, mimotopes and vaccines for fungal and encapsulated pathogens. *Trends in Microbiology* 9: 445-451.
131. Avci, F. 2013. Novel Strategies for Development of Next-Generation Glycoconjugate Vaccines. *Current Topics in Medicinal Chemistry* 13: 2535-2540.
132. Mitchison, N. 2004. Landmark - T-cell-B-cell cooperation. *Nature Reviews Immunology* 4: 308-312.
133. Kalka-Moll, W. M., A. O. Tzianabos, P. W. Bryant, M. Niemeyer, H. L. Ploegh, and D. L. Kasper. 2002. Zwitterionic polysaccharides stimulate T cells by MHC class II-dependent interactions. *J Immunol* 169: 6149-6153.
134. Avci, F. Y., X. Li, M. Tsuji, and D. L. Kasper. 2011. A mechanism for glycoconjugate vaccine activation of the adaptive immune system and its implications for vaccine design. *Nat Med* 17: 1602-1609.
135. Avci, F. Y., X. Li, M. Tsuji, and D. L. Kasper. 2012. Isolation of carbohydrate-specific CD4(+) T cell clones from mice after stimulation by two model glycoconjugate vaccines. *Nat Protoc* 7: 2180-2192.

136. Middleton, D. R., L. Sun, A. V. Paschall, and F. Y. Avci. 2017. T Cell-Mediated Humoral Immune Responses to Type 3 Capsular Polysaccharide of *Streptococcus pneumoniae*. *J Immunol* 199: 598-603.
137. Sun, X., G. Stefanetti, F. Berti, and D. L. Kasper. 2019. Polysaccharide structure dictates mechanism of adaptive immune response to glycoconjugate vaccines. *Proc Natl Acad Sci USA* 116: 193-198.
138. Lai, Z., and J. R. Schreiber. 2009. Antigen processing of glycoconjugate vaccines; the polysaccharide portion of the pneumococcal CRM(197) conjugate vaccine co-localizes with MHC II on the antigen processing cell surface. *Vaccine* 27: 3137-3144.
139. Muthukkumar, S., and K. E. Stein. 2004. Immunization with meningococcal polysaccharide-tetanus toxoid conjugate induces polysaccharide-reactive T cells in mice. *Vaccine* 22: 1290-1299.
140. Costantino, P., R. Rappuoli, and F. Berti. 2011. The design of semi-synthetic and synthetic glycoconjugate vaccines. *Expert Opinion on Drug Discovery* 6: 1045-1066.
141. Bardotti, A., G. Averani, F. Berti, S. Berti, V. Carinci, S. D'Ascenzi, B. Fabbri, S. Glannini, A. Giannozzi, C. Magagnoli, D. Proietti, F. Norelli, R. Rappuoli, S. Ricci, and P. Costantino. 2008. Physicochemical characterisation of glycoconjugate vaccines for prevention of meningococcal diseases. *Vaccine* 26: 2284-2296.
142. Kowarik, M., S. Numao, M. Feldman, B. Schulz, N. Callewaert, E. Kiermaier, I. Catrein, and M. Aebi. 2006. N-linked glycosylation of folded proteins by the bacterial oligosaccharyltransferase. *Science* 314: 1148-1150.
143. Ihssen, J., M. Kowarik, S. Dilettoso, C. Tanner, M. Wacker, and L. Thony-Meyer. 2010. Production of glycoprotein vaccines in *Escherichia coli*. *Microbial Cell Factories* 9.

144. Ravenscroft, N., M. A. Haeuptle, M. Kowarik, F. S. Fernandez, P. Carranza, A. Brunner, M. Steffen, M. Wetter, S. Keller, C. Ruch, and M. Wacker. 2016. Purification and characterization of a Shigella conjugate vaccine, produced by glycoengineering *Escherichia coli*. *Glycobiology* 26: 51-62.
145. Naegeli, A., and M. Aebi. 2015. Current Approaches to Engineering N-Linked Protein Glycosylation in Bacteria. *Methods Mol Biol* 1321: 3-16.
146. Faridmoayer, A., M. Fentabil, D. Mills, J. Klassen, and M. Feldman. 2007. Functional characterization of bacterial oligosaccharyltransferases involved in O-linked protein glycosylation. *Journal of Bacteriology* 189: 8088-8098.
147. Harding, C. M., and M. F. Feldman. 2019. Glycoengineering bioconjugate vaccines, therapeutics, and diagnostics in *E. coli*. *Glycobiology*.
148. Harding, C. M., M. A. Nasr, N. E. Scott, G. Goyette-Desjardins, H. Nothaft, A. E. Mayer, S. M. Chavez, J. P. Huynh, R. L. Kinsella, C. M. Szymanski, C. L. Stallings, M. Segura, and M. F. Feldman. 2019. A platform for glycoengineering a polyvalent pneumococcal bioconjugate vaccine using *E. coli* as a host. *Nat Commun* 10: 891.
149. Terra, V., D. Mills, L. Yates, S. Abouelhadid, J. Cuccui, and B. Wren. 2012. Recent developments in bacterial protein glycan coupling technology and glycoconjugate vaccine design. *Journal of Medical Microbiology* 61: 919-926.
150. Berti, F., and R. Adamo. 2013. Recent Mechanistic Insights on Glycoconjugate Vaccines and Future Perspectives. *Acs Chemical Biology* 8: 1653-1663.
151. Agard, N., J. Baskin, J. Prescher, A. Lo, and C. Bertozzi. 2006. A comparative study of bioorthogonal reactions with azides. *Acs Chemical Biology* 1: 644-648.

152. Nilo, A., M. Allan, B. Brogioni, D. Proietti, V. Cattaneo, S. Crotti, S. Sokup, H. Zhai, I. Margarit, F. Berti, Q. Hu, and R. Adamo. 2014. Tyrosine-Directed Conjugation of Large Glycans to Proteins via Copper-Free Click Chemistry. *Bioconjugate Chemistry* 25: 2105-2111.
153. Stefanetti, G., A. Saul, C. A. MacLennan, and F. Micoli. 2015. Click Chemistry Applied to the Synthesis of Salmonella Typhimurium O-Antigen Glycoconjugate Vaccine on Solid Phase with Sugar Recycling. *Bioconjug Chem* 26: 2507-2513.
154. Stefanetti, G., Q. Y. Hu, A. Usera, Z. Robinson, M. Allan, A. Singh, H. Imase, J. Cobb, H. Zhai, D. Quinn, M. Lei, A. Saul, R. Adamo, C. A. MacLennan, and F. Micoli. 2015. Sugar-Protein Connectivity Impacts on the Immunogenicity of Site-Selective Salmonella O-Antigen Glycoconjugate Vaccines. *Angew Chem Int Ed Engl* 54: 13198-13203.

Figure 1.1

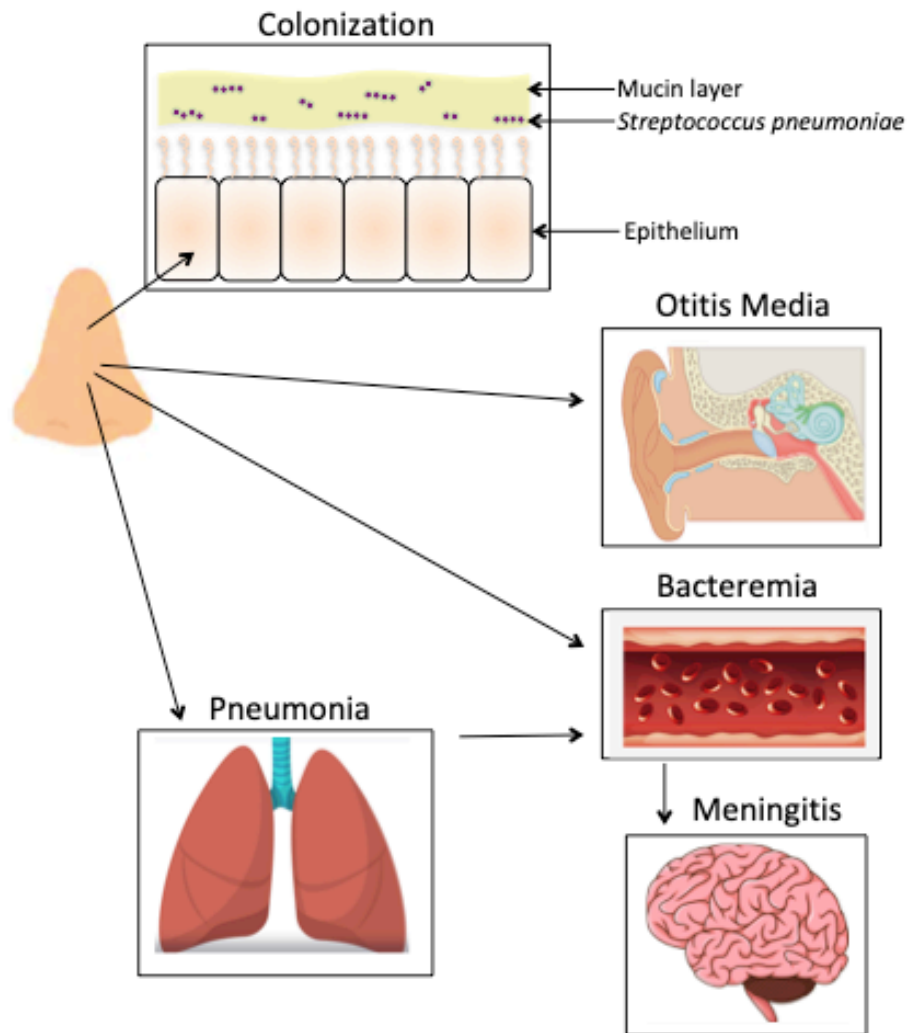


Figure 1.1

Streptococcus pneumoniae colonizes the nasopharynx of healthy host. Under high bacterial loads or inflammatory responses, Spn can disseminate to normally sterile tissues to cause invasive diseases.

Figure 1.2

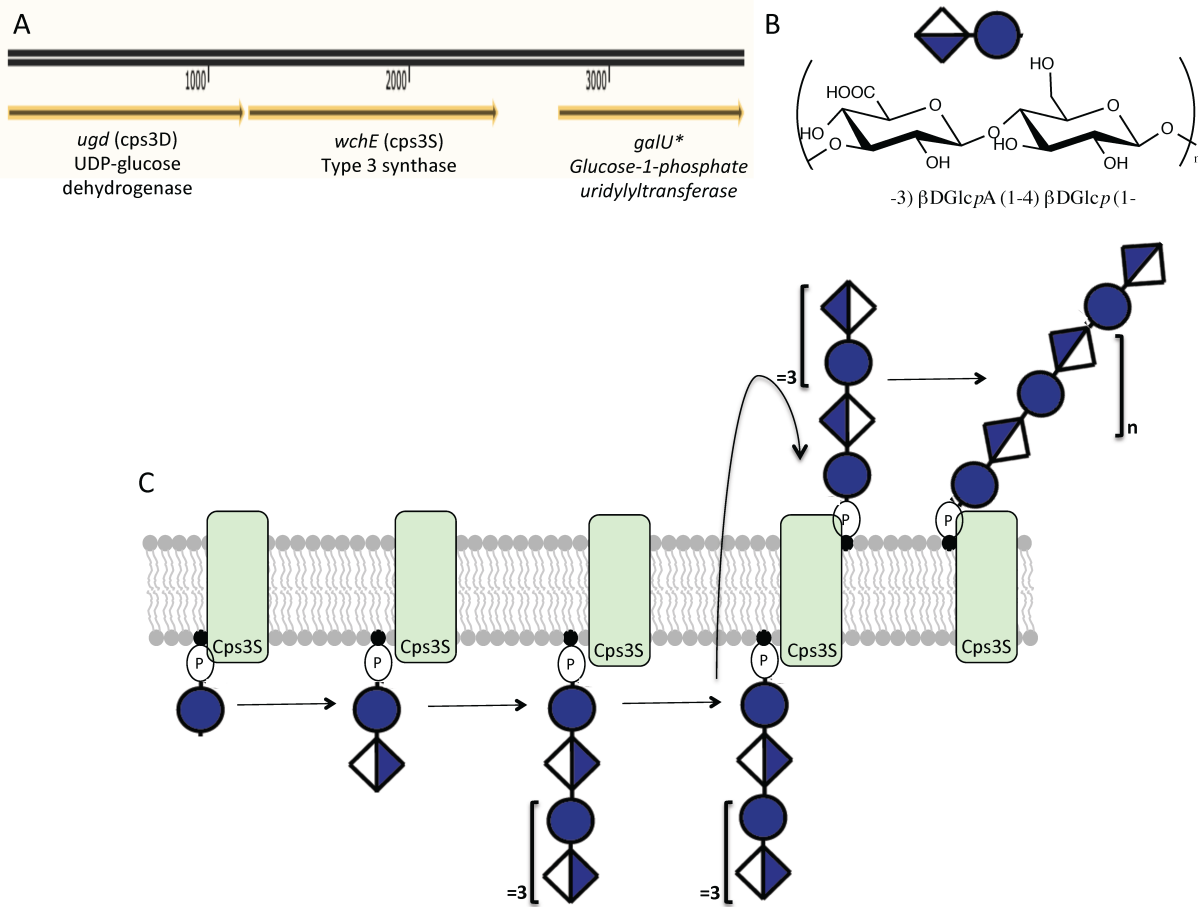


Figure 1.2

Streptococcus pneumoniae serotype 3 uses synthase-dependent synthesis. A.) Locus consists of UDP-glucose dehydrogenase (*cps3D*), Type 3 synthase (*cps3S*), and Glucose-1-phosphate uridylyltransferase (*galU*)(*dispensable for capsule production). B.) Polysaccharide is a linear disaccharide repeating unit structure consisting of $-3) \beta DGlcpA(1-4) \beta DGlcp(1-$. Half-filled blue diamond denotes glucuronic acid residues, blue circle denotes glucose residues. C.) Cps3S initiates synthesis by transferring glucose from UDP-glucose to the phosphatidyl glycerol (P) acceptor. The synthase then transfers glucuronic acid from UDP-glucuronic acid to the P-linked glucose. After the synthase extends the polymer to an octasaccharide, Cps3S will push the polysaccharide to the outside of the membrane where the chain length will extend until UDP-GlcA is depleted and local concentrations are insufficient for further polymerization.

Figure 1.3

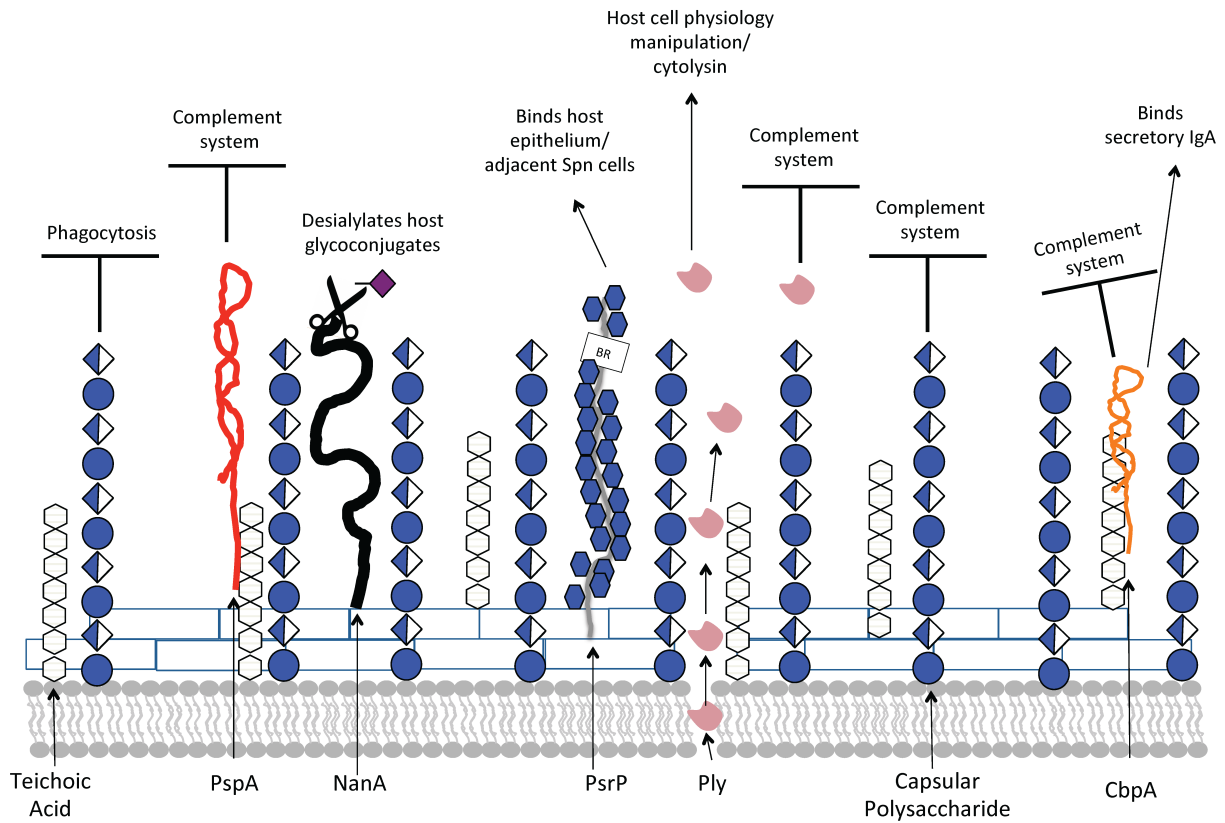


Figure 1.3

Virulence of *Streptococcus pneumoniae* is driven by multiple protein and carbohydrate factors. Important virulence determinants include: capsular polysaccharide, choline binding proteins (including PspA, and CbpA) that are non-covalently anchored to the surface through choline residues on teichoic acid, neuraminidases such as NanA, the cytolytic protein Ply, and major surface adhesion PsrP.

Figure 1.4

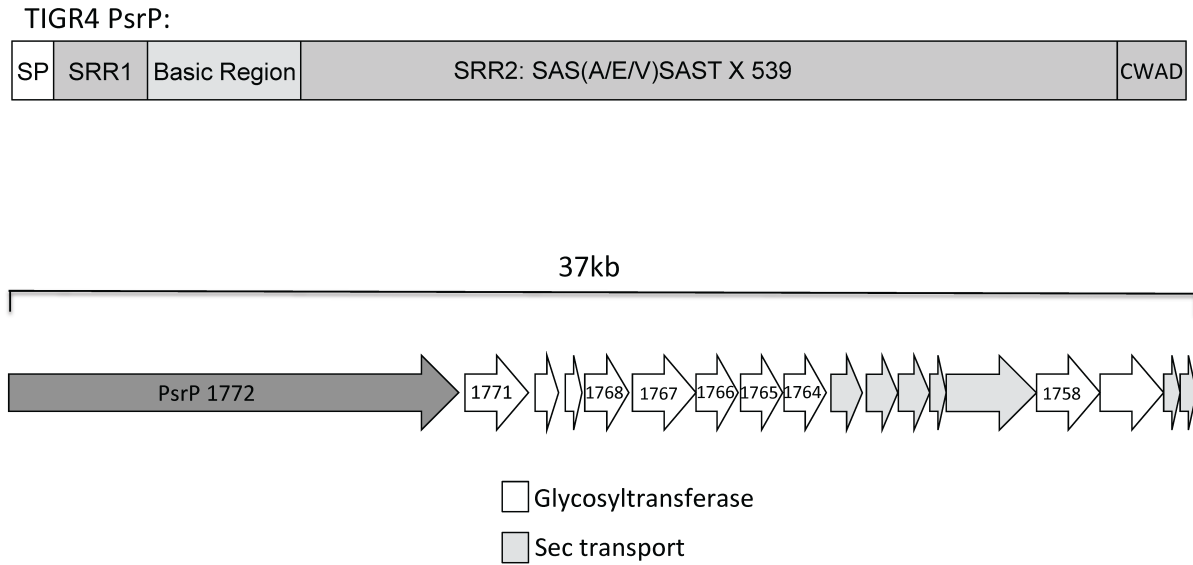


Figure 1.4

A.) Domain schematic of Pneumococcal serine rich protein (PsrP) from TIGR4 strain. PsrP consists of a N-terminal secretion signal peptide, a short serine-rich repeat 1 region, a basic region, a very long serine-rich repeat 2 region, and a cell-wall anchor domain at the C-terminus. B.) Genomic organization of PsrP-secY2A2 locus. Lightly shaded arrows are putative transport genes, whereas white arrows indicate putative or experimentally determined glycosyltransferases. Uniprot TIGR4 gene products SP_1772(PsrP) to SP_1755.

Figure 1.5

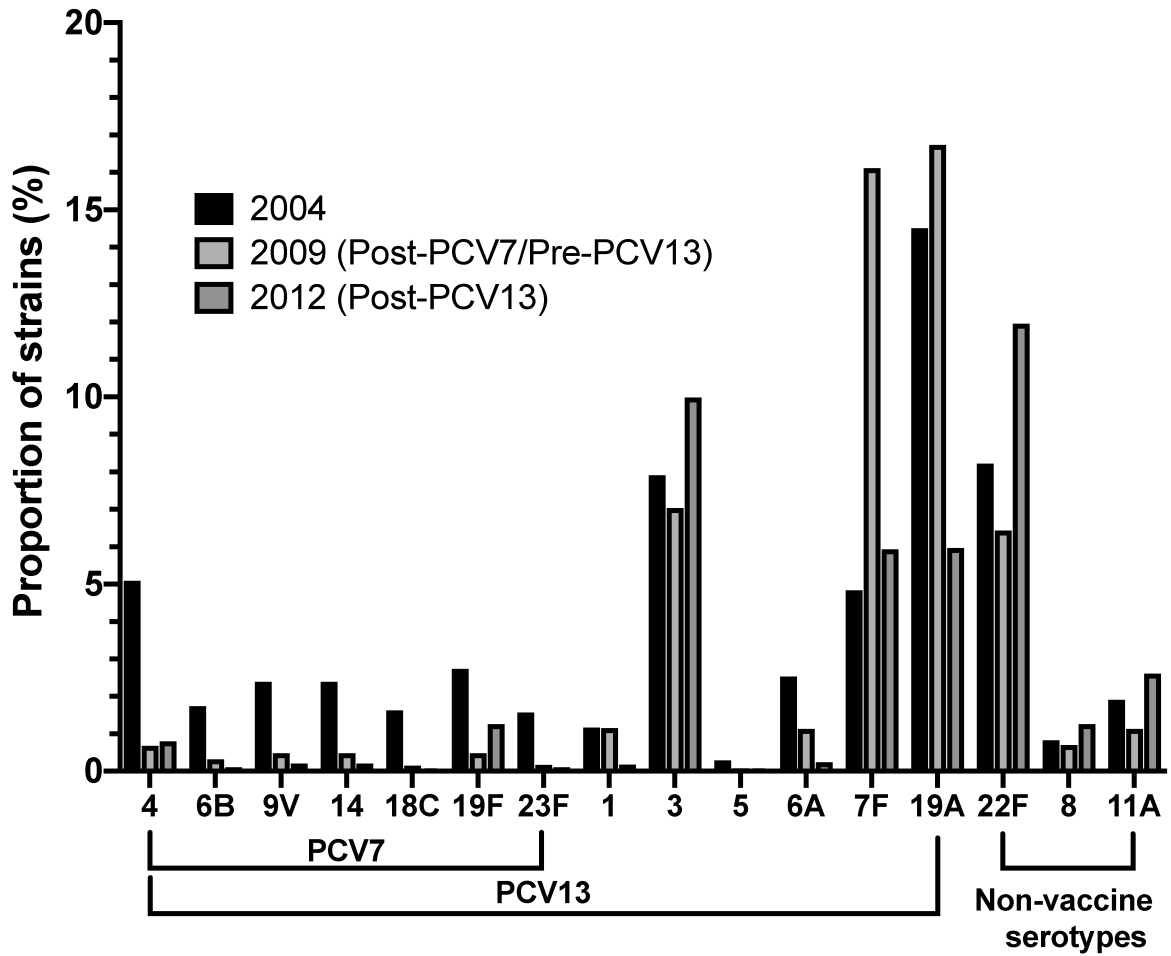


Figure 1.5
 Distribution of vaccine and non-vaccine serotypes before and after introduction of PCV13 glycoconjugate vaccine. Figure constructed from data introduced by Moore *et al.* 2015

Figure 1.6

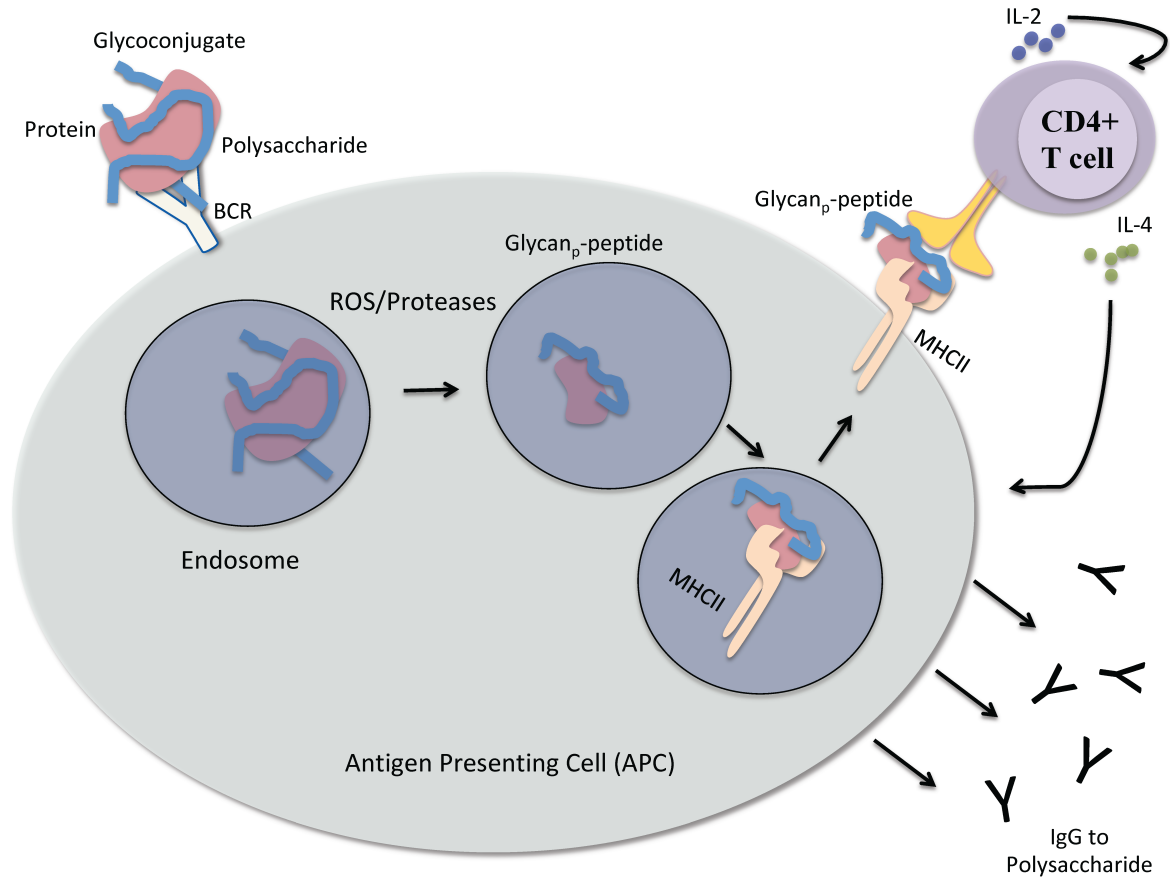


Figure 1.6

Mechanism of T cell activation by model glycoconjugate vaccines in a Tcarb dependent manner. Antigen processing and presentation leads to presentation of carbohydrate epitopes by MHCII to CD4+ T cells. Activation of CD4+ T cells leads to B cell induction to produce high affinity, long-lived IgG antibodies to the polysaccharide.

CHAPTER 2

T CELL-MEDIATED HUMORAL IMMUNE RESPONSES TO TYPE 3 CAPSULAR POLYSACCHARIDE OF *STREPTOCOCCUS PNEUMONIAE*

Dustin R Middleton, Lina Sun, Amy V. Paschall and Fikri Y. Avci

Accepted by *The Journal of Immunology*. Reprinted here with permission of publisher.

Abstract

Most pathogenic bacteria express surface carbohydrates called capsular polysaccharides (CPSs). CPSs are important vaccine targets since they are easily accessible and recognizable by the immune system. However, CPS-specific adaptive humoral immune responses can only be achieved by the covalent conjugation of CPSs with carrier proteins to produce glycoconjugate vaccines. We previously described a mechanism by which a model glycoconjugate vaccine can activate the adaptive immune system and demonstrated that the mammalian CD4⁺ T cell repertoire contains a population of carbohydrate-specific T cells (i.e., Tcarbs). In this study, we employ glycoconjugates of type 3 *Streptococcus pneumoniae* CPS (Pn3P) to assess whether the carbohydrate-specific adaptive immune response exemplified in our previous study can be applied to the conjugates of this lethal pathogen. Here, we provide evidence for the functional roles of Pn3P-specific CD4⁺ T cells utilizing mouse immunization schemes that induce Pn3P-specific immunoglobulin G (IgG) responses in a Tcarb-dependent manner.

Introduction

Exploiting their high antigenicity, capsular polysaccharides (CPSs) have been used as main components of glycoconjugate vaccines in clinical practice worldwide in the past three decades (1). Immunizations with glycoconjugates containing CPSs from *H. influenzae*, *S. pneumoniae*, and *N. meningitidis* have been utilized in preventing/controlling infectious diseases caused by these bacterial pathogens (2, 3). While glycoconjugate vaccines have provided great health benefits in controlling bacterial diseases, glycoconjugate construction has often been a random process of empirically linking two molecules (carbohydrate and protein) with minimum consideration of their mechanism of action (4), resulting in poorly characterized, heterogeneous

and variably immunogenic glycoconjugate vaccines (1, 5). Demystifying T cell activation mechanisms of glycoconjugate vaccines is a key step towards designing new-generation vaccines. We recently demonstrated a mechanism through which uptake of a glycoconjugate vaccine by antigen presenting cells (APCs) results in the presentation of a carbohydrate epitope by the major histocompatibility class II complex (MHCII), thus stimulating carbohydrate-specific CD4⁺ T cells (Tcarbs) (6-8).

In the present study, we employ model glycoconjugates of type 3 *Streptococcus pneumoniae* CPS (Pn3P) to examine whether the carbohydrate-specific adaptive immune responses exemplified in our previous findings apply to other carbohydrate antigens used in glycoconjugate vaccines. The Gram-positive pathogen *Streptococcus pneumoniae* can be sorted into over 90 capsular serotypes (9). Multiple studies have shown the ability of CPS-specific antibodies to provide protection from pneumococcal challenges (10, 11). However, most CPSs are poorly immunogenic, since they cannot, in their pure form, induce T cell dependent immune responses (4, 12). Immunization with glycoconjugates, as opposed to pure glycans, elicits T cell help for B cells that produce high-affinity IgG antibodies to the CPS component of the vaccine and induces memory B and T cell development (4, 12). Since the introduction of the first pneumococcal conjugate vaccine, PCV7, the incidence rate of pneumococcal disease has been reduced significantly (11). The current pneumococcal conjugate vaccine is the 13-valent Prevnar13®, encompassing CPSs from thirteen of the most prevalent serotypes of *S. pneumoniae* (11). The model conjugate vaccine used in this study is in fact a component of the existing 13-valent pneumococcal conjugate vaccine. *S. pneumoniae* remains among the most lethal infectious agents despite the availability of global vaccination programs (11, 13). The type 3 strain in particular is among the most virulent strains. Despite current vaccination programs, morbidity of

the type 3 strain remains high, raising questions regarding the efficacy of this vaccine (14). The knowledge gained in the present study may have implications in producing a highly protective knowledge-based pneumococcal vaccine.

Materials and Methods

Mice

Eight-week-old female BALB/c mice were obtained from Taconic Biosciences (Hudson, NY) and housed in the Coverdell Rodent Vivarium at the University of Georgia. Mice were kept in microisolator cages and handled under a laminar flow hood. All mouse experiments were in compliance with the University of Georgia Institutional Animal Care and Use Committee under the approved animal use protocol # A2013 12-011-Y1-A0.

Antigens

Purified Pn3P powder was obtained from American Type Cell Collection (Cat. #172-X). Pn3P was reduced to an average molecular weight of 100kDa by hydrolysis with 0.3M trifluoroacetic acid. Pn3P was conjugated to either ovalbumin (Sigma A7641) or keyhole limpet hemocyanin (Calbiochem 374805) through reductive amination as previously described (6, 7). Pn3P conjugates were isolated from unconjugated components by size exclusion chromatography (**Fig. 2.6**). A combination of phenol sulfuric acid and BCA assays using Pn3P and carrier proteins for standard curve generation confirmed that the conjugates consisted of 45-55% protein and 45-55% Pn3P (7).

Immunizations

Groups of BALB/c mice were immunized intraperitoneally on days 0 and 14 with 5 mg of antigen in phosphate buffered saline (PBS) mixed with 2% alhydrogel (Invivogen #vac-

alu-50) in a 3:1 ratio. Where indicated, mixtures consisted of quantities consistent with conjugate ratios.

Adoptive transfers

Groups of donor BALB/c mice were primed and boosted with 5 mg Pn3P or 10 mg of Pn3P-KLH subcutaneously at 3-week intervals. Mice were sacrificed 5 days after boost. CD4⁺ T cells from Pn3P and Pn3P-KLH primed mice were negatively selected using mouse CD4⁺ T lymphocyte enrichment magnetic beads (BD Biosciences 558131), and B cells from Pn3P-KLH primed mice were isolated using mouse B lymphocyte enrichment magnetic beads (BD Biosciences 557792). Isolation of a given cell type was confirmed by flow cytometry. CD4⁺ T cells (1×10^7) from either Pn3P or Pn3P-KLH immunized donors and B cells (1×10^7) from Pn3P-KLH immunized mice were adoptively transferred to recipient mice through tail vein injections in PBS. The recipient mice were then immunized with Pn3P-KLH or Pn3P-OVA 1 day after adoptive transfer.

Detection of Pn3P-specific serum antibodies

Mice were bled from the tail vein on days 14 and 21 during the prime-boost immunization experiments. Mice used in the adoptive transfer experiment were bled 3 days after booster immunization (4 days after transfer). Pn3P-specific antibodies in serum were detected by ELISA in 96 well plates coated with 2.5 mg/ml of Pn3P-HSA conjugate. Four immune sera per group were used in all ELISA experiments.

Opsonophagocytic killing assay

Opsonophagocytic killing assay was performed as previously described(15). Briefly, Type 3 *Streptococcus pneumoniae* WU2 strain (approximately 800 CFU/10 mL/well) was incubated with mouse sera samples (20 mL each at 1:30 dilutions) in duplicate wells in a 96-

well round-bottom plate for 30 minutes with shaking at room temperature in Opsonization Buffer B (sterile 1X PBS with $\text{Ca}^{++}/\text{Mg}^{++}$, 0.1% gelatin, and 5% heat-inactivated FetalClone). HL60 cells (generously provided by Moon Nahm, UAB) were cultured in RPMI with 10% heat-inactivated FetalClone (HyClone, SH30080.03) and 1% L-glutamine. HL60 cells were differentiated using 0.6% N,N-dimethylformamide (DMF, Fisher, D131-1) for three days, harvested, and resuspended in Opsonization Buffer B. Baby rabbit complement (Pel-Freez, 31061) was added to HL60 cells at 20% final volume, with a final cell concentration of 1×10^7 cells/mL. The HL60/complement mixture was added to the serum/bacteria at 5×10^5 cells/well. The reactions were incubated at 37°C for 1 hour with shaking. The reactions were stopped by incubating the plate(s) on ice for approximately 20 minutes. 10 mL of each reaction was diluted into a final volume of 50 mL and plated onto blood agar plates. Plates were incubated overnight at 30°C in anaerobic conditions and counted. Percent survival was calculated as each duplicate reaction subtracted from the mean values obtained for control samples (naïve serum, 100% survival).

Antibodies and Flow Cytometry

The following fluorophore-conjugated antibodies used in flow cytometry detection were purchased from Biolegend: anti-mouse CD3 ϵ (clone 145-2C11), anti-mouse CD4 (clone GK1.5), anti-mouse CD69 (clone H1.2F3). 5(6)-Carboxyfluorescein diacetate N-succinimidyl ester (CFSE) was purchased from Sigma. Surface staining of cell suspensions was performed in PBS/0.1% BSA/0.02% NaN_3 solution at 4°C. Samples were analyzed on CyAn (Beckman Coulter). Data were analyzed using FlowJo software (Tree Star).

ELISPOT Assay

Groups of BALB/c mice were immunized with 10ug of Pn3P-OVA emulsified in Freund's adjuvant (Thermo Scientific) by subcutaneously injection. CD4+ T cells were isolated from lymph nodes of Pn3P-OVA immunized mice and stimulated *in vitro* in the presence of irradiated APCs pulsed with indicated antigens. After 24hr stimulation, IL-2 production was detected by Enzyme-Linked ImmunoSpot (ELISPOT) assay using commercially available mouse ELISPOT reagent set (Cellular Technology Ltd) according to the manufacturer's protocol. The ELISPOT samples were analyzed by ImmunoSpot S6 analyzer using the ImmunoCapture 6.3 and ImmunoSpot 5.0 Pro DC software (Cellular Technology Ltd).

Generation of Pn3P-specific T cell Hybridomas

T-cell hybridomas were generated as previously described(16). Briefly, BALB/c mice were immunized with Pn3P-KLH emulsified in Freund's adjuvant (Thermo Scientific). Primary CD4+ T cells obtained from lymph node of immunized mice were re-stimulated in vitro with APCs that pulsed with Pn3P-KLH. Activated CD4+ T cells were fused with BW5147 T cell lymphoma cells at a ratio of 1:1. The T cell hybrids were selected in Dulbecco's Modified Eagle's Medium containing hypoxanthine-aminopterin-thymidine and screened for CD3 and CD4 expression. Antigen specificity was screened by activating the T hybridoma cells with appropriate antigens in the presence of APCs. Culture supernatant was collected after 24hrs stimulation to test IL-2 production by ELISA assay using paired rat monoclonal antibodies for mouse IL-2 (Biolegend).

Results

Carrier specific T cells are unable to boost Pn3P specific IgG titers

To assess the role of carbohydrate specific CD4⁺ T cells on the adaptive humoral immune response to Pn3P glycoconjugate, we performed a series of immunization experiments. We first performed primary immunizations to BALB/c mice with either KLH or Pn3P-KLH conjugate and 14 days later we performed booster immunizations with the Pn3P-KLH conjugate. On day 21, we compared Pn3P-specific IgG levels in the sera of the mice receiving primary and secondary immunizations (**Fig. 2.1A**). Mice that received the Pn3P-KLH conjugate in both primary and secondary immunizations produced high IgG titers, characteristic of a booster response. However, priming with KLH alone failed to generate a booster IgG response after the secondary immunization. If the Pn3P-KLH conjugate had induced T cell stimulation via a peptide epitope, the mice primed with either carrier alone or with the conjugate should have had comparable Pn3P IgG titers after boosting with the conjugate. We compared carrier specific IgG titers in mice immunized with conjugate versus carrier alone. KLH specific IgG levels were similar in these groups (**Fig. 2.7**). To determine whether the inability of the carrier to induce a priming response for a glycoconjugate boost is due to a lack of T-cell or B-cell priming, we immunized mice with an unconjugated mixture of Pn3P and KLH to provide T cells primed with KLH derived peptides, and B cells primed with Pn3P, and boosted these mice with the glycoconjugate (**Fig. 2.1A**). Again, priming with the mixture did not support a robust secondary antibody response to the polysaccharide upon boosting with the glycoconjugate (**Fig. 2.1A**). Regardless of whether the glycan was conjugated or not, similar Pn3P IgM levels were found in the sera of both groups of immunized mice, suggesting a similar level of B cell stimulation (**Fig.**

2.1B). Additional control groups of mice primed with no antigen (PBS) or Pn3P alone (**Fig. 2**) showed very low levels of serum IgG and IgM.

Boosting with alternate carrier protein conjugate generates high Pn3P IgG responses

In a separate immunization experiment we performed primary immunizations to groups of BALB/c mice with Pn3P-KLH and booster immunizations with a glycoconjugate containing the heterologous carrier protein, ovalbumin (OVA), to assess whether CD4⁺ T-cells specifically recognizing Pn3P epitopes help to induce the secondary humoral immune response to the glycoconjugate. Serum levels of Pn3P-specific IgG were measured after primary and secondary immunizations (**Fig. 2.2A**). Boosting of Pn3P-KLH-primed mice with Pn3P-OVA induced Pn3P-specific IgG titers consistent to those seen after priming and boosting with Pn3P-KLH or priming and boosting with Pn3P-OVA (**Fig. 2.2A**). Control groups included mice primed with Pn3P-KLH and boosted with a mixture of unconjugated Pn3P and OVA, and mice primed with Pn3P and boosted with Pn3P-OVA. Similar Pn3P IgM levels were found in the sera of all immunized mice, suggesting a similar level of B cell stimulation (**Fig. 2.2B**). In order to further confirm Pn3P specificity, we performed whole cell and competition ELISA experiments (**Fig. 2.8**). Serum IgGs bound to paraformaldehyde fixed whole Pn3 cells (WU2 strain) (**Fig. 1.3A**) whereas they failed to bind to Pn4 cells (TIGR4 strain) (data not shown). Additionally, prior incubation with soluble Pn3P inhibited IgGs from binding to the Pn3P-HSA coated plate whereas soluble Pn4P did not (**Suppl. Fig. 2.3B**). Observing a booster humoral immune response upon immunization with a heterologous carrier strongly suggests that T cell help for induction of Pn3P-specific immune responses is recruited primarily via recognition of a presented carbohydrate epitope. A key aspect of this experiment is to ensure that conjugate with OVA

carrier induces similar Pn3P IgG titers upon primary and secondary immunizations as does the conjugate with KLH carrier so alternate carrier data is comparable (**Fig. 2.2A**).

CD4⁺ T cells adoptively transferred from Pn3P-KLH immunized mice can be boosted by Pn3P-OVA in recipient mice

To directly examine the contribution of CD4⁺ T cells in the Pn3P-specific booster IgG responses, we performed an adoptive transfer experiment (**Fig. 2.3**). In this experiment groups of BALB/c donor mice were immunized with Pn3P or Pn3P-KLH. CD4⁺ T cells from each group were isolated and adoptively transferred to groups of recipient mice through tail-vein injections. Two groups of recipient mice received CD4⁺ T cells from mice immunized with Pn3P, and two groups of recipient mice received CD4⁺ T cells from mice immunized with Pn3P-KLH. All groups of recipient mice received splenic B cells obtained from Pn3P-KLH immunized mice to directly assess the functional role of CD4⁺ T cells in the polysaccharide specific IgG responses to glycoconjugate immunization. One day after receiving T and B cells, groups were immunized with Pn3P-KLH, or the glycoconjugate with alternate carrier protein, Pn3P-OVA (**Fig. 2.3A**). Titers of Pn3P specific IgG were determined in serum collected three days after immunization of recipient groups. Groups that received CD4⁺ T cells from Pn3P-KLH immunized donor mice displayed significantly higher Pn3P specific IgG titers than the groups that received CD4⁺ T cells from Pn3P immunized donor mice (**Fig. 2.3B**). Additionally, the booster IgG response in the Pn3P-KLH immunized group was comparable to the Pn3P-OVA group. Again, similar Pn3P specific IgM levels were found in the sera of all immunized mice (**Fig. 2.3C**). We then performed an opsonophagocytic killing assay to assess the functional capacity of these Pn3P specific IgGs (**Fig. 2.3D**). We observed that serum from mice that received CD4⁺ T cells from

Pn3P-KLH immunized mice demonstrated nearly complete killing of the WU2 strain, while serum from mice that received CD4⁺ T cells from Pn3P immunized mice showed minor killing activity.

In vitro stimulation of primary CD4⁺ T cells display carbohydrate specificity

To further investigate the CD4⁺ T cell responses to glycoconjugates, we isolated CD4⁺ T cells from lymph nodes of Pn3P-OVA immunized mice. These cells were stimulated *in vitro* with polysaccharide alone, the carrier protein ovalbumin, or the conjugate Pn3P-OVA in the presence of irradiated splenic APCs. T cell activation by these antigens was examined by detecting the CD69 expression by flow cytometry after 3 days of stimulation (**Fig. 2.4A-B**). A significantly higher percentage of T cells are activated by the conjugate *in vitro* than by the carrier protein or polysaccharide alone, an evidence for carbohydrate dependent recognition in this T cell population. Additionally, we looked at T cell proliferation by CFSE staining of the CD4⁺ T cells prior to *in vitro* stimulation. The T cell proliferation rate was measured by CFSE dilution after 5 days of culture (Fig. 4C-D). Again, a higher percentage of these cells proliferate upon stimulation with Pn3P-OVA conjugate compared to carrier protein alone. T cell activation was also tested by CD69 expression on CD4⁺ T cells from mice that were primed with Pn3P-OVA, and then boosted with Pn3P-KLH (**Fig. 2.4E**). We observed that *in vitro* stimulation by both conjugates activated a higher percentage of CD4⁺ T cells than their carriers alone or polysaccharide alone. Further evidence was obtained by stimulating CD4⁺ T cells from Pn3P-OVA-immunized mice with a heterologous (Pn3P-TT) conjugate compared with its carrier protein. Higher T cell activation was observed in response to the Pn3P-TT conjugate than the TT alone by measuring IL-2 production in an ELISPOT assay (**Fig. 2.9**).

Pn3P specific CD4+ T cell hybridoma generation

In order to begin assessing T cell specificity at the clonal level we generated T cell hybridomas by fusing primary CD4+ T cells from Pn3P-KLH immunized mice with BW5147 T cell lymphoma cells. After limiting dilutions, CD3+CD4+ hybridomas were then screened by incubation with Pn3P-KLH *in vitro* in the presence of irradiated APCs. Numerous T cell hybridomas were stimulated *in vitro* by Pn3P-KLH as measured by the production of Interleukin 2 (IL-2) using ELISA (**Fig. 2.5A**). Hybridomas that secreted high concentrations of IL2 compared to controls were tested for their carbohydrate specificity by incubation with Pn3P-OVA, Pn3P-KLH, and the carrier proteins alone. Four select hybridomas shown here (**Fig. 2.5B**) were consistently stimulated by glycoconjugates, no matter which carrier protein, without responding to the carriers alone, indicating a carbohydrate dependent recognition by these cells.

Discussion

Despite the availability of a glycoconjugate vaccine against *S. pneumoniae*, it remains one of the world's most deadly pathogens. The current 13-valent vaccine induces variable immune responses to each serotype and is not as effective against serotype 3, an exceptionally virulent serotype (17, 18). Studies have shown that multivalent glycoconjugate vaccines encompassing serotype 3 CPS have impaired booster responses, and fail to protect from otitis media infections from serotype 3 (19). In addition, individuals vaccinated with PCV13 require higher opsonophagocytosis assay serum titers for serotype 3 in comparison with other serotypes(20)

T cell responses described here are consistent with our previous findings(6,7) Upon immunization, a very small percentage of T cells that recognize carbohydrate epitopes are expanded. Through *in vitro* expansion, this Tcarb population could be enriched. In addition to our own studies, multiple past and present studies demonstrate the presence of Tcarb populations

recognizing carbohydrate epitopes of glycoconjugate vaccines(21-24). This work contributes to the universalization of Tcarb mediated immune responses and generalizable vaccine development strategies against bacterial pathogens. Future studies on cloning the T cell populations described here will shed light on functional properties of Tcarb populations and structural requirements for their T cell receptor engagement with carbohydrate epitopes and MHCII complexes. Further identification of Tcarb epitopes generated through processing and presentation of pneumococcal glycoconjugate vaccines by the antigen presenting cells will have direct implications in producing future knowledge-based vaccines that are target-specific, structurally designed, highly immunogenic and protective, and produced at much lower cost, thus allowing a much wider use on a global scale than current vaccines to control or eliminate invasive pneumococcal diseases (13).

References

1. Avci, F. 2013. Novel Strategies for Development of Next-Generation Glycoconjugate Vaccines. *Current Topics in Medicinal Chemistry* 13: 2535-2540.
2. Trotter, C. L., J. McVernon, M. E. Ramsay, C. G. Whitney, E. K. Mulholland, D. Goldblatt, J. Hombach, and M. P. Kieny. 2008. Optimising the use of conjugate vaccines to prevent disease caused by Haemophilus influenzae type b, Neisseria meningitidis and Streptococcus pneumoniae. *Vaccine* 26: 4434-4445.
3. Weintraub, A. 2003. Immunology of bacterial polysaccharide antigens. *Carbohydr. Res.* 338: 2539-2547.
4. Avci, F. Y., and D. L. Kasper. 2010. How Bacterial Carbohydrates Influence the Adaptive Immune System. *Annual Review of Immunology* 28: 107-130.
5. Costantino, P., R. Rappuoli, and F. Berti. 2011. The design of semi-synthetic and synthetic glycoconjugate vaccines. *Expert Opin Drug Discov* 6: 1045-1066.
6. Avci, F. Y., X. M. Li, M. Tsuji, and D. L. Kasper. 2011. A mechanism for glycoconjugate vaccine activation of the adaptive immune system and its implications for vaccine design. *Nature Medicine* 17: 1602-1610.
7. Avci, F. Y., X. M. Li, M. Tsuji, and D. L. Kasper. 2012. Isolation of carbohydrate-specific CD4(+) T cell clones from mice after stimulation by two model glycoconjugate vaccines. *Nature Protocols* 7: 2180-2192.

8. Avci, F. Y., X. M. Li, M. Tsuji, and D. L. Kasper. 2013. Carbohydrates and T cells: A sweet twosome. *Seminars in Immunology* 25: 146-151.
9. Geno, K. A., G. L. Gilbert, J. Y. Song, I. C. Skovsted, K. P. Klugman, C. Jones, H. B. Konradsen, and M. H. Nahm. 2015. Pneumococcal Capsules and Their Types: Past, Present, and Future. *Clinical Microbiology Reviews* 28: 871-899.
10. MacLeod, C. M., R. G. Hodges, M. Heidelberger, and W. G. Bernhard. 1945. Prevention of pneumococcal pneumonia by immunization with specific capsular polysaccharides. *J. Exp. Med.* 82: 445-465.
11. Torres, A., P. Bonanni, W. Hryniewicz, M. Moutschen, R. R. Reinert, and T. Welte. 2015. Pneumococcal vaccination: what have we learnt so far and what can we expect in the future? *Eur J Clin Microbiol Infect Dis* 34: 19-31.
12. Mitchison, N. A. 2004. T-cell-B-cell cooperation. *Nat Rev Immunol* 4: 308-312.
13. Huang, S. S., K. M. Johnson, G. T. Ray, P. Wroe, T. A. Lieu, M. R. Moore, E. R. Zell, J. A. Linder, C. G. Grijalva, J. P. Metlay, and J. A. Finkelstein. 2011. Healthcare utilization and cost of pneumococcal disease in the United States. *Vaccine* 29: 3398-3412.
14. Demczuk, W. H., I. Martin, A. Griffith, B. Lefebvre, A. McGeer, M. Lovgren, G. J. Tyrrell, S. Desai, L. Sherrard, H. Adam, M. Gilmour, G. G. Zhanel, N. Toronto Bacterial Diseases, and N. Canadian Public Health Laboratory. 2013. Serotype distribution of invasive *Streptococcus pneumoniae* in Canada after the introduction of the 13-valent pneumococcal conjugate vaccine, 2010-2012. *Can J Microbiol* 59: 778-788.
15. Burton, R. L., and M. H. Nahm. 2012. Development of a fourfold multiplexed opsonophagocytosis assay for pneumococcal antibodies against additional serotypes and

- discovery of serological subtypes in *Streptococcus pneumoniae* serotype 20. *Clin Vaccine Immunol* 19: 835-841.
16. Nandakumar, S., S. Kannanganat, K. M. Dobos, M. Lucas, J. S. Spencer, S. Fang, M. A. McDonald, J. Pohl, K. Birkness, V. Chamcha, M. V. Ramirez, B. B. Plikaytis, J. E. Posey, R. R. Amara, and S. B. Sable. 2013. O-mannosylation of the Mycobacterium tuberculosis adhesin Apa is crucial for T cell antigenicity during infection but is expendable for protection. *PLoS Pathog* 9: e1003705.
 17. Dagan, R., S. Patterson, C. Juergens, D. Greenberg, N. Givon-Lavi, N. Porat, A. Gurtman, W. C. Gruber, and D. A. Scott. 2013. Comparative immunogenicity and efficacy of 13-valent and 7-valent pneumococcal conjugate vaccines in reducing nasopharyngeal colonization: a randomized double-blind trial. *Clin Infect Dis* 57: 952-962.
 18. Gruber, W. C., D. A. Scott, and E. A. Emini. 2012. Development and clinical evaluation of Prevnar 13, a 13-valent pneumococcal CRM197 conjugate vaccine. *Ann N Y Acad Sci* 1263: 15-26.
 19. Hausdorff, W. P., R. Dagan, F. Beckers, and L. Schuerman. 2009. Estimating the direct impact of new conjugate vaccines against invasive pneumococcal disease. *Vaccine* 27: 7257-7269.
 20. Kieninger, D. M., K. Kueper, K. Steul, C. Juergens, N. Ahlers, S. Baker, K. U. Jansen, C. Devlin, W. C. Gruber, E. A. Emini, D. A. Scott, and s. group. 2010. Safety, tolerability, and immunologic noninferiority of a 13-valent pneumococcal conjugate vaccine compared to a 7-valent pneumococcal conjugate vaccine given with routine pediatric vaccinations in Germany. *Vaccine* 28: 4192-4203.

21. Polonskaya, Z., S. Deng, A. Sarkar, L. Kain, M. Comellas-Aragones, C. S. McKay, K. Kaczanowska, M. Holt, R. McBride, V. Palomo, K. M. Self, S. Taylor, A. Irimia, S. R. Mehta, J. M. Dan, M. Brigger, S. Crotty, S. P. Schoenberger, J. C. Paulson, I. A. Wilson, P. B. Savage, M. G. Finn, and L. Teyton. 2017. T cells control the generation of nanomolar-affinity anti-glycan antibodies. *J Clin Invest* 127: 1491-1504.
22. Sun, L., D. R. Middleton, P. L. Wantuch, A. Ozdilek, and F. Y. Avci. 2016. Carbohydrates as T-cell antigens with implications in health and disease. *Glycobiology*.
23. Lai, Z., and J. R. Schreiber. 2009. Antigen processing of glycoconjugate vaccines; the polysaccharide portion of the pneumococcal CRM(197) conjugate vaccine co-localizes with MHC II on the antigen processing cell surface. *Vaccine* 27: 3137-3144.
24. Muthukkumar, S., and K. E. Stein. 2004. Immunization with meningococcal polysaccharide-tetanus toxoid conjugate induces polysaccharide-reactive T cells in mice. *Vaccine* 22: 1290-1299.

Figure 2.1

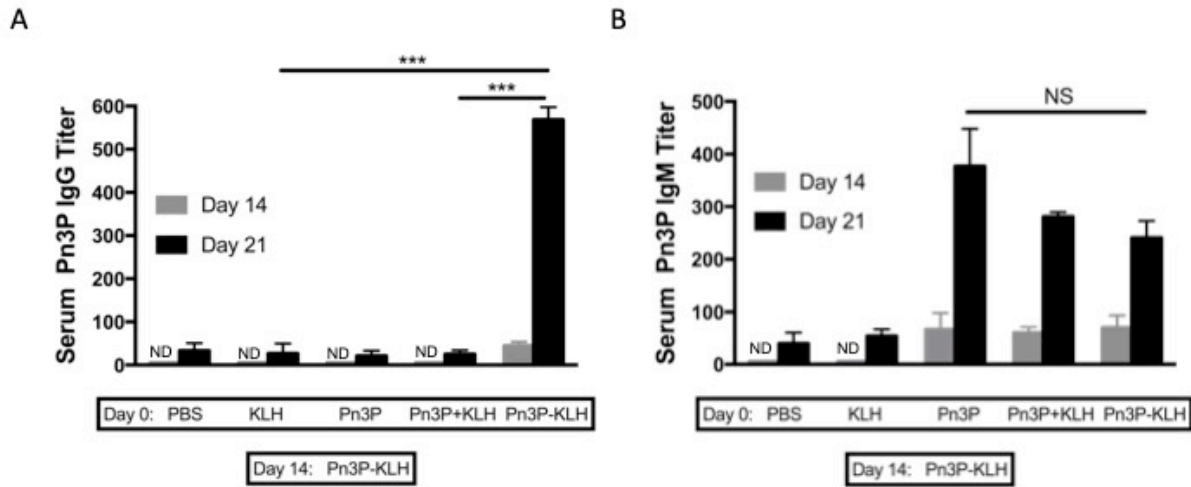


Figure 2.1. Conjugate Immunizations. Pn3P IgG (A) and IgM (B) titers in BALB/c mice primed (day 0) and boosted (day 14) with different antigen combinations, as measured by ELISA in serum obtained on day 14 (pre-boost) and 21. n=4/group. Serum titers are reported as the reciprocal dilution that results in an OD of 0.5 at 405nm. Statistical significance was determined with the two-tailed student's t-test. P<0.001. NS=not significant. ND=not detectable.

Figure 2.2

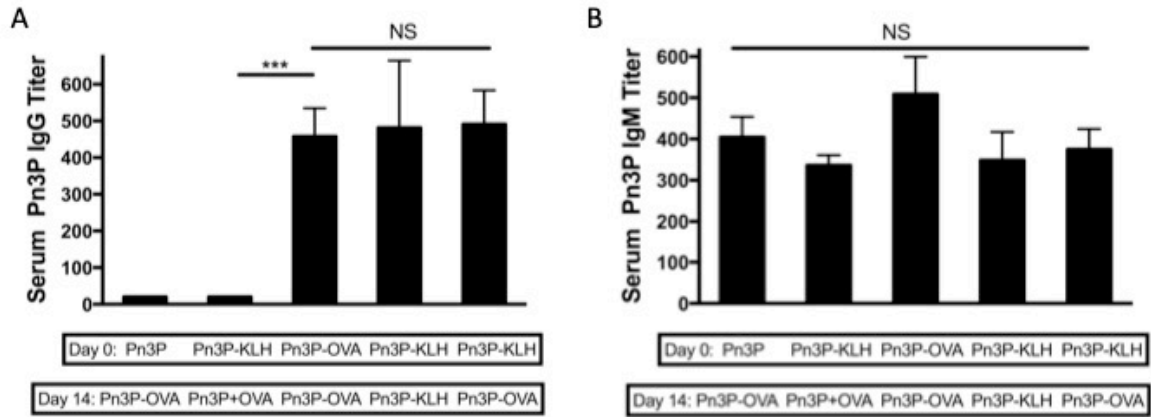


Figure 2.2. Heterologous carrier immunizations. Pn3P IgG (A) and IgM (B) titers in BALB/c mice primed (day 0) and boosted (day 14) with different antigen combinations, as measured by ELISA in serum obtained on day 21. n=4/group. Serum titers are reported as the reciprocal dilution that results in an OD of 0.5 at 405nm. Statistical significance was determined with the two-tailed student's t-test. P<0.001. NS=not significant

Figure 2.3

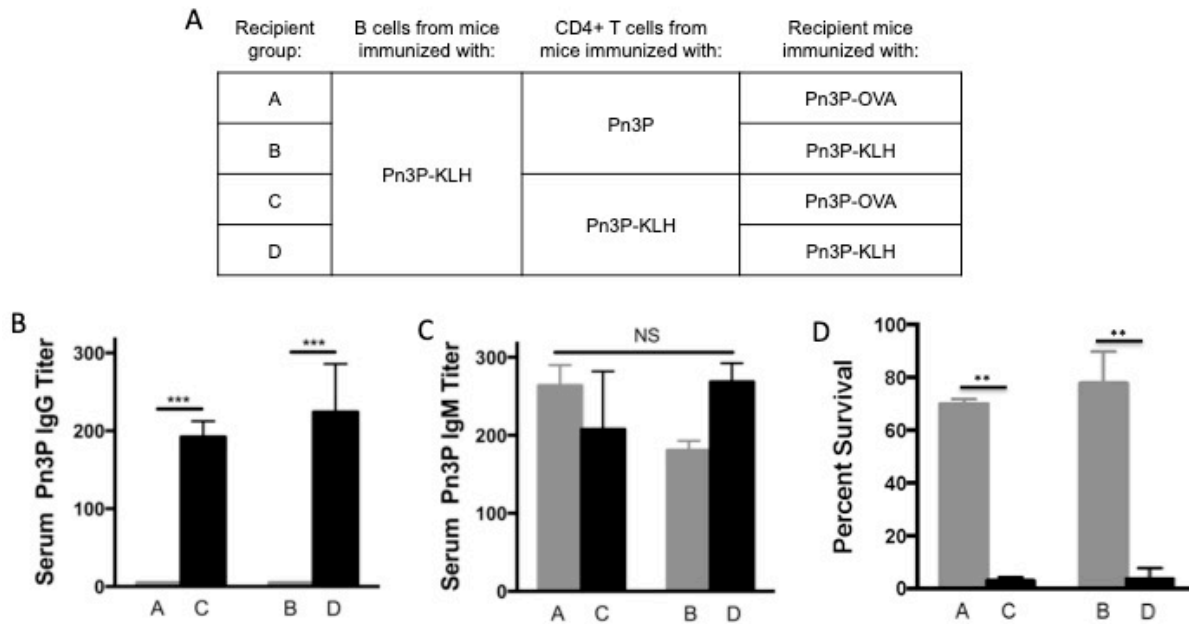


Figure 2.3. CD4+ T cells adoptively transferred from donor mice immunized with Pn3P-KLH provides the T cell help for Pn3P-specific secondary immune responses in the recipient mice upon their immunization with Pn3P-OVA (A). Pn3P IgG (B) and IgM (C) titers in BALB/c mice that received CD4+ T cells and B cells from immunized donor mice and were immunized with Pn3P-KLH or Pn3P-OVA (day 0), as measured by ELISA in serum obtained on day 3. n=4/group. Serum titers are reported as the reciprocal dilution that results in an OD of 0.5 at 405nm. Functional test of Pn3P specific antibodies in serum using opsonophagocytic killing assay (D) Statistical significance was determined with the two-tailed student's t-test. *** P<0.001. NS= not significant

Figure 2.4

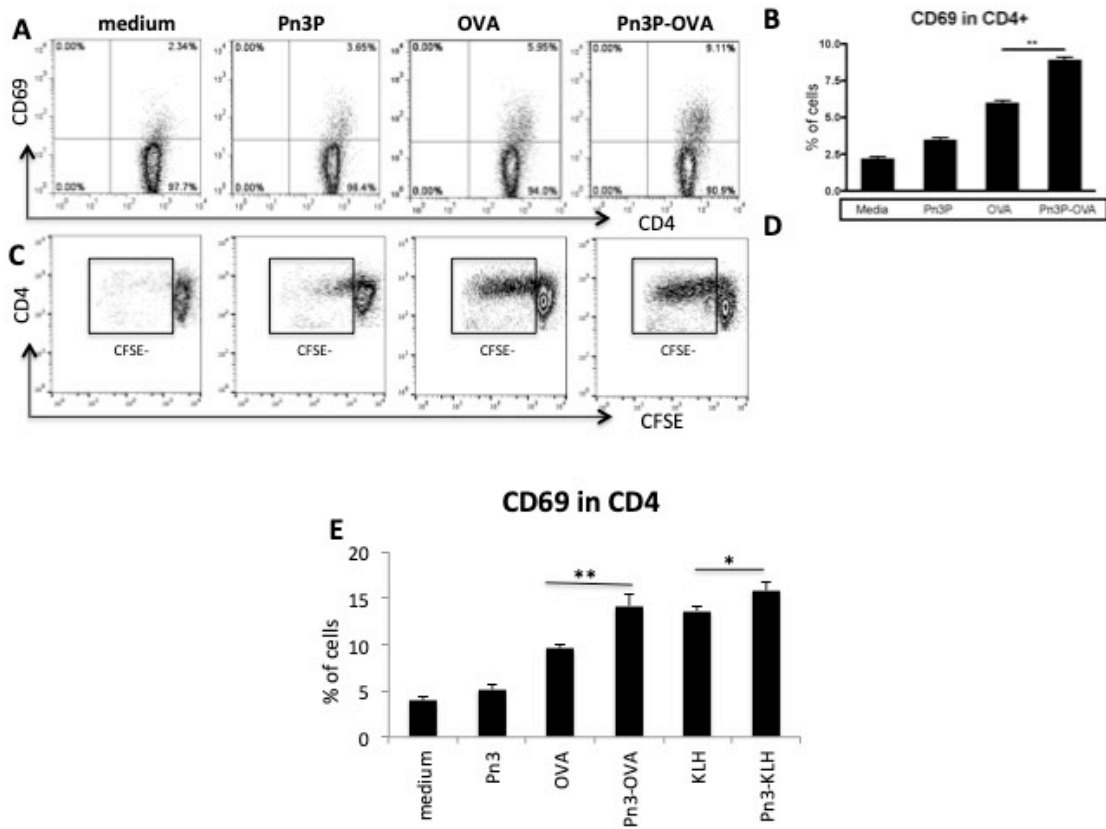


Figure 2.4. Evidence for Pn3P specific CD4⁺ T cell response after Pn3P conjugates immunization. (A-D) CD4⁺ T cells were isolated from lymph nodes of Pn3P-OVA immunized mice and stimulated *in vitro* in the presence of irradiated APCs (CD3 depleted mouse splenic mononuclear cells) pulsed with indicated antigens. T cell activation and proliferation were detected by flow cytometry. Representative FACS profiles (A) and the percentile (B) of CD69 expression on CD4⁺ T cells after 3 days stimulation were shown. (C, D) CD4⁺ T cells were labeled with CFSE fluorescence before culture. CFSE dilution as T cell proliferation rate was measured after 5 days stimulation. (E) The response of CD4⁺ T cells from Pn3P-OVA primed and Pn3P-KLH boosted mice to indicate Pn3P conjugates or carrier proteins were detected as mentioned above. Representative results are shown from one of three independent experiments performed. Data were shown as mean+SD. *P<0.05, **P<0.01, ***P<0.001.

Figure 2.5

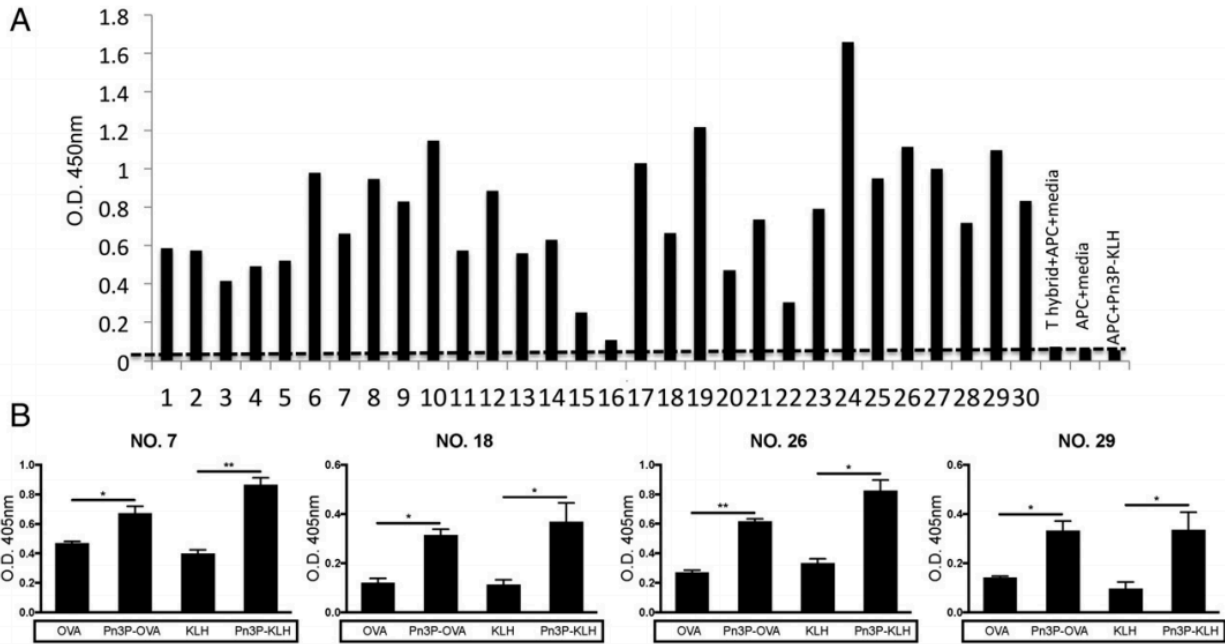


Figure 2.5. Generation of Pn3P specific CD4⁺ T cell hybridomas. Pn3P conjugate specific T cell hybridomas were generated by fusion of primary CD4⁺ T cells isolated from Pn3P-KLH immunized mice with BW5147 T cell lymphoma cells. T hybridoma cell lines positive for both CD3 and CD4 expression were selected to investigate their response to Pn3P-KLH antigen. (A) Antigen specificity of T hybridoma cell lines was determined by their ability to produce IL-2 using ELISA assays in the presence of irradiated APCs and Pn3P-KLH antigen. T hybridoma cell lines with higher IL-2 level than control groups were selected out for fine specificity of antigen recognition. (B) Four representative CD4⁺ T hybridoma cell lines were selected and tested their ability to produce IL-2 using ELISA assays in the presence of APCs pulsed with Pn3P conjugates or carrier proteins.

Figure 2.6

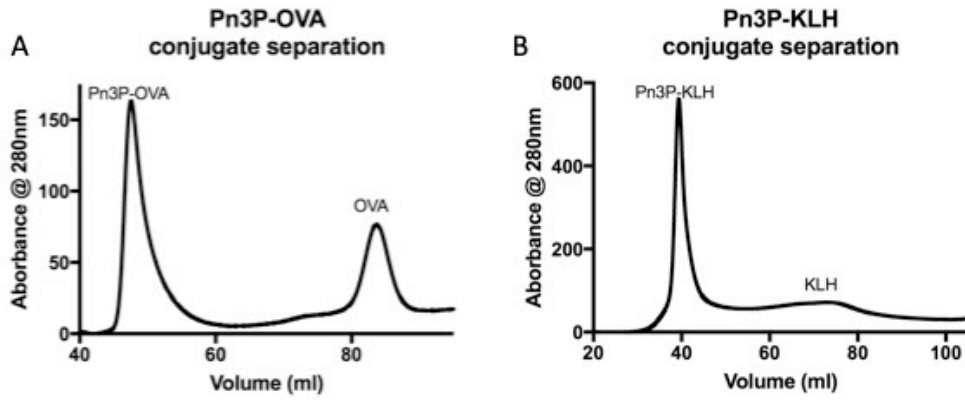


Figure 2.6. Purification of Glycoconjugates A) Superdex 200 (OVA) and B) Sephacryl 300 (KLH) elution profiles of glycoconjugates. Conjugates fractions were collected, desalted, and lyophilized for long-term storage.

Figure 2.7

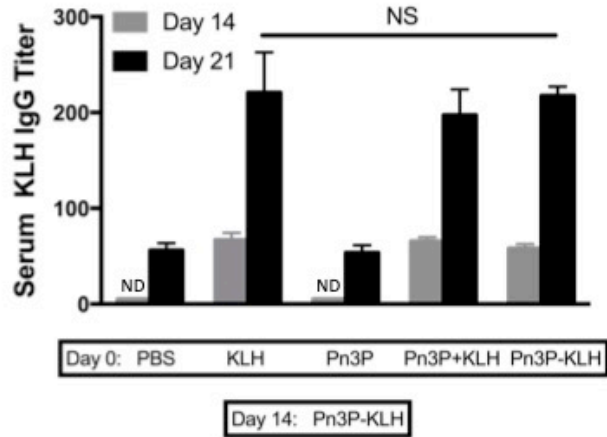


Figure 2.7. Conjugate Immunizations. KLH IgG titers in BALB/c mice primed (day 0) and boosted (day 14) with different antigen combinations, as measured by ELISA in serum obtained on day 14 (pre-boost) and 21. n=4/group. Serum titers are reported as the reciprocal dilution that results in an OD of 0.5 at 405nm. ND=Not Detected. Statistical significance was determined with the two-tailed student's t-test.

Figure 2.8

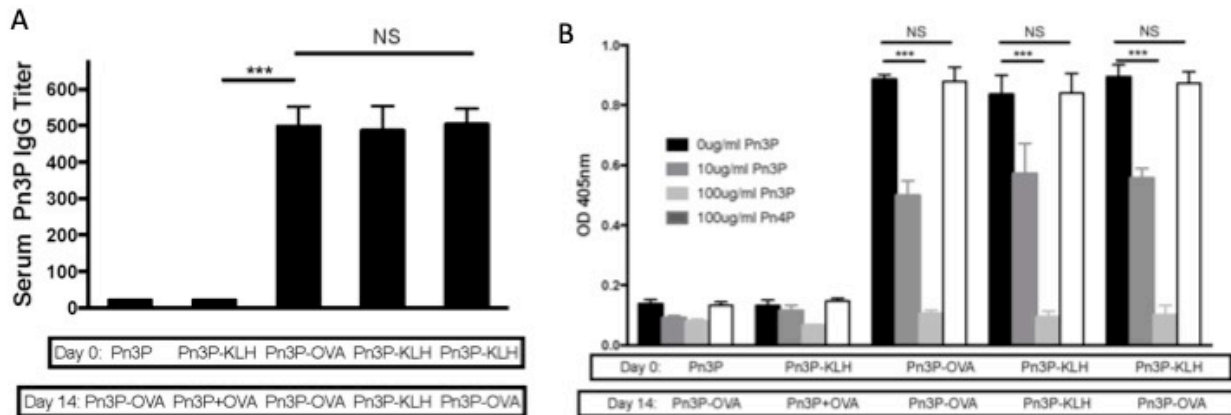


Figure 2.8. Heterologous carrier immunizations. (A) Whole fixed Pn3 cell ELISA detecting Pn3P IgG titers in BALB/c mice primed (day 0) and boosted (day 14) with different antigen combinations, as measured by ELISA in serum obtained on day 21. n=4/group. Serum titers are reported as the reciprocal dilution that results in an OD of 0.5 at 405nm. (B) Competition experiment using increasing doses of soluble Pn3P to compete for Pn3P specific IgGs in BALB/c mice primed (day 0) and boosted (day 14) with different antigen combinations, as measured by ELISA in serum obtained on day 21. Statistical significance was determined with the two-tailed student's t-test. P<0.001. NS=not significant

Figure 2.9

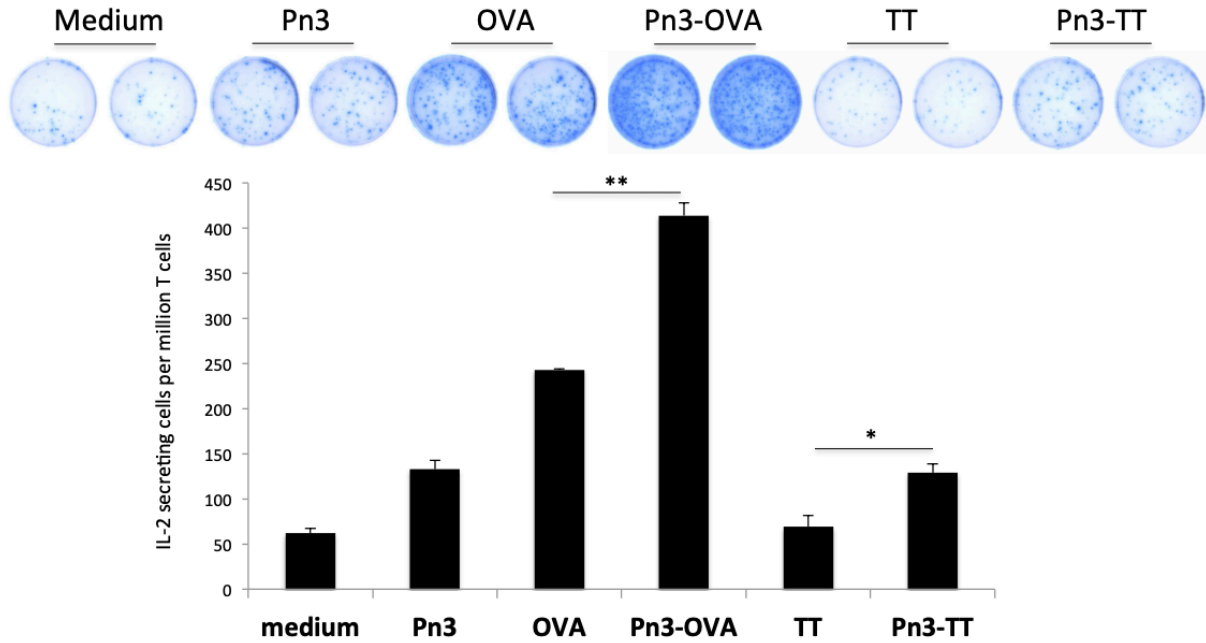


Figure 2.9. Presence of CD4⁺ T cells that recognize Pn3P epitopes after Pn3P-OVA immunization. CD4⁺ T cells were isolated from lymph nodes of Pn3P-OVA immunized mice and stimulated *in vitro* in the presence of irradiated APCs pulsed with Pn3P, homologous (Pn3P-OVA) or heterologous (Pn3P-TT) conjugates and carrier proteins. IL-2 production was detected by ELISPOT assay. Representative results are shown from one of three independent experiments performed. Data were shown as mean±SD. *P<0.05, **P<0.01, ***P<0.001

CHAPTER 3

IDENTIFICATION AND CHARACTERIZATION OF THE *STREPTOCOCCUS*
PNEUMONIAE TYPE 3 CAPSULE-SPECIFIC GLYCOSIDE HYDROLASE OF
PAENIBACILLUS SPECIES 32352

Dustin R Middleton, Xing Zhang, Paeton L. Wantuch, Ahmet Ozdilek, Xinyue Liu, Rachel
Lopilato, Nikhil Gangasani, Robert Bridger, Lance Wells, Robert J. Linhardt, and Fikri Y. Avci

Accepted by *Glycobiology*. Reprinted here with permission of publisher.

Abstract

Bacillus circulans Jordan 32352 was isolated from decaying organic matter in the New Jersey soil in the early 1930s. This soil-dwelling bacterium produced an enzyme capable of degrading the type 3 capsular polysaccharide (Pn3P) of *Streptococcus pneumoniae* (Spn). Early reports of this enzyme, Pn3Pase, demonstrated its inducibility by, and specificity for Pn3P. We set out to identify and clone this enzyme for its recombinant expression and characterization. We first sequenced the genome of this bacterial species, and reclassified the Pn3Pase producing bacterium as *Paenibacillus species* 32352. We identified the putative protein of Pn3Pase through mass spectrometry-based proteomics and cloned the gene for recombinant expression. We then characterized the oligosaccharide products generated upon the enzymatic depolymerization of Pn3P. Sequence analysis suggests that this glycoside hydrolase (GH) belongs to a new Carbohydrate-Active enzyme (CAZy) GH family. To our knowledge, this is the only enzyme to demonstrate Pn3P depolymerization activity.

Introduction

In 1930, Avery and Dubos isolated an organism from soil taken from cranberry bogs, which was capable of depolymerizing type 3 capsular polysaccharide of *Streptococcus pneumoniae* (Pn3P), a linear polymer of $-3)\beta\text{GlcA}(1-4)\beta\text{Glc}(1-$ (1, 2). The expression of this enzyme (Pn3Pase) was inducible in the presence of Pn3P, and the bacterium was able to grow with Pn3P as the sole carbon source. They described this bacterium as a sporulating, gram-negative, aerobic bacillus with peritrichous flagella. A few years later, Sickles and Shaw isolated two additional similar strains demonstrating the same enzymatic activity targeting Pn3P (3, 4). These strains were designated as *Bacillus palustris*, before being accepted as synonymous to *Bacillus circulans* (4-6). Besides Pn3Pase, these strains demonstrated the ability to produce enzymes capable of depolymerizing *S. pneumoniae* capsular serotypes 2 and 8, although soluble protein in cell free extracts were inactive against these polysaccharides (3, 7). There are numerous possible practical applications for these strains and enzymes. For example, investigators have applied the Sickles and Shaw Pn3Pase enzyme while examining Pn3P biosynthesis as well as its immunological properties (8-11).

We obtained the '*Bacillus circulans* Jordan strain 32352' (i.e., the Sickles and Shaw strain) from American Type Culture Collection, and sequenced its genome (12). 16S rRNA analysis revealed that this bacterium belonged in the *Paenibacillae* genus, and it is now identified as *Paenibacillus sp.* 32352 (Pbac). *Paenibacillus* species are of growing interest since the genus was established in 1991 (13). These microbes are a rich source of extracellular enzymes that catalyze a variety of reactions, which have demonstrated utility in numerous agricultural and medical applications (14-19). Database for carbohydrate-active enzyme annotation (dbCAN) of the *Paenibacillus sp.* 32352 genome indicates 665 carbohydrate active

entries out of 7200 predicted genes, 252 of those exhibiting glycoside hydrolase- or polysaccharide lyase- like architecture (20).

We set out to determine the identity of the gene producing Pn3Pase in order to express, utilize, and study the enzyme's unique Pn3P-specific activity. Here, we have identified the *Paenibacillus* Pn3Pase through proteomics of culture supernatant preparations with Pn3P supplemented minimal media growth. We have cloned the Pn3Pase gene and expressed the active enzyme in *E. coli*. We have also identified kinetic parameters, characterized oligosaccharide products, and determined optimal conditions for Pn3P depolymerization by Pn3Pase.

Results

Pn3P utilization induces expression of genes organized into locus

We began by culturing Pbac in minimal M9 media with either 2% glucose or Pn3P as the sole carbon source. Pbac growth was monitored by OD 600 nm for 14 h to achieve maximum Pn3Pase production, (**Figure 3.1A**). Pbac was able to grow and utilize Pn3P and glucose, but was unable to utilize cellulose. Supernatants from these cultures were concentrated 20×, and proteins were visualized by coomassie staining. In the Pn3P growth conditions a prominent band ~55 kDa was observed (**Figure 3.1B**). Proteomic analysis of these samples by LC-MS/MS identified numerous proteins that were present in both samples. Two proteins, however, were significantly enriched in the Pn3P growth condition as highlighted in **Table 3.1**.

These two Pn3P induced Pbac proteins appear to be organized into a locus of Pn3P utilization (**Figure 3.1C**) consisting of ABC-type polysaccharide transport system, permease

component (Pbac_3556), probable ABC transporter permease protein ytcP (Pbac_3555), lipoprotein (Pbac_3554), DNA-binding response regulator, AraC family (Pbac_3553), multidomain protein with a surface-layer homology region and immunoglobulin-like motif (Pbac_3552), and a hypothetical protein (Pbac_3551). Since two of these proteins are more abundant in the Pn3P growth conditions, we compared the transcription of three genes of this locus with the commonly expressed surface layer protein (Pbac_1521) in the glucose and Pn3P samples by RT-PCR. The transcription of genes 3551, 3552, and 3554 increase ~130-fold with Pn3P utilization, while mRNA expression of Pbac_1521 is unchanged between the two growth conditions (**Figure 3.1D**). The only major difference observed at the protein level, based on coomassie stain (**Figure 3.1B**) of the culture supernatant of Pn3P induced culture, is the dominant Pbac_3554 product. The sensitivity provided by mass spectrometry allowed us to identify Pbac_3551 in the supernatant as well, although at low abundance. While transcript levels are increased dramatically for all genes that were tested in this locus, some of these proteins may be more closely associated with the cell surface and not efficiently shed similarly to Pbac_3554.

Pn3Pase identification and domain analysis

Pbac_3554, Pbac_3552, and Pbac_3551 were cloned and expressed in *E. coli* BL21 (DE3) cells to determine which upregulated gene product was responsible for Pn3P depolymerase activity. The hypothetical protein Pbac_3551 (Accession WP_079915027), with primary sequence shown in **Figure 3.2A** was expressed and purified by immobilized metal affinity chromatography (**Figure 3.2B**). Initial preparations have yielded ~2.5mg/L of BL21 culture. Pbac_3551 (hypothetical protein) demonstrated rapid and efficient hydrolysis of tritium

radio-isotope labeled Pn3P, as shown by counts per min shift to lower molecular weight oligosaccharides when reaction products were separated by size exclusion chromatography (**Figure 3.2C**). Reactions of recombinant Pn3Pase with unlabeled Pn3P were performed, spotted on a PVDF membrane, and probed with a Pn3P monoclonal antibody. Reactivity to the monoclonal antibody was completely abolished after 4 h Pn3Pase treatment of Pn3P (**Figure 3.2D**).

The translated protein sequence of Pbac_3551 consists of 1,545 amino acids. Predicted cleavage of the signal peptide by SignalP 4.1 server (21) from residues 1-40 would yield a mature protein of 164.1 kDa. Protein sequence analysis and classification by InterPro online software (22) recognized homology to glycoside hydrolase, family 39 (GH39) at the N-terminus, most similar to the β -xylosidase from *Thermoanaerobacterium saccharolyticum* (beta/alpha)₈ barrel region (23). Other regions related to galactose-binding domain-like related to carbohydrate-binding module, family 6 (CBM6) from 621-765, a domain of unknown function DUF1080 from 781-950 with structural similarity to an endo-1,3-1,4-beta glucanase belonging to glycoside hydrolase, family 16 (GH16), and a concanavalin A-like lectin/glucanase domain from 1,209-1,348 (**Figure 3.2E**) were found. Based on carbohydrate active enzyme (CAZy) database, although segments of this enzyme display some homology to numerous carbohydrate active proteins, no overall homology to known glycoside hydrolase families across the length of the enzyme exist (data not shown). This unique enzyme will potentially be sorted into a new dedicated glycoside hydrolase family related to clan GH-A. Clan GH-A are retaining enzymes with a catalytic domain displaying a (beta/alpha)₈ barrel fold (24).

Characterization of oligosaccharide products

The oligosaccharide products of Pn3Pase hydrolysis were separated by size exclusion chromatography. This hydrolysis yielded two major product peaks eluting late in the Superdex peptide column corresponding to a tetrasaccharide and hexasaccharide (**Figures 3.3A-C**). The identities of these peaks were confirmed as tetrasaccharide (**Figure 3.3B**) and hexasaccharide (**Figure 3.3C**) by electrospray ionization mass spectrometry. Mass spectrometry data is summarized in **Table 3.2**.

The characterization of oligosaccharide products by NMR spectroscopy is presented in **Figure 3.4**. All anomeric proton signals are assigned in representative ^1H NMR spectra of tetra- and hexa- saccharides (**Figure 3.4**). Anomeric proton signals of residue **A**, **C** and **E** at ~ 4.70 ppm were overlapped with HOD peak (**Figures 3.4A, 4D**) but showed up in 2D HSQC spectrum (**Figures 3.4B, E**). The $^3J_{HH}$ coupling constants of B-1 and D-1 were 8.22 Hz, demonstrating β -linkages. The signals at 5.15 ($^3J_{HH} = 3.69$) and 4.58 ($^3J_{HH} = 8.05$) ppm correspond to α - and β -configuration of GlcA residue **F**, respectively. By combining HSQC and COSY experiments (**Figures 3.4C, F**), we were able to identify that proton signal of F-5 possessed a high chemical shift (~ 4.05 ppm) suggesting that GlcA residue (**F**) was at the reducing end of the carbohydrate chain. These data demonstrate that Pn3Pase cleaves the $\beta(1-4)$ linkage between glucuronic acid and glucose in the polysaccharide chain.

Pn3Pase activity analysis

A time course experiment was performed using tritiated Pn3P and the recombinant Pn3Pase to understand whether this enzymatic degradation proceeds through endolytic or exolytic cleavage. Reaction products were separated by size exclusion chromatography after

proceeding for the given time. Low molecular weight oligosaccharides are generated early on in the reaction (**Figure 3.5A**). Both an increase in CPM for the oligosaccharide elution volume, and corresponding decrease in CPM for the higher molecular weight polymer over time suggest an exolytic type cleavage (**Figure 3.5A**) that preferentially generates tetrasaccharides and hexasaccharides (**Figure 3.3A**). A gradual shift of the peak from left to right over time would be indicative of true random endolytic cleavage.

Two-hour reactions were performed in three different buffers at pH 6.0, 7.2, and 8.0, detecting the concentration of reducing end glucuronic acid by the p-hydroxybenzoic acid hydrazide (PAHBAH) method (25) to determine the optimum reaction conditions for Pn3Pase. Pn3Pase displays slightly better activity in sodium phosphate buffer at pH 7.2 than in MES buffer pH 6.0, but performs significantly worse in Tris buffer at pH 8.0 (**Figure 3.5B**). Further optimization focusing on metal-ion dependence was performed with Mg^{2+} and Ca^{2+} in Tris-HCl pH 7.4. Pn3Pase displays a concentration-dependent increase in activity with addition of Ca^{2+} or Mg^{2+} , as it produces a higher concentration of reducing end GlcA in presence of 10 mM of these divalent cations (**Figure 3.5C**). Surprisingly, Pn3Pase activity is minimal at 23°C, optimal at 30°C, and slightly less than optimal at 37°C, the temperature at which all other experiments are carried out (**Figure 3.5D**). Our initial kinetic analyses determined the K_m and V_{max} to be 108.4 μ g/mL and 24.82 μ moles/min/mg respectively.

Discussion

The *Paenibacillus* genus, literal Latin translation, “almost *Bacillus*,” was ruled distinct from true *Bacillus* species when phylogenetic analysis on 16S rRNA gene sequences was performed for a number of strains previously defined as *Bacillus* (6). Sequence analysis showed

that several bacterial strains sorted into this genus, required reassignment. Species belonging to this genus have been obtained from diverse ecological niches (26) from aquatic (27) to desert environments (28), and from hot springs (29) to extreme cold regions (30). Many *Paenibacillus* species are found in soil (3, 31) and plant root environments (32), however, a number are isolated from human samples as well (33). *Paenibacillus* species are a rich source for a variety of agricultural, biomedical, and industrial products (26). Extracellular enzymes demonstrating numerous activities (34) have applications in production of a variety of industrially significant materials (26). A number of these species are efficient nitrogen fixers that have been applied agriculturally to promote crop growth (35). In addition, protective action of novel antimicrobial peptides and compounds obtained from *Paenibacilli* has been demonstrated (36).

While *Paenibacillus sp.* 32352 was isolated from a soil source (3), it is appropriate to question the evolutionary pressure to obtain enzymes capable of acting on a human pathogen Spn CPS. Based on earlier studies, this particular strain demonstrates the ability to degrade three distinct pneumococcal CPSs (3, 9). Whether these are the natural substrates for the enzymes, or whether other soil dwelling microbes or plant matter possess similar glycan residues and linkages remains to be investigated.

However originally acquired, *Paenibacillus sp.* 32352 has adapted the Pn3Pase described here to play an important functional role in its metabolism. Early reports by Torriani and Pappenheimer on this species indicated the ability to induce Pn3Pase activity in culture supernatant by addition of Pn3P in the growth medium (7). The “inducibility” was in contrast to the Avery and Dubos findings that Pn3Pase formation only occurred in conditions where Pn3P is present as a sole carbon source(2). Here, we demonstrate that while Pn3P is not required for

bacterial growth, it can serve as the sole nutrition source. Moreover, our data indicate that presence of Pn3P in the Pbac culture medium induces the expression of Pn3Pase.

Our attempts to purify multi-milligram quantities of active, native Pn3Pase from an induced culture of this strain were unsuccessful, though Pn3P depolymerizing activity can be detected in these culture supernatant preparations. In this study, we have identified and cloned the Pn3Pase gene from *Paenibacillus sp.* 32352. We have fully characterized the oligosaccharide products. Kinetic values found in this manuscript will serve as initial parameters towards future structure-activity relationship studies of this enzyme. Future structural studies will determine factors of substrate specificity, active site residues, and catalytic mechanism of this unique glycoside hydrolase. In addition, future experiments will assess this enzyme's utility as a treatment for serotype 3 Spn infections by stripping the capsular polysaccharide (CPS) from the bacterial surface. The capsular polysaccharide is a major virulence factor for type 3 strains, as non-encapsulated mutants fail to colonize (37). The virulence mechanisms of CPS is to help Spn evade the immune system through resisting or inhibiting its phagocytosis by host macrophages while also limiting mucus-mediated clearance (38). The Pn3P component of the current 13-valent vaccine (PCV13) induces variable immune responses to serotype 3 (39, 40). Individuals vaccinated with PCV13 require higher opsonophagocytosis assay serum titers for serotype 3 in comparison with other serotypes (41). Despite current vaccination programs against Spn, it remains one of the world's most lethal pathogens. Inefficiencies in current vaccination and antibiotic administration necessitate the discovery of alternative therapeutic approaches for controlling these and other encapsulated pathogens.

Materials and methods

Bacterial strains and growth conditions

Paenibacillus sp. 32352 (ATCC 14175) was cultured aerobically with shaking at 37°C on Tryptic Soy Agar with 5% sheep blood (Hardy Diagnostics), or in minimal medium (M9 Teknoba) culture containing 1 mM MgSO₄, 1 mM biotin, 1mM thiamin, and 2% glucose (Sigma Aldrich) or Pn3P powder (ATCC 172-X) as sole carbon source. *Streptococcus pneumoniae* type 3 (WU2 strain) and acapsular derivative (JD908), generous gifts from Moon Nahm (University of Alabama at Birmingham), were cultured aerobically without shaking at 37 °C on Tryptic Soy Agar with 5% sheep blood (TSAB), or in Todd Hewitt Broth plus 0.5% yeast extract (THY) (BD Biosciences).

Proteomics of culture supernatants

Paenibacillus sp. 32352 was cultured in 5 ml of minimal medium M9 containing 2% (w/v) carbon source, as described above. Bacterial cultures were harvested at mid-log phase (OD_{600nm} 0.6). Culture supernatants were passed through a 0.45 µm syringe filter and concentrated to 1/20th culture volume using a microsep advance centrifugal device with 10K molecular weight cutoff (Pall). Protein concentration was determined by bicinchoninic acid assay. An in-solution trypsin digestion was performed as described previously (42). Briefly, 20 mg protein from culture supernatant protein was reduced by incubation with 10 mM DTT for 1 h at 56 °C, followed by carboxyamidomethylation with 55 mM iodoacetamide in the dark at room temperature for 45 min, and then digested with 1 mg of sequencing grade trypsin (Promega) in 40 mM ammonium bicarbonate overnight at 37 °C. Trypsin digest was stopped with 1% trifluoroacetic acid and incubation on ice for 30 min. The resulting peptides were cleaned up using C18 spin columns (G Biosciences), dried down, and reconstituted in 0.1% formic acid. The

peptides were analyzed on a Orbitrap Fusion Tribrid mass spectrometer (Thermo Fisher Scientific) interfaced with an UltiMate 3000 RSLCnano HPLC system (Thermo Fisher Scientific). Peptides were resolved on an Acclaim™ PepMap™ RSLC C18 column (75 µm ID x 15 cm; 2 µm particle size) at a flow rate of 200 nL/min using a linear gradient of 1-100% solvent B (0.1% formic acid in 80% acetonitrile) over 60 min and a total run time of 90 min. Data-dependent acquisition was carried out using the Orbitrap mass analyzer collecting full scans of 200-2000 m/z range at 60,000 mass resolution. Most intense precursor ions were selected using top speed mode with a maximum cycle time of 3 s. Precursor ions with charge state 2-5 were selected with dynamic exclusion set to exclude precursors for 20 s following a third selection within 10 s. Selected precursors were fragmented using collision-induced dissociation (CID) set to 38%, and resulting MS/MS ions were scanned out in the ion trap. The raw MS/MS spectra were searched against the Rapid Annotation Server(43) (RAST) annotated genome database for *Paenibacillus sp.* 32352 using SEQUEST HT in Proteome Discoverer 1.4 (Thermo Fisher Scientific) with precursor mass tolerance of 10 ppm and fragment tolerance of 0.3 Da. Static modification of +57.021 Da (carbamidomethylation of cysteine residues), and dynamic modification of +15.995 Da (oxidation of methionine residues) were allowed in the search parameters. Results were filtered at a 1% false discovery rate for peptide assignments.

Gene expression

Comparison of the levels of transcript expression from the Pn3P induced locus was performed by RT-PCR. *Paenibacillus sp.* 32352 was cultured in 5 ml of minimal medium containing 2% (w/v) carbon source, as described above. Triplicate bacterial cultures were harvested at mid-log phase (OD 600 nm 0.6), RNA was purified using E.N.Z.A. Bacterial RNA

Kit, followed by TRIzol (Thermo Fisher Scientific) extraction of RNA from contaminating genomic DNA as described previously (44). RNA purity was assessed with nanodrop, and 1 µg of RNA was used for reverse transcription reaction using iscript CDNA synthesis kit (BioRad). Quantitative real time-PCR was performed in a 96-well plate on a MyiQ system (BioRad) with iQ SYBR green mastermix. Primers used in RT-PCR are listed in **Table 3.3**. The reactions were carried out in 20 µl, consisting of 10 µl of SYBR Green mix, 20 ng of cDNA, and 1 µM primer mix. The reaction conditions were 95 °C 180 s, followed by 45 cycles of 95 °C for 10 s, 55 °C for 20 s, and 72 °C for 30 s. The data were normalized to 16S rRNA transcript levels, and changes in expression level were calculated as fold change compared with cultures of minimal medium with glucose supplement.

Production of recombinant Pn3Pase

The coding region of Pbac_3551 (ref seq WP_079915027), Pbac_3552 (ref seq WP_079915028), and Pbac_3554 (ref seq WP_079915030.1) (minus predicted signal peptide and stop codon) were amplified from *Paenibacillus sp.* 32352 genomic DNA (DNeasy blood and tissue kit, Qiagen) using 2× platinum superfi mastermix (Thermo Fisher Scientific) with overhang containing B-sites to facilitate gateway cloning (45) via BP reaction (Thermo Fisher Scientific) into pDONR221. Primers for cloning are listed in **Table 3.3**. After DH5α transformation and DNA sequence confirmation, an LR-clonase reaction was performed to insert the gene into the pET-DEST42 (Thermo Fisher Scientific) destination vector for the expression of a carboxy-terminal His₆-tagged fusion protein in *E. coli* BL21(DE3) cells. BL21(DE3) cells transformed with the pET-DEST42-“Pn3Pase” plasmid were grown in LB medium supplemented with 100 µg/ml ampicillin at 37 °C, and cell density was monitored by absorbance at 600 nm. Once the OD 600 nm reached 0.6, the cells were transferred into 25 °C, protein

expression was induced by the addition of Isopropyl β -D-1-thiogalactopyranoside to a final concentration of 1 mM and the cell culture was allowed to incubate for 8 h (until A_{600} reached ~ 1.1). Cells were harvested by centrifugation. Cells were then resuspended in phosphate-buffered saline (PBS, pH 7.2) with 1 mg/ml lysozyme for 20 min at 30 °C, probe sonicated for 2 min (four cycles of 20 s on, 10 s off), clarified by centrifugation at $17,000 \times g$ for 1 h at 4 °C, and passed through a 0.45 μ m syringe filter. Recombinant Pn3Pase was purified by Ni^{2+} -NTA resin at 4 °C, eluted with 300 mM imidazole and buffer exchanged into PBS pH 7.2. Protein concentration was determined by bicinchoninic acid assay. Purity was assessed by visualizing proteins on stain free tris-glycine gel (BioRad) using gel doc EZ imager (BioRad).

Enzyme assays

Tritiated Pn3P assays- Recombinant enzyme activity against type 3 capsular polysaccharide was assayed by incubation of 0.2 μ g/ml recombinant protein, or heat killed control, with 10 mg/ml ^3H -Pn3P in PBS. The reaction was stopped after 2 h by heating at 100 °C for 5 min. Reaction mixture was separated on a superdex peptide 10/300 GL column (GE) on an NGC discoverer FPLC system (BioRad). Fractions of 1ml were collected, and counts per min in each fraction were counted in a Tri-Carb 2910 TR liquid scintillation analyzer (Perkin Elmer). Time course experiments were analyzed by the same method.

Reducing end sugar assays- recombinant Pn3Pase hydrolysis activity was determined by measuring the increase in reducing ends using the *p*-hydroxybenzoic acid hydrazide (PAHBAH) method (25). A reaction mixture (200 μ l) containing 20 μ g Pn3P, and 1 μ g recombinant Pn3Pase in either 50 mM MOPS-NaOH (pH 6.0), 50 mM sodium phosphate buffer (pH 7.2), or 20 mM Tris-HCl (pH 8.0), was incubated at 37 °C for 1 h and then heated at 100 °C for 5 min to stop. Reaction mixture (40 μ l) was mixed with 120 μ l of 1% (w/v) PAHBAH-HCL solution, heated at

100 °C for 5 min. Absorbance at 405 nm was measured on a Biotek synergy H1 microplate reader in a clear bottom 96-well microplate. Concentrations of reducing sugars were calculated based on GlcA standard curves generated by the same method in respective buffers. Metal dependence assays were performed similarly with addition of MgCl₂ or CaCl₂ in Tris buffer (pH 7.4).

Enzyme Kinetics

The Michaelis-Menten constant (K_m) and the maximum velocity (V_{max}) of Pn3Pase were measured using Pn3P as substrate (average molecular weight: 400,000 Da). The substrate was used at eight concentrations (3200 nM, 1600 nM, 800 nM, 400 nM, 200 nM, 100 nM, 50 nM and 25nM) in phosphate buffered saline at pH 7.4. Pn3Pase was added at 1µg/mL and the reactions were incubated at 37°C. Reactions were stopped at 0,4,8,12,16, and 20 minutes (corresponding to approximately 10% of total depolymerization yielding mostly tetrasaccharides) by boiling the reaction at 100°C for 5 minutes. The amount of product formed was measured using PAHBAH-HCl, as described above, with tetrasaccharides obtained from enzymatic depolymerization to generate a standard curve for data fitting. Initial velocity was calculated using the amount of product formed in the linear region of absorbance. Initial velocities of each substrate concentration were inserted into the Michaelis-Menten equation to determine K_m and V_{max} .

Oligosaccharide analysis

Pn3P powder (2 mg) was incubated with 100 mg of Pn3Pase at 37 °C for 48 h. The reaction was stopped by heating at 100 °C for 5 min, and loaded onto Superdex peptide 10/300 GL column (GE). Products were separated in phosphate buffered saline at a flow rate of 1 ml/min and monitored by refractive index. Fractions (0.5 ml) were collected and oligosaccharide

peaks were purified, desalted into water on a packed fine P2 column (Biorad). Desalted oligos were lyophilized and subject to ESI-MS for mass determination and NMR for structural and reducing end identification.

NMR

Oligosaccharides were dissolved in 400 μL $^2\text{H}_2\text{O}$ (99.9 %, Sigma-Aldrich, St. Louis, MO) and lyophilized three-times to remove the exchangeable protons. The samples were re-dissolved in 400 μl 99.96 % $^2\text{H}_2\text{O}$ and transferred to NMR microtubes. ^1H spectroscopy, ^{13}C spectroscopy, ^1H - ^1H correlated spectroscopy (COSY), and ^1H - ^{13}C heteronuclear single quantum coherence spectroscopy (HSQC) experiments were all performed at 298 K on Bruker 600 or 800 MHz spectrometer with Topspin 2.1.6 software.

References

1. Avery, O. T., and R. Dubos. 1930. The specific action of a bacterial enzyme on pneumococci of type III. *Science* 72: 151-152.
2. Dubos, R., and O. T. Avery. 1931. Decomposition of the capsular polysaccharide of pneumococcus type III by a bacterial enzyme *J Exp Med* 54: 51-71.
3. Sickles, G. M., and M. Shaw. 1934. A Systematic Study of Microorganisms Which Decompose the Specific Carbohydrates of the Pneumococcus. *J Bacteriol* 28: 415-431.
4. Uetanabaro, A. P., C. Wahrenburg, W. Hunger, R. Pukall, C. Spröer, E. Stackebrandt, V. P. de Canhos, D. Claus, and D. Fritze. 2003. *Paenibacillus agarexedens* sp. nov., nom. rev., and *Paenibacillus agaridevorans* sp. nov. *Int J Syst Evol Microbiol* 53: 1051-1057.
5. Nakamura, L., and J. Swezey. 1983. Taxonomy of *Bacillus circulans* Jordan 1890-Base Composition and Reassociation of Deoxyribonucleic Acid. *International Journal of Systematic Bacteriology* 33: 46-52.
6. Ash, C., F. G. Priest, and M. D. Collins. 1993. Molecular identification of rRNA group 3 bacilli (Ash, Farrow, Wallbanks and Collins) using a PCR probe test. Proposal for the creation of a new genus *Paenibacillus*. *Antonie Van Leeuwenhoek* 64: 253-260.
7. Torriani, A., and A. M. Pappenheimer. 1962. Inducible polysaccharide depolymerases of *Bacillus palustris*. *J Biol Chem* 237: 3-13.
8. C.E., R., and S. G. R. 1946. Studies of anti-pneumococcal serum; complement-fixing activity of fractionated rabbit serum. *J Immunol* 54: 267-274.

9. Shaw, M., and G. M. Sickles. 1950. Production of specific pneumococcus carbohydrate-splitting enzymes in media to which the specific substrate was not added. *J Immunol* 64: 27-32.
10. Forsee, W. T., R. T. Cartee, and J. Yother. 2009. Characterization of the lipid linkage region and chain length of the celluburonic acid capsule of *Streptococcus pneumoniae*. *J Biol Chem* 284: 11826-11835.
11. Forsee, W. T., R. T. Cartee, and J. Yother. 2006. Role of the carbohydrate binding site of the *Streptococcus pneumoniae* capsular polysaccharide type 3 synthase in the transition from oligosaccharide to polysaccharide synthesis. *J Biol Chem* 281: 6283-6289.
12. Middleton, D. R., W. Lorenz, and F. Y. Avci. 2017. Complete Genome Sequence of the Bacterium *Bacillus circulans* Jordan Strain 32352. *Genome Announcements* (In press).
13. Agard, N., J. Baskin, J. Prescher, A. Lo, and C. Bertozzi. 2006. A comparative study of bioorthogonal reactions with azides. *Acs Chemical Biology* 1: 644-648.
14. Chung, J., S. Kim, K. Choi, and J. O. Kim. 2015. Degradation of polyvinyl alcohol in textile waste water by *Microbacterium barkeri* KCCM 10507 and *Paenibacillus amylolyticus* KCCM 10508. *Environ Technol*: 1-7.
15. Konishi, J., and K. Maruhashi. 2003. 2-(2'-Hydroxyphenyl)benzene sulfinate desulfinate from the thermophilic desulfurizing bacterium *Paenibacillus* sp. strain A11-2: purification and characterization. *Appl Microbiol Biotechnol* 62: 356-361.
16. Knolhoff, A. M., J. Zheng, M. A. McFarland, Y. Luo, J. H. Callahan, E. W. Brown, and T. R. Croley. 2015. Identification and Structural Characterization of Naturally-Occurring Broad-Spectrum Cyclic Antibiotics Isolated from *Paenibacillus*. *J Am Soc Mass Spectrom* 26: 1768-1779.

17. Oliveira, A., M. Leite, L. D. Kluskens, S. B. Santos, L. D. Melo, and J. Azeredo. 2015. The First *Paenibacillus* larvae Bacteriophage Endolysin (PlyPI23) with High Potential to Control American Foulbrood. *PLoS One* 10: e0132095.
18. Guo, Y., E. Huang, C. Yuan, L. Zhang, and A. E. Yousef. 2012. Isolation of a *Paenibacillus* sp. strain and structural elucidation of its broad-spectrum lipopeptide antibiotic. *Appl Environ Microbiol* 78: 3156-3165.
19. Pasari, N., N. Adlakha, M. Gupta, Z. Bashir, G. H. Rajacharya, G. Verma, M. Munde, R. Bhatnagar, and S. S. Yazdani. 2017. Impact of Module-X2 and Carbohydrate Binding Module-3 on the catalytic activity of associated glycoside hydrolases towards plant biomass. *Sci Rep* 7: 3700.
20. Yin, Y., X. Mao, J. Yang, X. Chen, F. Mao, and Y. Xu. 2012. dbCAN: a web resource for automated carbohydrate-active enzyme annotation. *Nucleic Acids Res* 40: W445-451.
21. Petersen, T. N., S. Brunak, G. von Heijne, and H. Nielsen. 2011. SignalP 4.0: discriminating signal peptides from transmembrane regions. *Nat Methods* 8: 785-786.
22. Finn, R. D., T. K. Attwood, P. C. Babbitt, A. Bateman, P. Bork, A. J. Bridge, H. Y. Chang, Z. Dosztányi, S. El-Gebali, M. Fraser, J. Gough, D. Haft, G. L. Holliday, H. Huang, X. Huang, I. Letunic, R. Lopez, S. Lu, A. Marchler-Bauer, H. Mi, J. Mistry, D. A. Natale, M. Necci, G. Nuka, C. A. Orengo, Y. Park, S. Pesseat, D. Piovesan, S. C. Potter, N. D. Rawlings, N. Redaschi, L. Richardson, C. Rivoire, A. Sangrador-Vegas, C. Sigrist, I. Sillitoe, B. Smithers, S. Squizzato, G. Sutton, N. Thanki, P. D. Thomas, S. C. Tosatto, C. H. Wu, I. Xenarios, L. S. Yeh, S. Y. Young, and A. L. Mitchell. 2017. InterPro in 2017-beyond protein family and domain annotations. *Nucleic Acids Res* 45: D190-D199.

23. Yang, J. K., H. J. Yoon, H. J. Ahn, B. I. Lee, J. D. Pedelacq, E. C. Liong, J. Berendzen, M. Laivenieks, C. Vieille, G. J. Zeikus, D. J. Vocadlo, S. G. Withers, and S. W. Suh. 2004. Crystal structure of beta-D-xylosidase from *Thermoanaerobacterium saccharolyticum*, a family 39 glycoside hydrolase. *J Mol Biol* 335: 155-165.
24. Henrissat, B., and A. Bairoch. 1996. Updating the sequence-based classification of glycosyl hydrolases. *Biochem J* 316 (Pt 2): 695-696.
25. Blakeney, A., and L. Mutton. 1980. A Simple Colorimetric Method for the Determination of Sugars in Fruit and Vegetables. *Journal of the Science of Food and Agriculture* 31: 889-897.
26. Grady, E., J. MacDonald, L. Liu, A. Richman, and Z. Yuan. 2016. Current knowledge and perspectives of *Paenibacillus*: a review. *Microbial Cell Factories* 15.
27. Baik, K. S., H. N. Choe, S. C. Park, E. M. Kim, and C. N. Seong. 2011. *Paenibacillus wooonensis* sp. nov., isolated from wetland freshwater. *Int J Syst Evol Microbiol* 61: 2763-2768.
28. Lim, J. M., C. O. Jeon, J. C. Lee, L. H. Xu, C. L. Jiang, and C. J. Kim. 2006. *Paenibacillus gansuensis* sp. nov., isolated from desert soil of Gansu Province in China. *Int J Syst Evol Microbiol* 56: 2131-2134.
29. Bouraoui, H., H. Rebib, M. Ben Aissa, J. P. Touzel, M. O'donohue, and M. Manai. 2013. *Paenibacillus marinum* sp. nov., a thermophilic xylanolytic bacterium isolated from a marine hot spring in Tunisia. *J Basic Microbiol* 53: 877-883.
30. Kishore, K. H., Z. Begum, A. A. Pathan, and S. Shivaji. 2010. *Paenibacillus glacialis* sp. nov., isolated from the Kafni glacier of the Himalayas, India. *Int J Syst Evol Microbiol* 60: 1909-1913.

31. Shida, O., H. Takagi, K. Kadowaki, L. K. Nakamura, and K. Komagata. 1997. Transfer of *Bacillus alginolyticus*, *Bacillus chondroitinus*, *Bacillus curdlanolyticus*, *Bacillus glucanolyticus*, *Bacillus kobensis*, and *Bacillus thiaminolyticus* to the genus *Paenibacillus* and emended description of the genus *Paenibacillus*. *Int J Syst Bacteriol* 47: 289-298.
32. Li, Q. Q., X. K. Zhou, L. Z. Dang, J. Cheng, W. N. Hozzein, M. J. Liu, Q. Hu, W. J. Li, and Y. Q. Duan. 2014. *Paenibacillus nicotianae* sp. nov., isolated from a tobacco sample. *Antonie Van Leeuwenhoek* 106: 1199-1205.
33. Leão, R. S., R. H. Pereira, A. G. Ferreira, A. N. Lima, R. M. Albano, and E. A. Marques. 2010. First report of *Paenibacillus cineris* from a patient with cystic fibrosis. *Diagn Microbiol Infect Dis* 66: 101-103.
34. Hong, T. Y., and M. Meng. 2003. Biochemical characterization and antifungal activity of an endo-1,3-beta-glucanase of *Paenibacillus* sp. isolated from garden soil. *Appl Microbiol Biotechnol* 61: 472-478.
35. Xie, J. B., Z. Du, L. Bai, C. Tian, Y. Zhang, J. Y. Xie, T. Wang, X. Liu, X. Chen, Q. Cheng, S. Chen, and J. Li. 2014. Comparative genomic analysis of N₂-fixing and non-N₂-fixing *Paenibacillus* spp.: organization, evolution and expression of the nitrogen fixation genes. *PLoS Genet* 10: e1004231.
36. Allard, S., A. Enurah, E. Strain, P. Millner, S. L. Rideout, E. W. Brown, and J. Zheng. 2014. In situ evaluation of *Paenibacillus alvei* in reducing carriage of *Salmonella enterica* serovar Newport on whole tomato plants. *Appl Environ Microbiol* 80: 3842-3849.
37. Magee, A. D., and J. Yother. 2001. Requirement for capsule in colonization by *Streptococcus pneumoniae*. *Infect Immun* 69: 3755-3761.

38. Nelson, A. L., A. M. Roche, J. M. Gould, K. Chim, A. J. Ratner, and J. N. Weiser. 2007. Capsule enhances pneumococcal colonization by limiting mucus-mediated clearance. *Infect Immun* 75: 83-90.
39. Dagan, R., S. Patterson, C. Juergens, D. Greenberg, N. Givon-Lavi, N. Porat, A. Gurtman, W. C. Gruber, and D. A. Scott. 2013. Comparative immunogenicity and efficacy of 13-valent and 7-valent pneumococcal conjugate vaccines in reducing nasopharyngeal colonization: a randomized double-blind trial. *Clin Infect Dis* 57: 952-962.
40. Gruber, W. C., D. A. Scott, and E. A. Emini. 2012. Development and clinical evaluation of Prevnar 13, a 13-valent pneumococcal CRM197 conjugate vaccine. *Ann N Y Acad Sci* 1263: 15-26.
41. Kieninger, D. M., K. Kueper, K. Steul, C. Juergens, N. Ahlers, S. Baker, K. U. Jansen, C. Devlin, W. C. Gruber, E. A. Emini, D. A. Scott, and s. group. 2010. Safety, tolerability, and immunologic noninferiority of a 13-valent pneumococcal conjugate vaccine compared to a 7-valent pneumococcal conjugate vaccine given with routine pediatric vaccinations in Germany. *Vaccine* 28: 4192-4203.
42. Lim, J. M., D. Sherling, C. F. Teo, D. B. Hausman, D. Lin, and L. Wells. 2008. Defining the regulated secreted proteome of rodent adipocytes upon the induction of insulin resistance. *J Proteome Res* 7: 1251-1263.
43. Aziz, R. K., D. Bartels, A. A. Best, M. DeJongh, T. Disz, R. A. Edwards, K. Formsma, S. Gerdes, E. M. Glass, M. Kubal, F. Meyer, G. J. Olsen, R. Olson, A. L. Osterman, R. A. Overbeek, L. K. McNeil, D. Paarmann, T. Paczian, B. Parrello, G. D. Pusch, C. Reich, R.

- Stevens, O. Vassieva, V. Vonstein, A. Wilke, and O. Zagnitko. 2008. The RAST Server: rapid annotations using subsystems technology. *BMC Genomics* 9: 75.
44. Rio, D. C., M. Ares, G. J. Hannon, and T. W. Nilsen. 2010. Purification of RNA using TRIzol (TRI reagent). *Cold Spring Harb Protoc* 2010: pdb.prot5439.
45. Walhout, A. J., G. F. Temple, M. A. Brasch, J. L. Hartley, M. A. Lorson, S. van den Heuvel, and M. Vidal. 2000. GATEWAY recombinational cloning: application to the cloning of large numbers of open reading frames or ORFeomes. *Methods Enzymol* 328: 575-592.

Figure 3.1

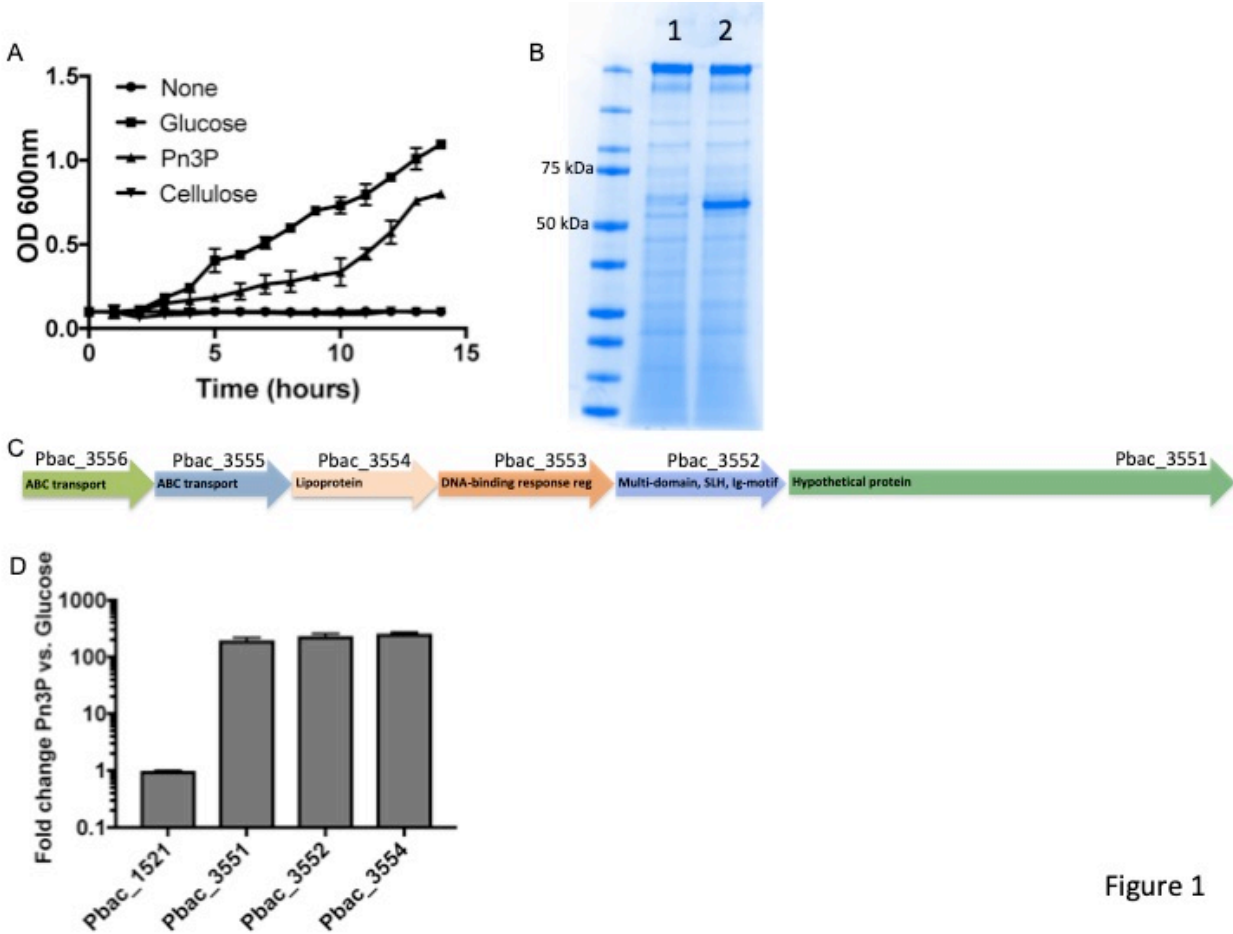


Figure 1

Figure 3.1. Culture of *Paenibacillus sp.* 32352 in minimal medium with Pn3P as carbon source.

(A) Growth of *Paenibacillus sp.* 32352 (Pbac) on minimal medium plus 2% (w/v) glucose, Pn3P, cellulose, or nothing as carbon source. (B) SDS-PAGE coomassie blue stained gel of concentrated culture supernatant of Pbac grown on glucose (1) or Pn3P (2). (C) Proposed locus of Pn3P utilization organization based on the Rapid Annotation Server (43) (RAST) annotation. (D) Real-Time PCR of select genes within putative locus in Pbac grown on 2% glucose or Pn3P, shown as fold change in expression in Pn3P culture versus glucose culture. SLH (Surface layer homology) Ig-motif (Immunoglobulin-like motif)

Table 3.1

Table 3.1. Proteomic identification of culture supernatant proteins of Paenibacillus sp. 32352 grown in Pn3P. Highlighted are proteins unique to Pn3P grown culture.

Gene	Description	Score	Coverage	# Unique Peptides	# PSMs [^]	# AAs	MW [kDa]
Pbac_3554	*Lipoprotein	1301.24	82.02	49	597	506	55.9
Pbac_1521	Ig-like, group 2, Surface layer protein	450.46	50.17	44	218	1190	128.7
Pbac_6539	Hypothetical protein	237.19	31.20	17	82	577	64.1
Pbac_5871	NLP/P60 family protein	103.53	61.54	6	35	156	16.9
Pbac_1659	Alpha/beta hydrolase fold (EC 3.8.1.5)	94.98	66.07	13	72	280	30.1
	Hypothetical protein						
Pbac_3551	NCBI ref seq: WP_079915027	39.14	16.70	6	53	1545	168.0

[^]PSM, peptide spectral matches, filtered at a 1% false discovery rate. Proteins considered with >30 PSM.

Figure 3.2

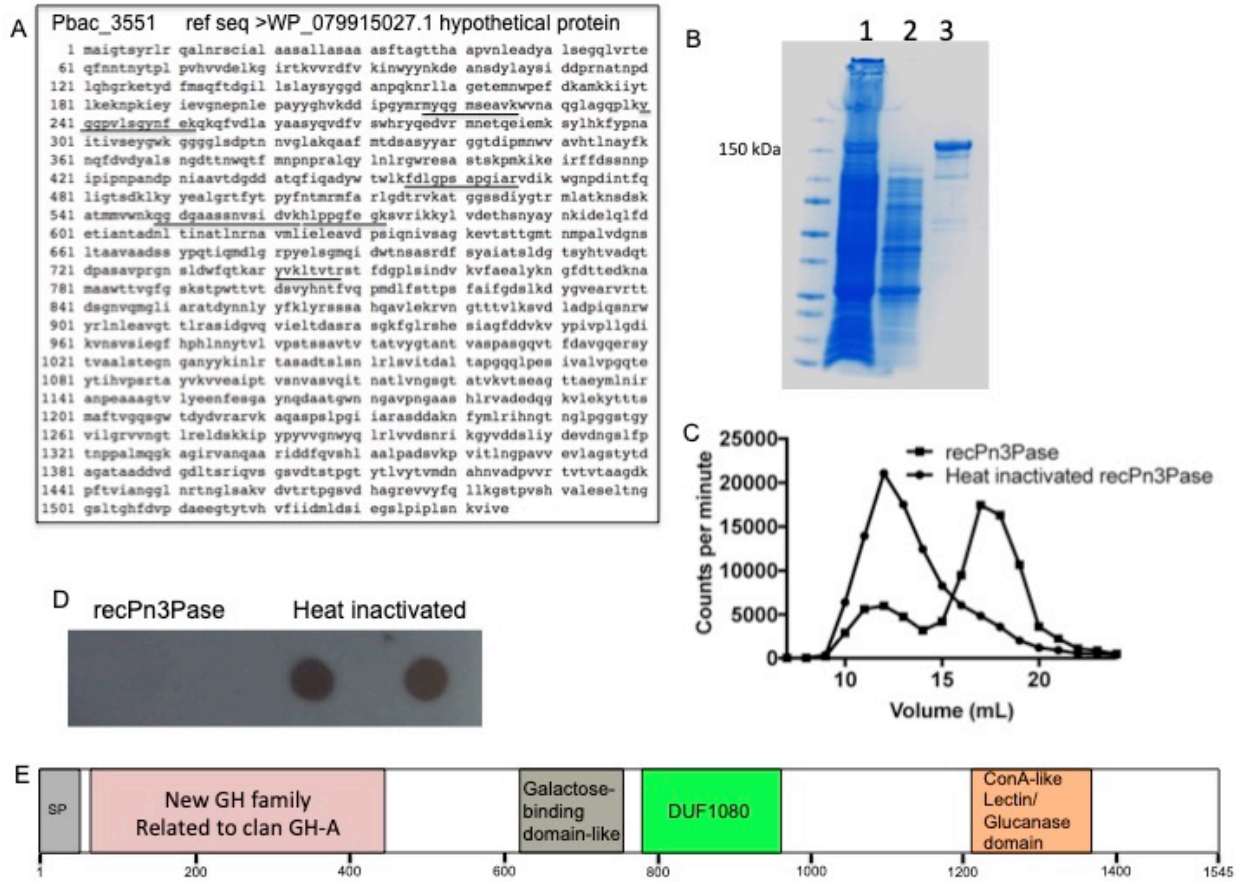


Figure 3.2. Pn3Pase identification and domain schematic of amino acid sequence.

(A) Amino acid sequence and accession of Pn3Pase. Underlined are tryptic peptides identified with high confidence by proteome discoverer software. (B) Purification is His-tagged recombinant Pn3Pase by Nickel-NTA column. Lane 1) uncaptured flow-through 2) 5X concentrated wash 3) elution. (C) Separation of recombinant Pn3Pase depolymerized tritium radioisotope labeled Pn3P by size exclusion chromatography, measured by counts per minute in each 1 ml fraction. (D) Dot blot of recombinant Pn3Pase depolymerized cold Pn3P probed with Pn3P monoclonal antibody (E) Schematic of predicted domains of Pn3Pase by InterPro.

Figure 3.3

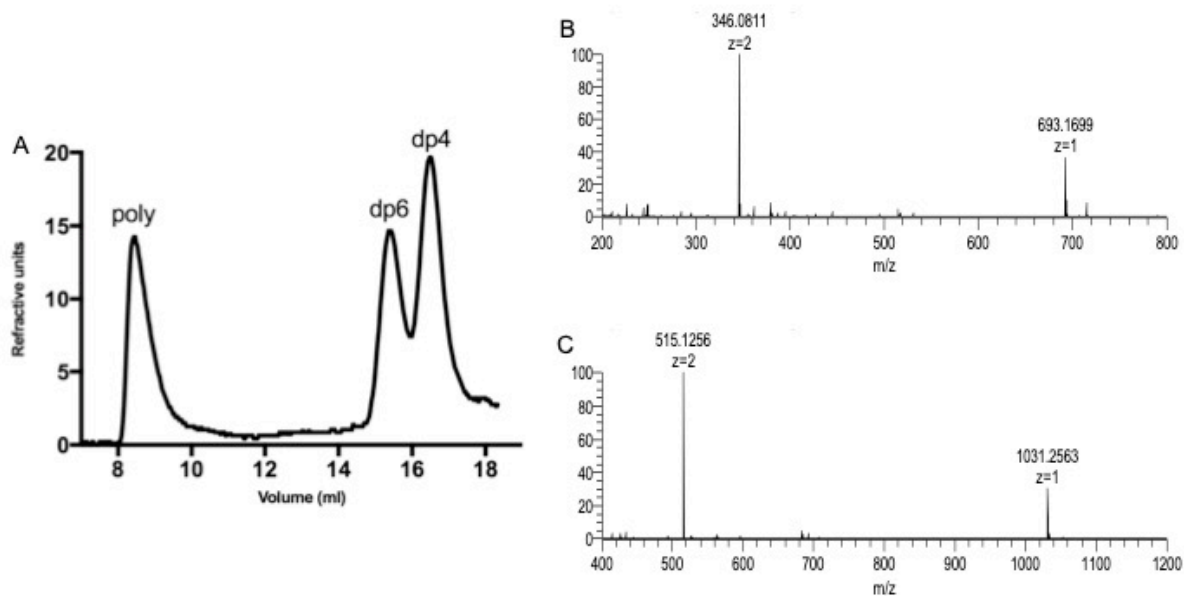


Figure 3.3 Identification of oligosaccharide products by electrospray ionization mass spectrometry. Separation of oligosaccharide products (A) and mass spectra of the tetrasaccharide (B) and the hexasaccharide (C). Experimental molecular weights and the accuracies are shown in **Table 3.2**

Table 3.2

Table 3.2. Different charge states of the tetrasaccharide and hexasaccharide detected by mass spectrometry.

	<i>m/z</i> observed	Charge state	Experimental M	Theoretical M	Error (ppm)
Tetrasaccharide	693.1699	1	694.1777	694.1804	-3.85
	346.0811	2	694.1779	694.1804	-3.66
Hexasaccharide	1031.2563	1	1032.2641	1032.2653	-1.13
	515.1256	2	1032.2669	1032.2653	1.51

Figure 3.4

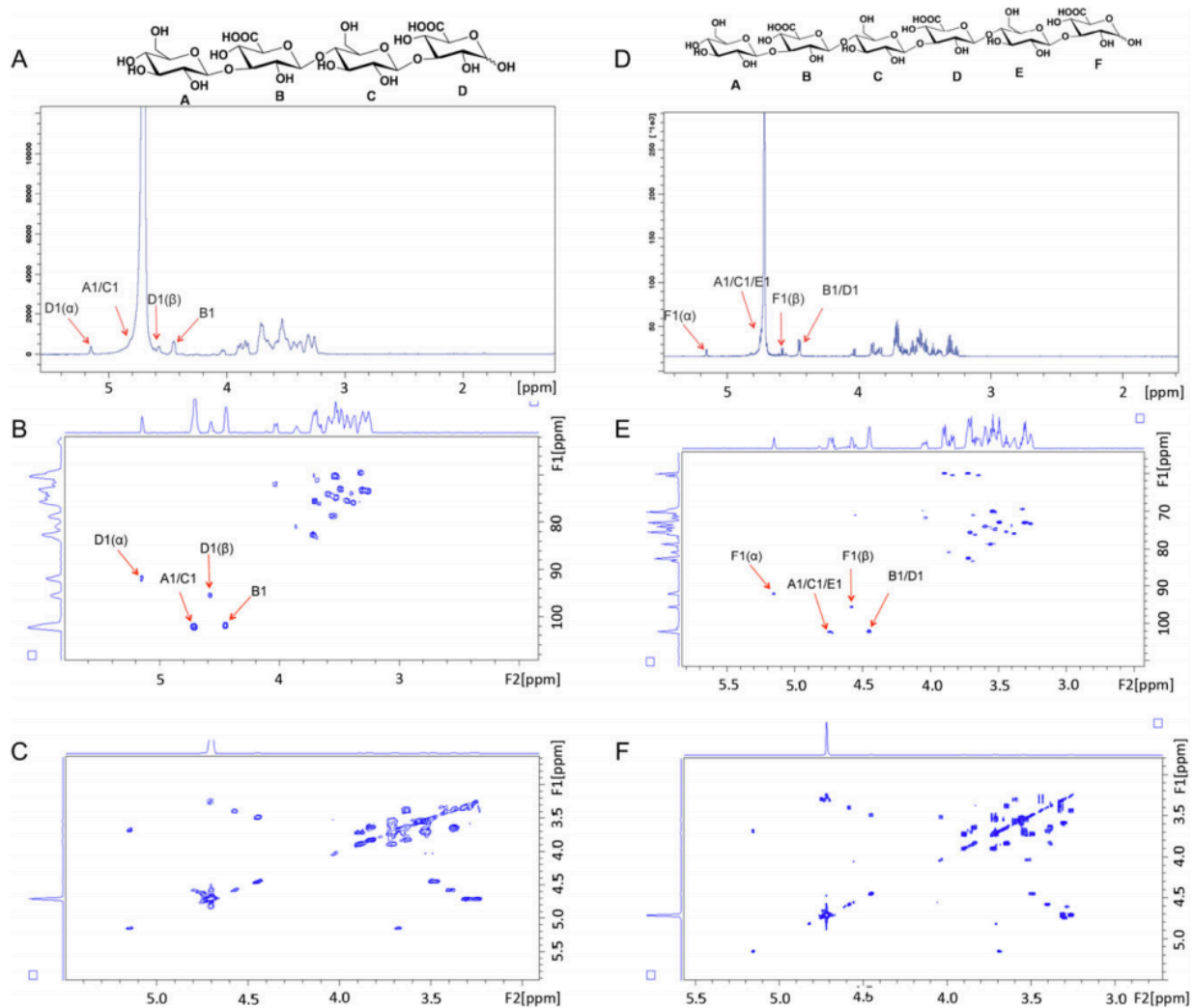


Figure 3.4. Nuclear Magnetic Resonance characterization of oligosaccharide products.

^1H NMR spectrum (A), 2D HSQC NMR spectrum (B), and 2D COSY NMR spectrum (C) of the Pn3 tetrasaccharide. ^1H NMR spectrum (D), 2D HSQC NMR spectrum (E), and 2D COSY NMR spectrum (F) of the Pn3 hexasaccharide.

Figure 3.5

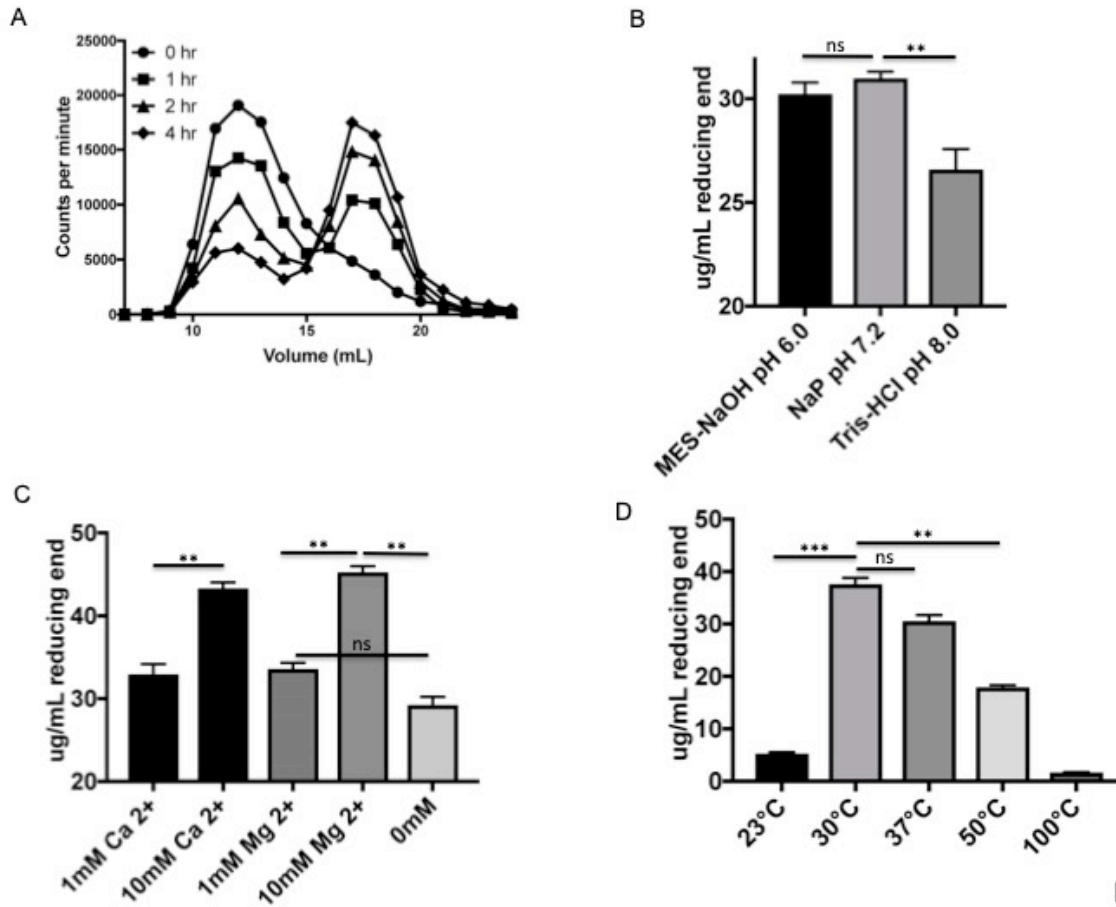


Figure 5

Figure 3.5. Activity assessment of Pn3Pase.

(A) Time course assay of recombinant Pn3Pase depolymerized tritium radioisotope labeled Pn3P separated by size exclusion chromatography, measured by counts per min in each 1 ml fraction. (B) Optimization of recombinant Pn3Pase in three different buffer conditions, measured by concentration of glucuronic acid reducing end generated in mg/ml. (C) Metal dependence determination with Mg²⁺ and Ca²⁺ reaction supplements, measured by concentration of glucuronic acid reducing end generated in ug/ml. (D) Temperature dependence of recombinant Pn3Pase, measured by concentration of glucuronic acid reducing end generated in mg/ml. Statistical significance was determined with the two-tailed Student *t*-test *** P<0.001 ** P<0.01 ns- not significant

CHAPTER 4

ENZYMATIC HYDROLYSIS OF PNEUMOCOCCAL CAPSULAR POLYSACCHARIDE

RENDERS THE BACTERIUM VULNERABLE TO HOST DEFENSE

Dustin R Middleton, Amy V. Paschall, Jeremy A. Duke, and Fikri Y. Avci

Accepted by *Infection and Immunity*. Reprinted here with permission of publisher.

Abstract

Despite a century of investigation, *Streptococcus pneumoniae* (*Spn*) remains a major human pathogen, causing a number of diseases such as pneumonia, meningitis, and otitis media. Like many encapsulated pathogens, the capsular polysaccharide (CPS) of *Spn* is a critical component for colonization and virulence in mammalian hosts. This study aimed to evaluate the protective role of a glycoside hydrolase, Pn3Pase, targeting the CPS of type 3 *Spn*, which is one of the most virulent serotypes. We have assessed the ability of Pn3Pase to degrade the capsule on a live type 3 strain. Through *in vitro* assays we observed that Pn3Pase treatment increases the bacterium's susceptibility to phagocytosis by macrophages and complement-mediated killing by neutrophils. We have demonstrated that *in vivo* Pn3Pase treatment reduces nasopharyngeal colonization, and protects mice from sepsis caused by type 3 *Spn*. Due to the increasing shifts in serotype distribution, rise in drug resistant strains, and poor immune responses to vaccine-included serotypes, it is necessary to investigate approaches to combat pneumococcal infections. This study evaluates the interaction of pneumococcal CPS with host at molecular, cellular and systemic levels and offers an alternative therapeutic approach for diseases caused by *Spn* through enzymatic hydrolysis of the CPS.

Introduction

Streptococcus pneumoniae (*Spn*), the causal agent of pneumonia, meningitis, and otitis media, remains a major threat to human health. This bacterium can stably colonize the human nasopharynx as a part of the normal commensal microflora (1-3). Colonization is the primary mode of transmission and a key step in the initiation of disease, despite asymptomatic carriage (4, 5). A critical component for survival within the host and full pathogenicity of most *Spn*

strains is the capsular polysaccharide (CPS) (6, 7). The CPS is a large and distinct polysaccharide structure coating the entire surface of the bacterium. The capsule helps *Spn* evade the host immune system through resisting or inhibiting its phagocytosis by host macrophages while also limiting mucus-mediated clearance (8-11). The requirement of the CPS in bacterial virulence, surface accessibility, and antigenicity, has made it a target in vaccination studies for over 100 years (12-16). Great strides have been made at increasing the immunogenicity and efficacy of pneumococcal vaccines that utilize the CPS by conjugation to a protein carrier (17, 18).

Spn has over 90 unique capsular serotypes, each differing in monosaccharide composition and linkage, as well as other modifications such as acetylation (14). Current pneumococcal vaccines aim to provide serotype-specific protection for some of the most relevant clinical serotypes (12, 14). The use of the 7 and 13-valent pneumococcal conjugate vaccines, PCV7 and PCV13 (Prevnar; Pfizer) has been a major success; reducing invasive pneumococcal disease (IPD) rates significantly in both vaccinated and unvaccinated populations (15, 19-22).

While the conjugate vaccines have been effective for preventing carriage and IPD caused by most included serotypes, the exception has been serotype 3. The pneumococcal type 3 polysaccharide (Pn3P) component of the current PCV13 induces variable immune responses to *Spn* serotype 3, (23-25). Pn3P is a linear polymer of $-3)\beta\text{GlcA}(1-4)\beta\text{Glc}(1-$ disaccharide repeating units with an average molecular weight of >400 kDa (26, 27). It was noted that significantly higher serum titers are required for serotype 3 in comparison with other serotypes for opsonophagocytic killing of *Spn* (14, 28, 29). Numerous animal model and epidemiology studies have associated type 3 strains with increased virulence and death risk compared to other pneumococcal serotypes (30-32). A recent case report demonstrated a fatal case of IPD caused

by serotype 3, highlighting increased complications and generally poor outcomes associated with this invasive serotype (33). In addition, recent data indicate that *Spn* strains are resistant to one or more antibiotics in 30% of IPD cases (34). The Centers for Disease Control and Prevention predict a rise in antibiotic-resistance features of *Spn* (35, 36).

The inability of vaccination to provide adequate protection against one of the most aggressive serotypes of this major human pathogen necessitates the urgent exploration of alternative approaches for type 3 pneumococcal infections. This, along with a rise in the prevalence of antibiotic resistant strains (37, 38) led us to revisit early studies by Avery and Dubos, who discovered a soil dwelling bacterium producing an enzyme that hydrolyzes Pn3P (39-41). Previously, we have identified this bacterium as a *Paenibacillus* species, cloned its type 3 specific glycosyl hydrolase, Pn3Pase and characterized its degradation products (26, 42). In light of the continued prevalence, and severity of serotype 3 *Spn*, we postulated the potential use of this purified protein as a therapeutic agent for hyper virulent serotype 3 infections. Here, we investigated the ability of Pn3Pase to degrade the capsule on a live virulent type 3 *Spn* strain and therefore render the bacterium susceptible to host immune clearance.

Results

Pn3Pase removes capsule from growing type 3 *Spn*

The encapsulated type 3 WU2 strain was cultured for 10 hours with the recombinant enzyme added to the growth medium and bacterial growth was monitored by measuring OD at 600 nm to assess effects of Pn3Pase treatment on growing type 3 *Spn*. Pn3Pase treatment of cells demonstrated no adverse growth or cytotoxic effects on the bacteria (**Fig 4.1A**). In the same experiment, we obtained comparable CFU values for both enzyme treated and non-treated

groups at two-hour intervals (data not shown). To assess direct impact of enzyme treatment on bacterial survival, a log-phase culture was isolated and suspended in nutrient-free buffer with active, or heat inactivated Pn3Pase. Enzyme treated cells showed comparable counts to inactivated and PBS controls over the 8-hour time course (**Fig 4.1B**).

The bacterial cells grown in the presence of Pn3Pase were then examined by competition ELISA to determine if the enzyme led to efficient capsule removal in the growing cultures. After treatment, fixed whole cells, at two different concentrations, were used to compete for Pn3P specific antibodies binding to the Pn3P coated plate. The acapsular WU2 mutant strain (JD908) showed minimal to no inhibition of antibody binding due to its lack of capsule. Heat inactivated Pn3Pase treated cells demonstrated the highest percent inhibition as cell surfaces should be fully decorated with CPS. With active Pn3Pase treatment, inhibition of antibody binding begins to decrease in a Pn3Pase concentration dependent manner (**Fig 4.2A**), suggesting that the enzyme strips the capsule from live, growing type 3 *Spn*.

A time course experiment was performed in which the bacterial cells were grown to mid-log phase, suspended in PBS, and treated with Pn3Pase for 0, 1, 2, or 4 hours. The Pn3Pase dose was lowered to 1mg/ml for this assay given that the WU2 strain should not be actively growing and therefore not producing a substantial amount of new CPS under these conditions. At each time point, the treated cells were fixed and examined by competition ELISA as described above. The acapsular WU2 mutant strain (JD908), again, showed minimal to no inhibition due to its lack of capsule. Untreated cells exhibited the highest percent inhibition, indicative of a cell surface fully decorated with CPS. With increasing Pn3Pase incubation time, inhibition of antibody binding begins to decrease significantly, appearing essentially acapsular after 2- or 4-hour treatments (**Fig 4.2B**).

The Pn3Pase treated cells were visualized by transmission electron microscopy and compared to the cells treated with heat inactivated Pn3Pase. The heat inactivated enzyme treated cells displayed a thick, complete CPS coat across their surface (Fig 2C), undoubtedly distinct from the acapsular mutant (**Fig 4.2D**). The capsule layer of the enzyme treated cells exhibited little to no capsule (**Fig 4.2E**), appearing as acapsular.

Pn3Pase treatment of type 3 *Spn* allows phagocytic cell uptake and killing

A major virulence mechanism of the CPS is to provide the bacterium the ability to resist phagocytosis by host phagocytic cells (1, 6). To investigate the effect of Pn3Pase treatment on uptake by macrophages *in vitro*, we stained mid-log phase bacterial cultures with carboxyfluorescein succinimidyl ester (CFSE) and then treated with Pn3Pase followed by incubation with RAW 264.7 macrophages. Macrophages were then washed extensively and imaged by fluorescent microscopy (**Fig 4.3A**). The extent of bacterial uptake by macrophages was quantified by flow cytometry (**Fig 4.3B**). Bacteria treated with the enzyme were taken up by macrophages significantly more than the encapsulated strain. We then determined the percentage of fluorescent macrophages, representing the phagocytosis of fluorescent bacteria (**Figs 4.3C-D**). The encapsulated type 3 strain incubated with heat inactivated Pn3Pase had minimal fluorescently labeled phagocytes whereas Pn3Pase treated bacteria were as efficiently taken up by the macrophages as the acapsular mutant strain. Uptake was partially dependent on complement as evidenced by higher bacterial uptake in the presence of complement (**Fig 4.3C**). Pn3Pase treatment rendered the bacteria more susceptible to phagocytic engulfment by RAW macrophages in a dose dependent manner, while even high doses of the inactivated enzyme had no significant effect on bacterial uptake (**Fig 4.3D**).

Complement deposition on the pneumococcal surface is an important mechanism aiding in efficient phagocytosis and clearance (10, 11). Since CPS provides complement evasive properties to the bacterium (10, 11), we investigated the effect of capsule removal by Pn3Pase treatment on C3b deposition on the bacterial surface. The encapsulated type 3 WU2 strain was treated with active or inactive Pn3Pase. The untreated type 3 strain and the acapsular mutant were included as additional controls. Bacteria were then incubated with normal mouse serum, washed, and stained with FITC-conjugated antibody to mouse complement. Fixed samples were then analyzed with flow cytometry. In a dose dependent manner, Pn3Pase treatment increased the deposition of complement on the bacterial surface, reaching the levels of deposition on the acapsular strain. Complement had minimal binding to the bacteria either untreated or treated with inactivated-Pn3Pase (**Fig 4.4**).

The standard *in vitro* assay to assess phagocytic killing of *Spn* is an opsonophagocytosis assay (OPA) in which HL-60 cells are differentiated into neutrophils to engulf and clear antibody opsonized bacteria. This method has been widely used to measure the quality of antibody responses in numerous vaccine studies (43-48). Neutrophils are one of the most important components of innate immunity against pathogenic bacteria in the lungs (49-51). While the focus of this study is not on humoral immune responses to *Spn*, we have used a modified OPA to evaluate complement-mediated neutrophil killing of type 3 *Spn* treated with Pn3Pase *in vitro*. Encapsulated type 3 *Spn* was incubated with active or heat inactivated Pn3Pase. Differentiated HL-60 cells were pre-incubated with active or heat-inactivated complement. The mixture of HL-60 cells and complement was added to the bacteria and incubated at 37°C for 1 hour. To quantify the surviving bacteria in the experimental groups, the reaction mixtures were plated and CFUs were counted the next day. Percent survival was calculated as each duplicate reaction

normalized to mean values obtained for control samples (reactions without neutrophils, 100% survival). The enzyme-untreated, encapsulated type 3 strain was able to escape neutrophil killing to show maximum survival while the acapsular mutant strain was reduced to nearly 40% viability upon incubation with active complement and neutrophils (**Fig 4.5**). Pn3Pase treatment to remove the capsule rendered the type 3 strain susceptible to complement dependent neutrophil killing similar to the acapsular strain (**Fig 4.5**).

Pn3Pase limits nasopharyngeal colonization

To investigate the enzyme's protective abilities *in vivo* we first performed an intranasal colonization experiment with BALB/c mice. Nasal colonization by *Spn* is essential for transition to invasive pneumococcal disease (4, 5). It is established that the capsule of this strain is required for intranasal colonization(6). Therefore, we used the nasal colonization model to assess the ability of Pn3Pase to reduce bacterial colonization in the nasopharynx through removal of the capsule of the colonizing type 3 strain. We first confirmed that the acapsular mutant, JD908, failed to colonize the nasopharynx (data not shown). Groups of mice were then intranasally inoculated with 10^6 log-phase wildtype (wt) encapsulated bacteria in 10 μ l PBS. All inocula were chased with either Pn3Pase or buffer control. Groups were dosed with the enzyme at either day 0, day 0 and 3, or day 0, 3, and 7 to assess the effects of multiple administrations. Mice were euthanized, and bacterial load was quantified on day 10. Nasal lavage fluid was obtained, serially diluted, and plated to enumerate the bacterial load. Vehicle control treated mice were colonized with significantly higher bacterial loads than mice treated with only a single dose of Pn3Pase. Administration of two or three doses of Pn3Pase made the majority of the animal lavage fluid void of any viable bacterial colonies (**Fig 4.6A**). Lung homogenates and serum samples showed

no evidence of a bacterial burden (data not shown). Signature pro-inflammatory cytokine levels were measured in the nasal lavage fluid by ELISA (52). Vehicle treated mice had significantly increased levels of the cytokines IL-6 and TNF α compared to Pn3Pase treated animals, a reflection of a continued host inflammatory response to the bacterial burden in this group (**Figs 4.6B-C**) (52). A significant reduction in IL-6 and TNF α was observed in most animals even after a single dose of Pn3Pase on day 0. The mouse with higher bacterial load in the single dose group contributed to the increased cytokine levels in this group.

Pn3Pase protects mice from lethal challenge

To further assess Pn3Pase for its protective abilities and evaluate the utility of Pn3Pase as a therapeutic agent, we employed an intraperitoneal (I.P.) sepsis model (53, 54). Groups of mice were infected with 5×10^3 CFU of log-phase WU2 type 3 strain of *Spn*. We assessed the effect of a single dose of 5 μ g or 0.5 μ g, administered at time 0, 12, or 24 hours post infection. Control groups treated with heat inactivated enzyme died within 48 hours of infection. Regardless of the enzyme dose or the timing of the administration, all treated groups displayed no signs of illness and experienced full protection from the I.P. challenge (**Fig 4.7**).

Discussion

This study aimed to evaluate the protective role of a carbohydrate-degrading enzyme (glycoside hydrolase), Pn3Pase, targeting the capsular polysaccharide of the pathogenic bacterium, serotype 3 *Streptococcus pneumoniae* (*Spn*). Invasive pneumococcal diseases (IPD) caused by *Spn* have been a major threat to human health with alarming mortality rates. Despite a global vaccination program and the use of antibiotics *Spn* remains among the deadliest infectious agents worldwide. Pneumococcal vaccines are made empirically and are variably/poorly

immunogenic especially among elderly and immunocompromised individuals. Widespread use of antibiotics against IPD led to spread of drug resistance pneumococcal strains. This study offers an alternative targeted therapeutic approach to the shortcomings of the incumbent vaccine and antibiotic solutions to IPD. The results presented here indicate that enzymatic hydrolysis of the CPS may be a valid alternative or complementary therapeutic approach for diseases caused by *Spn* and other important encapsulated pathogens such as *Neisseria meningitidis* and Methicillin-Resistant *Staphylococcus aureus* (MRSA).

In this study, we first assessed the ability of Pn3Pase to degrade the capsule on a live type 3 strain. We found that the enzyme could efficiently remove the capsule from live pneumococci while demonstrating no bactericidal effects on the cells. This could potentially serve as a tool to shed light on host-capsule interactions, or to understand novel biological roles for the type 3 CPS. Through *in vitro* assays we observed that Pn3Pase treatment increases the bacterium's susceptibility to phagocytosis by a macrophage cell line. These results were promising since the capsule is a major host immune evasion component that allows *Spn* to resist engulfment by host phagocytes (9). We further investigated how Pn3Pase influences killing by neutrophils. We found that enzyme treatment significantly increased complement-mediated killing by the neutrophils. We have demonstrated that a single dose of Pn3Pase reduces murine nasopharyngeal colonization by type 3 *Spn* significantly, indicating that the enzyme may function as a prophylactic measure to control colonization by this serotype in at-risk populations. Finally, an intraperitoneal challenge was performed to assess the protective capacity of Pn3Pase in a sepsis model. We determined that a single dose of 5 μ g given at time 0 post-infection protects mice from sepsis caused by type 3 *Spn*. Additionally and surprisingly, a single dose of 0.5 μ g administered 24 hours after infection was also able to protect 100% of the challenged mice from the bacterial

challenge while control treated animals did not survive longer than 48 hours. The robust protective capacity of Pn3Pase in this model demonstrates the enzymatic activity is sufficient within the host to effectively degrade the capsule even at low doses.

Given that Pn3Pase has therapeutic potential for pneumococcal infections, practical issues pertaining to the application of the enzyme such as immunogenicity, administration routes, and substrate specificity will need to be addressed (55). Our preliminary assessment of antibody titers generated against Pn3Pase in the challenge experiments observed no IgM or IgG response generated against the effective dose of the enzyme. Preliminary activity assays have been performed on the most similar mammalian glycan structures such as hyaluronic acid, $-4)\beta\text{GlcA}(1-3)\beta\text{GlcNAc}(1-$ and chondroitin, $-4)\beta\text{GlcA}(1-3)\beta\text{GalNAc}(1-$ to assess potential relaxed substrate specificity. We have found this enzyme to be specific for the type 3 structure. Future studies will evaluate humoral and cellular immune responses to Pn3Pase and investigate alternative routes of administration such as intravenous for a bacteremia model, or aerosolized spray for a pneumonia model. A useful example of enzyme delivery to the respiratory tract by aerosol spray is the recombinant human deoxyribonuclease known as Pulmozyme, used to relieve airway obstruction by secreted DNA in cystic fibrosis patients(56).

In addition to the high potential of Pn3Pase as a therapeutic enzyme, this glycosyl hydrolase has unique properties from a structure/function point of view in that it does not fall into a currently established glycosyl hydrolase Carbohydrate Active enZYme (CAZY) family (57). Further examination of structural properties of this protein may lead to the discovery of structurally similar enzymes with activities toward other unique bacterial CPSs. Future investigations will explore the existence of enzymes for use against other prevalent pneumococcal serotypes and other encapsulated pathogenic bacteria. Based on earlier studies,

the native species expressing Pn3Pase has the capacity to degrade two additional pneumococcal CPSs (58, 59). While this Pn3Pase expressing *Paenibacillus* species was isolated from the soil (26, 42, 59), it is befitting to question why this species would evolve to possess such enzymes that are capable of degrading capsules of a human pathogen. Whether these are the natural substrates for the enzymes, indicating co-evolutionary relationship, or whether other soil-dwelling microbes or plants express similar glycan residues and linkages remains to be explored.

In summary, this study serves as the first comprehensive evaluation of the protective role of a glycoside hydrolase, Pn3Pase, debilitating an otherwise lethal bacterial pathogen through targeting its capsular polysaccharide.

Materials and Methods

Bacterial strains and growth conditions

Streptococcus pneumoniae type 3 (WU2 strain) and acapsular derivative (JD908) (60, 61), generous gifts from Moon Nahm (University of Alabama at Birmingham), were cultured aerobically without shaking at 37 °C on Tryptic Soy Agar with 5% sheep blood (TSAB), or in Todd Hewitt Broth plus 0.5% yeast extract (THY) (BD Biosciences).

Mice

Eight-week-old female BALB/c mice were obtained from Taconic Biosciences (Hudson, NY) and housed in the Central Animal Facility at the University of Georgia. Mice were kept in microisolator cages and handled under BSL-2 hoods.

Production of recombinant Pn3Pase

Pn3Pase was produced as described previously with minor modifications(26). Briefly, BL21(DE3) cells transformed with the pET-DEST42-“Pn3Pase” plasmid were grown in Terrific Broth supplemented with 100 µg/ml ampicillin at 37 °C, and cell density was monitored by absorbance at 600 nm. Once the OD 600 nm reached 1.0, the cells were transferred into 18 °C. Protein expression was induced by the addition of Isopropyl β-D-1-thiogalactopyranoside to a final concentration of 1 mM and the cell culture was allowed to incubate for 18 h. Cells were harvested by centrifugation, resuspended in phosphate-buffered saline (PBS, pH 7.2) and lysed by pressure lysis. The lysate was clarified by centrifugation at 17,000 × g for 1 h at 4°C, and passed through a 0.45 µm syringe filter. Recombinant Pn3Pase was purified by Ni²⁺-NTA resin at 4 °C, eluted with 300 mM imidazole and buffer exchanged into PBS pH 7.2. Protein concentration was determined by the bicinchoninic acid assay according to the instructions of the manufacturer. Purity was evaluated by coomassie staining.

Pn3Pase treatment of type 3 *S. pneumoniae*

Fresh *Streptococcus pneumoniae* type 3 (WU2) and acapsular derivative (JD908) colonies on TSAB plates were inoculated to 0.1 OD 600 nm in THY broth and cultured as described above. WU2 growth in presence of 100 mg/ml Pn3Pase was monitored over the course of 10 h by measuring OD 600 nm. WU2 was grown in presence of 2 mg/ml, 10 mg/ml, or 10 mg/ml heat inactivated Pn3Pase for 6 hours, serially diluted, and plated to determine colony forming units. Cultures were harvested by centrifugation, washed in PBS, fixed in 2% paraformaldehyde for 20 min on ice, washed once more, and suspended in 1 ml PBS. For the time course experiment, WU2 and the acapsular strain were grown to mid-log phase (OD 600 nm of 0.6), harvested by centrifugation, washed in PBS, and then suspended in 1 ml PBS. Then, 1

mg/ml Pn3Pase was added and incubated at 37 °C for the 1, 2, or 4 hours. Treated cells were serially diluted, and plated to determine colony forming units, fixed in 2% paraformaldehyde for 20 min on ice, washed once more, and suspended in 1 ml PBS.

Competition ELISA

ELISA plates (96 well, Nunc) were coated with 5 mg/ml Pn3P in 0.1 M carbonate buffer (pH 9.0) overnight at room temperature. Plates were washed 4-times with PBS +0.1% Tween (PBS-T) 20 using a Biotek 405/LS microplate washer. After 1 h blocking at room temperature with 1% BSA in PBS, microplate wells were incubated for 2 h at room temperature with fixed, treated cells that were pre-incubated for 30 min with Pn3P specific anti-serum in PBS-T. Plates were washed, and then incubated for 2 h at room temperature with 1:2000 dilution of goat anti-mouse IgG-AP (Southern Biotech #1030-04) in PBS-T. After washing, plates were incubated for ~30 min at 37 °C with 2 mg/ml phosphatase substrate (Sigma S0942) in 1 M Tris 0.3 mM MgCl₂. Absorbance at 405 nm was measured on a Biotek synergy H1 microplate reader. Percent inhibition of antibody binding was calculated by $((\text{Uninhibited}_{\text{OD405}} - \text{Inhibited}_{\text{OD405}}) / \text{Uninhibited}_{\text{OD405}}) \times 100$.

Electron microscopy

Electron microscopy was performed by the Georgia Electron Microscopy core facility at the University of Georgia according to a modified method by Hammerschmidt et al. (62). Treated cells were fixed in 2% glutaraldehyde, 2% paraformaldehyde, 0.075M lysine-acetate and 0.075% ruthenium red in PBS buffer for 1 h on ice and then rinsed 2× with buffer containing 0.15% ruthenium red, 15 min per rinse. Cells were then fixed in 1% osmium tetroxide in buffer containing 0.15% ruthenium red for 1 h at room temperature followed by two rinses in buffer containing 0.15% ruthenium red, 15 min per rinse. Pellet was dehydrated in a graded ethanol

series (30%, 50%, 75%, 95%, 100% and 100%) and two changes in 100% acetone, 15 min each step. Pellet was then infiltrated with 25% Spurr's resin and 75% acetone - 2 h followed by sequential infiltration with 50% Spurr's resin and 50% acetone, 75% Spurr's resin and 25% acetone, 100% Spurr's resin and then polymerized in a 70 °C oven for 24 h. Samples were sectioned at 60 nm with a Diatome diamond knife and picked up on slot grids. Grids were post-stained on drops of uranyl acetate and lead citrate, 5 min each and rinsed with H₂O 30 s between stains. Samples were scoped using a JEOL JEM 1011 TEM (JEOL USA, Peabody, MA) operated at 80 kV.

Phagocytosis

Mid-log phase WU2 and JD908 (acapsular) cultures were washed and stained with 10 mM Carboxyfluorescein succinimidyl ester (CFSE) for 30 minutes at room temperature. The WU2 strain was concurrently treated with 2 mg/ml of active or heat-inactivated Pn3Pase. Bacterial cell pellets were washed extensively, suspended in 1 ml sterile PBS. 10⁷ bacteria were added to a confluent monolayer of murine leukemia virus transformed macrophage line, RAW 264.7 (American Type Culture Collection (ATCC) Manassas, VA) with active or heat-inactivated baby rabbit complement (Pel-Freez) in a 24 well plate and incubated for 1 hour at 37°C. Wells were washed 4x with PBS to remove extracellular bacteria. Macrophages were fixed with 2% paraformaldehyde at 4°C for 15 minutes and removed from the plate. For microscopy, cells were incubated at room temperature for 30 minutes with a 1/500 dilution of biotinylated wheat germ agglutinin (Vector labs) in 1% bovine serum albumin followed by a 30-minute room temperature incubation with a 1/1000 dilution of streptavidin APC (Biolegend). Cells were imaged with a 40X objective lens. Flow cytometry was performed on a Beckman Cytoflex S cytometer and analyzed by FlowJo. Cells were gated on the macrophage population by scatter plot. A non-

CFSE labeled control served to gate highly fluorescent cell populations. The Pn3Pase dose dependent experiment was performed as above with addition of active complement.

Complement deposition

A complement deposition assay was performed as described previously(63). Type 3 WU2 and acapsular (JD908) strains of bacteria were resuspended in 3% BSA in PBS. Aliquots (in duplicate wells on a 96-well round-bottom plate) were stained with Hoechst 33342 and treated with inactivated or functional Pn3Pase at 5 or 50 mg/ml for 1 hour at 37°C. Normal mouse serum (1:10 dilution) was added to the samples for 30 minutes at 37°C. Cells were washed and stained with FITC-conjugated goat antibody to mouse complement (MP BioMedical, Santa Ana, CA) at 4°C for 30 minutes. Samples were washed with 3% BSA in PBS and resuspended in 2% paraformaldehyde to fix. Samples were then analyzed with flow cytometry. Mean fluorescent intensity (MFI) of FITC-A was calculated from gating of Hoechst-positive cells.

Modified OPA

An opsonophagocytic killing assay was performed as described previously with modifications (43). Briefly, the type 3 WU2 and acapsular (JD908) strains were incubated in duplicate wells in a 96-well round-bottom plate for 1 hour or 4 hours at 37°C with or without Pn3Pase (inactivated or functional at concentrations of 5 or 50 ug/ml) in opsonization buffer B (OBB, sterile 1X PBS with $\text{Ca}^{++}/\text{Mg}^{++}$, 0.1% gelatin, and 5% heat-inactivated FetalClone). Human promyelocytic leukemia cell line, HL-60 (ATCC Manassas, VA) were cultured in RPMI with 10% heat-inactivated FetalClone (HyClone) and 1% L-glutamine. HL-60 cells were differentiated using 0.6% N,N-dimethylformamide (DMF, Fisher) for three days before performing the OPA assay, harvested, and resuspended in OBB. Active or heat-inactivated (no complement) baby rabbit complement (Pel-Freez) was added to HL-60 cells at 1:5 final volume. The HL-60/complement

mixture was added to the serum/bacteria at 5×10^5 cells/well (for controls, no HL-60/complement was added; equal volumes of OBB buffer was added instead). The final reactions were incubated at 37°C for 1 hour. The reactions were stopped by incubating the samples on ice for approximately 20 minutes. Then, 10 ml of each reaction was diluted to a final volume of 50 ml and plated onto blood agar plates in duplicate. Plates were incubated overnight at 30°C in anaerobic conditions and counted the next day. Percent survival was calculated as each duplicate reaction normalized to mean values obtained for control samples (reactions without HL-60 cells, 100% survival).

Murine intranasal colonization

An intranasal colonization was performed essentially as described by Puchta *et al*(64). Mid-log phase WU2 cultures were washed with sterile PBS and suspended at a concentration of 10^8 CFU/ml or 10^6 CFU/10 ml. Groups of 5 to 10 unanesthetized 8-week-old female BALB/c mice (Taconic) were intranasally inoculated with 10^6 CFU/10 ml as previously described. Mice were either inoculated with 10 ml of PBS as vehicle on day 0,3, and 7 or treated by administering 50mg of Pn3Pase in 10 ml PBS on day 0, 0 and 3, or 0,3, and 7. Nasal lavage fluid was obtained on day 10 by flushing out the nasopharynx with PBS by insertion of a 25 gauge needle into the trachea to expel 500 ml through the nares. Serial dilutions of the nasal lavage fluid were plated on Tryptic Soy Agar with 5% sheep blood (TSAB), to enumerate the colony forming units. A sandwich ELISA (Biolegend mouse ELISA MAX) was performed according to manufacturers instructions to determine IL-6 and TNF α cytokine levels in the lavage fluid.

Murine sepsis challenge

Mid-log phase WU2 cultures were washed with sterile PBS and suspended at a concentration of 5×10^3 CFU/100 mL. Groups of 4 unanesthetized 8-week-old female BALB/c mice (Taconic)

were injected intraperitoneally (I.P.) with 5×10^3 CFU. Control mice were injected I.P. with 5mg of heat inactivated Pn3Pase in 100 mL of PBS at time 0, or directly after infection. Treated mice were administered I.P. 0.5 mg or 5 mg of Pn3Pase in 100 mL PBS at time 0, 12, or 24 hours post infection. Animals were monitored every 12 hours.

Ethics statement

All mouse experiments were in compliance with the University of Georgia Institutional Animal Care and Use Committee under the approved animal use protocol 2478 A2016 11-022-Y1-A0. Our animal use protocol adheres to the principles outlined in *U.S Government Principles for the Utilization and Care of Vertebrate Animals Used in Testing, Research and Training*, the *Animal Welfare Act*, the *Guide for the Care and Use of Laboratory Animals*, and the *AVMA Guidelines for the Euthanasia of Animals*.

Acknowledgements

We thank Dr. Moon Nahm (University of Alabama Birmingham) for providing us with the type 3 WU2 strain and the acapsular WU2 mutant strain (JD908) of *S. pneumoniae*. We thank Dr. Christine Szymanski for her critical review. TEM work was conducted in the Georgia Electron Microscope Lab at the University of Georgia, Athens, GA, USA.

References

1. Jochems, S. P., J. N. Weiser, R. Malley, and D. M. Ferreira. 2017. The immunological mechanisms that control pneumococcal carriage. *PLoS Pathog* 13: e1006665.
2. Austrian, R. 1986. Some aspects of the pneumococcal carrier state. *J Antimicrob Chemother* 18 Suppl A: 35-45.
3. Goldblatt, D., M. Hussain, N. Andrews, L. Ashton, C. Virta, A. Melegaro, R. Pebody, R. George, A. Soininen, J. Edmunds, N. Gay, H. Kayhty, and E. Miller. 2005. Antibody responses to nasopharyngeal carriage of *Streptococcus pneumoniae* in adults: a longitudinal household study. *J Infect Dis* 192: 387-393.
4. Bogaert, D., R. De Groot, and P. W. Hermans. 2004. *Streptococcus pneumoniae* colonisation: the key to pneumococcal disease. *Lancet Infect Dis* 4: 144-154.
5. Simell, B., K. Auranen, H. Käyhty, D. Goldblatt, R. Dagan, K. L. O'Brien, and P. C. Group. 2012. The fundamental link between pneumococcal carriage and disease. *Expert Rev Vaccines* 11: 841-855.
6. Magee, A. D., and J. Yother. 2001. Requirement for capsule in colonization by *Streptococcus pneumoniae*. *Infect Immun* 69: 3755-3761.
7. Watson, D. A., and D. M. Musher. 1990. Interruption of capsule production in *Streptococcus pneumoniae* serotype 3 by insertion of transposon Tn916. *Infect Immun* 58: 3135-3138.

8. Nelson, A. L., A. M. Roche, J. M. Gould, K. Chim, A. J. Ratner, and J. N. Weiser. 2007. Capsule enhances pneumococcal colonization by limiting mucus-mediated clearance. *Infect Immun* 75: 83-90.
9. Bruyn, G. A., B. J. Zegers, and R. van Furth. 1992. Mechanisms of host defense against infection with *Streptococcus pneumoniae*. *Clin Infect Dis* 14: 251-262.
10. Winkelstein, J. A. 1984. Complement and the host's defense against the pneumococcus. *Crit Rev Microbiol* 11: 187-208.
11. Winkelstein, J. A. 1981. The role of complement in the host's defense against *Streptococcus pneumoniae*. *Rev Infect Dis* 3: 289-298.
12. Grabenstein, J. D., and K. P. Klugman. 2012. A century of pneumococcal vaccination research in humans. *Clin Microbiol Infect* 18 Suppl 5: 15-24.
13. MacLeod, C. M., R. G. Hodges, M. Heidelberger, and W. G. Bernhard. 1945. Prevention of pneumococcal pneumonia by immunization with specific capsular polysaccharides. *J. Exp. Med.* 82: 445-465.
14. Geno, K. A., G. L. Gilbert, J. Y. Song, I. C. Skovsted, K. P. Klugman, C. Jones, H. B. Konradsen, and M. H. Nahm. 2015. Pneumococcal Capsules and Their Types: Past, Present, and Future. *Clin Microbiol Rev* 28: 871-899.
15. Wantuch, P. L., and F. Y. Avci. 2018. Current status and future directions of invasive pneumococcal diseases and prophylactic approaches to control them. *Hum Vaccin Immunother*: 1-19.
16. Avci, F., and D. Kasper. 2010. How Bacterial Carbohydrates Influence the Adaptive Immune System. *Annu Rev Immunol* 28: 107-130.

17. Avci, F. 2013. Novel Strategies for Development of Next-Generation Glycoconjugate Vaccines. *Current Topics in Medicinal Chemistry* 13: 2535-2540.
18. Avci, F., X. Li, M. Tsuji, and D. Kasper. 2011. A mechanism for glycoconjugate vaccine activation of the adaptive immune system and its implications for vaccine design. *Nat Med* 17: 1602-U1115.
19. Alicino, C., C. Paganino, A. Orsi, M. Astengo, C. Trucchi, G. Icardi, and F. Ansaldi. 2017. The impact of 10-valent and 13-valent pneumococcal conjugate vaccines on hospitalization for pneumonia in children: A systematic review and meta-analysis. *Vaccine* 35: 5776-5785.
20. Bonten, M. J., S. M. Huijts, M. Bolkenbaas, C. Webber, S. Patterson, S. Gault, C. H. van Werkhoven, A. M. van Deursen, E. A. Sanders, T. J. Verheij, M. Patton, A. McDonough, A. Moradoghli-Haftvani, H. Smith, T. Mellelieu, M. W. Pride, G. Crowther, B. Schmoele-Thoma, D. A. Scott, K. U. Jansen, R. Lobatto, B. Oosterman, N. Visser, E. Caspers, A. Smorenburg, E. A. Emini, W. C. Gruber, and D. E. Grobbee. 2015. Polysaccharide conjugate vaccine against pneumococcal pneumonia in adults. *N Engl J Med* 372: 1114-1125.
21. Tin Tin Htar, M., A. L. Stuurman, G. Ferreira, C. Alicino, K. Bollaerts, C. Paganino, R. R. Reinert, H. J. Schmitt, C. Trucchi, T. Vestraeten, and F. Ansaldi. 2017. Effectiveness of pneumococcal vaccines in preventing pneumonia in adults, a systematic review and meta-analyses of observational studies. *PLoS One* 12: e0177985.
22. Harboe, Z. B., T. Dalby, D. M. Weinberger, T. Benfield, K. Mølbak, H. C. Slotved, C. H. Suppli, H. B. Konradsen, and P. Valentiner-Branth. 2014. Impact of 13-valent

- pneumococcal conjugate vaccination in invasive pneumococcal disease incidence and mortality. *Clin Infect Dis* 59: 1066-1073.
23. Dagan, R., S. Patterson, C. Juergens, D. Greenberg, N. Givon-Lavi, N. Porat, A. Gurtman, W. C. Gruber, and D. A. Scott. 2013. Comparative immunogenicity and efficacy of 13-valent and 7-valent pneumococcal conjugate vaccines in reducing nasopharyngeal colonization: a randomized double-blind trial. *Clin Infect Dis* 57: 952-962.
 24. Gruber, W. C., D. A. Scott, and E. A. Emini. 2012. Development and clinical evaluation of Prevnar 13, a 13-valent pneumococcal CRM197 conjugate vaccine. *Ann N Y Acad Sci* 1263: 15-26.
 25. Richter, S. S., K. P. Heilmann, C. L. Dohrn, F. Riahi, D. J. Diekema, and G. V. Doern. 2013. Pneumococcal serotypes before and after introduction of conjugate vaccines, United States, 1999-2011(1.). *Emerg Infect Dis* 19: 1074-1083.
 26. Middleton, D. R., X. Zhang, P. L. Wantuch, A. Ozdilek, X. Liu, R. LoPilato, N. Gangasani, R. Bridger, L. Wells, R. J. Linhardt, and F. Y. Avci. 2018. Identification and characterization of the *Streptococcus pneumoniae* type 3 capsule-specific glycoside hydrolase of *Paenibacillus* species 32352. *Glycobiology* 28: 90-99.
 27. Li, G., L. Li, C. Xue, D. Middleton, R. J. Linhardt, and F. Y. Avci. 2015. Profiling pneumococcal type 3-derived oligosaccharides by high resolution liquid chromatography-tandem mass spectrometry. *Journal of chromatography. A* 1397: 43-51.
 28. Kieninger, D. M., K. Kueper, K. Steul, C. Juergens, N. Ahlers, S. Baker, K. U. Jansen, C. Devlin, W. C. Gruber, E. A. Emini, D. A. Scott, and s. group. 2010. Safety, tolerability, and immunologic noninferiority of a 13-valent pneumococcal conjugate vaccine

- compared to a 7-valent pneumococcal conjugate vaccine given with routine pediatric vaccinations in Germany. *Vaccine* 28: 4192-4203.
29. Jackson, L., H. El Sahly, S. George, P. Winokur, K. Edwards, R. Brady, N. Roupael, W. Keitel, M. Mulligan, R. Burton, A. Nakamura, J. Ferreria, and M. Nahm. 2018. Randomized clinical trial of a single versus a double dose of 13-valent pneumococcal conjugate vaccine in adults 55 through 74 years of age previously vaccinated with 23-valent pneumococcal polysaccharide vaccine. *Vaccine* 36: 606-614.
30. Briles, D. E., M. J. Crain, B. M. Gray, C. Forman, and J. Yother. 1992. Strong association between capsular type and virulence for mice among human isolates of *Streptococcus pneumoniae*. *Infect Immun* 60: 111-116.
31. Weinberger, D. M., Z. B. Harboe, E. A. Sanders, M. Ndiritu, K. P. Klugman, S. Rückinger, R. Dagan, R. Adegbola, F. Cutts, H. L. Johnson, K. L. O'Brien, J. A. Scott, and M. Lipsitch. 2010. Association of serotype with risk of death due to pneumococcal pneumonia: a meta-analysis. *Clin Infect Dis* 51: 692-699.
32. Martens, P., S. W. Worm, B. Lundgren, H. B. Konradsen, and T. Benfield. 2004. Serotype-specific mortality from invasive *Streptococcus pneumoniae* disease revisited. *BMC Infect Dis* 4: 21.
33. Sugimoto, N., Y. Yamagishi, J. Hirai, D. Sakanashi, H. Suematsu, N. Nishiyama, Y. Koizumi, and H. Mikamo. 2017. Invasive pneumococcal disease caused by mucoid serotype 3 *Streptococcus pneumoniae*: a case report and literature review. *BMC Res Notes* 10: 21.

34. Kim, L., L. McGee, S. Tomczyk, and B. Beall. 2016. Biological and Epidemiological Features of Antibiotic-Resistant *Streptococcus pneumoniae* in Pre- and Post-Conjugate Vaccine Eras: a United States Perspective. *Clin Microbiol Rev* 29: 525-552.
35. Li, Y., B. J. Metcalf, S. Chochua, Z. Li, R. E. Gertz, H. Walker, P. A. Hawkins, T. Tran, C. G. Whitney, L. McGee, and B. W. Beall. 2016. Penicillin-Binding Protein Transpeptidase Signatures for Tracking and Predicting β -Lactam Resistance Levels in *Streptococcus pneumoniae*. *MBio* 7.
36. Metcalf, B. J., R. E. Gertz, R. A. Gladstone, H. Walker, L. K. Sherwood, D. Jackson, Z. Li, C. Law, P. A. Hawkins, S. Chochua, M. Sheth, N. Rayamajhi, S. D. Bentley, L. Kim, C. G. Whitney, L. McGee, B. Beall, and A. B. C. s. team. 2016. Strain features and distributions in pneumococci from children with invasive disease before and after 13-valent conjugate vaccine implementation in the USA. *Clin Microbiol Infect* 22: 60.e69-60.e29.
37. Obolski, U., J. Lourenço, C. Thompson, R. Thompson, A. Gori, and S. Gupta. 2018. Vaccination can drive an increase in frequencies of antibiotic resistance among nonvaccine serotypes of. *Proc Natl Acad Sci U S A* 115: 3102-3107.
38. Zhao, C., Z. Li, F. Zhang, X. Zhang, P. Ji, J. Zeng, B. Hu, Z. Hu, K. Liao, H. Sun, R. Zhang, B. Cao, C. Zhuo, W. Jia, Y. Mei, Y. Chu, X. Xu, Q. Yang, Y. Jin, Q. Fu, H. Li, L. Wang, Y. Ni, H. Liang, and H. Wang. 2017. Serotype distribution and antibiotic resistance of *Streptococcus pneumoniae* isolates from 17 Chinese cities from 2011 to 2016. *BMC Infect Dis* 17: 804.
39. Avery, O. T., and R. Dubos. 1930. The specific action of a bacterial enzyme on pneumococci of type III. *Science* 72: 151-152.

40. Dubos, R., and O. T. Avery. 1931. Decomposition of the capsular polysaccharide of pneumococcus type III by a bacterial enzyme *J Exp Med* 54: 51-71.
41. Avery, O. T., and R. Dubos. 1931. The protective action of a specific enzyme against type III pneumococcus infection in mice. *J Exp Med* 54: 73-89.
42. Middleton, D. R., W. Lorenz, and F. Y. Avci. 2017. Complete Genome Sequence of the Bacterium *Bacillus circulans* Jordan Strain 32352. *Genome Announcements* (In press).
43. Burton, R. L., and M. H. Nahm. 2012. Development of a fourfold multiplexed opsonophagocytosis assay for pneumococcal antibodies against additional serotypes and discovery of serological subtypes in *Streptococcus pneumoniae* serotype 20. *Clin Vaccine Immunol* 19: 835-841.
44. Daniels, C. C., K. H. Kim, R. L. Burton, S. Mirza, M. Walker, J. King, Y. Hale, P. Coan, D. K. Rhee, M. H. Nahm, and D. E. Briles. 2013. Modified opsonization, phagocytosis, and killing assays to measure potentially protective antibodies against pneumococcal surface protein A. *Clin Vaccine Immunol* 20: 1549-1558.
45. Fleck, R. A., S. Romero-Steiner, and M. H. Nahm. 2005. Use of HL-60 cell line to measure opsonic capacity of pneumococcal antibodies. *Clin Diagn Lab Immunol* 12: 19-27.
46. Romero-Steiner, S., C. E. Frasch, G. Carlone, R. A. Fleck, D. Goldblatt, and M. H. Nahm. 2006. Use of opsonophagocytosis for serological evaluation of pneumococcal vaccines. *Clin Vaccine Immunol* 13: 165-169.
47. Song, J. Y., M. A. Moseley, R. L. Burton, and M. H. Nahm. 2013. Pneumococcal vaccine and opsonic pneumococcal antibody. *J Infect Chemother* 19: 412-425.

48. Middleton, D. R., L. Sun, A. V. Paschall, and F. Y. Avci. 2017. T Cell-Mediated Humoral Immune Responses to Type 3 Capsular Polysaccharide of *J Immunol* 199: 598-603.
49. Craig, A., J. Mai, S. Cai, and S. Jeyaseelan. 2009. Neutrophil recruitment to the lungs during bacterial pneumonia. *Infect Immun* 77: 568-575.
50. Lu, Y. J., J. Gross, D. Bogaert, A. Finn, L. Bagrade, Q. Zhang, J. K. Kolls, A. Srivastava, A. Lundgren, S. Forte, C. M. Thompson, K. F. Harney, P. W. Anderson, M. Lipsitch, and R. Malley. 2008. Interleukin-17A mediates acquired immunity to pneumococcal colonization. *PLoS Pathog* 4: e1000159.
51. Zhang, Z., T. B. Clarke, and J. N. Weiser. 2009. Cellular effectors mediating Th17-dependent clearance of pneumococcal colonization in mice. *J Clin Invest* 119: 1899-1909.
52. Blanchette-Cain, K., C. A. Hinojosa, R. Akula Suresh Babu, A. Lizcano, N. Gonzalez-Juarbe, C. Munoz-Almagro, C. J. Sanchez, M. A. Bergman, and C. J. Orihuela. 2013. *Streptococcus pneumoniae* biofilm formation is strain dependent, multifactorial, and associated with reduced invasiveness and immunoreactivity during colonization. *MBio* 4: e00745-00713.
53. Briles, D. E., M. Nahm, K. Schroer, J. Davie, P. Baker, J. Kearney, and R. Barletta. 1981. Antiphosphocholine antibodies found in normal mouse serum are protective against intravenous infection with type 3 streptococcus pneumoniae. *J Exp Med* 153: 694-705.
54. Chiavolini, D., G. Pozzi, and S. Ricci. 2008. Animal models of *Streptococcus pneumoniae* disease. *Clin Microbiol Rev* 21: 666-685.

55. Fenton, M., P. Ross, O. McAuliffe, J. O'Mahony, and A. Coffey. 2010. Recombinant bacteriophage lysins as antibacterials. *Bioeng Bugs* 1: 9-16.
56. Fuchs, H. J., D. S. Borowitz, D. H. Christiansen, E. M. Morris, M. L. Nash, B. W. Ramsey, B. J. Rosenstein, A. L. Smith, and M. E. Wohl. 1994. Effect of aerosolized recombinant human DNase on exacerbations of respiratory symptoms and on pulmonary function in patients with cystic fibrosis. The Pulmozyme Study Group. *N Engl J Med* 331: 637-642.
57. Henrissat, B., and A. Bairoch. 1996. Updating the sequence-based classification of glycosyl hydrolases. *Biochem J* 316 (Pt 2): 695-696.
58. Shaw, M., and G. M. Sickles. 1950. Production of specific pneumococcus carbohydrate-splitting enzymes in media to which the specific substrate was not added. *J Immunol* 64: 27-32.
59. Sickles, G. M., and M. Shaw. 1934. A Systematic Study of Microorganisms Which Decompose the Specific Carbohydrates of the Pneumococcus. *J Bacteriol* 28: 415-431.
60. Dillard, J. P., M. W. Vandersea, and J. Yother. 1995. Characterization of the cassette containing genes for type 3 capsular polysaccharide biosynthesis in *Streptococcus pneumoniae*. *J Exp Med* 181: 973-983.
61. Dillard, J. P., and J. Yother. 1994. Genetic and molecular characterization of capsular polysaccharide biosynthesis in *Streptococcus pneumoniae* type 3. *Mol Microbiol* 12: 959-972.
62. Hammerschmidt, S., S. Wolff, A. Hocke, S. Rosseau, E. Müller, and M. Rohde. 2005. Illustration of pneumococcal polysaccharide capsule during adherence and invasion of epithelial cells. *Infect Immun* 73: 4653-4667.

63. Hyams, C., E. Camberlein, J. M. Cohen, K. Bax, and J. S. Brown. 2010. The *Streptococcus pneumoniae* capsule inhibits complement activity and neutrophil phagocytosis by multiple mechanisms. *Infect Immun* 78: 704-715.
64. Puchta, A., C. P. Verschoor, T. Thurn, and D. M. Bowdish. 2014. Characterization of inflammatory responses during intranasal colonization with *Streptococcus pneumoniae*. *J Vis Exp*: e50490.

Figure 4.1

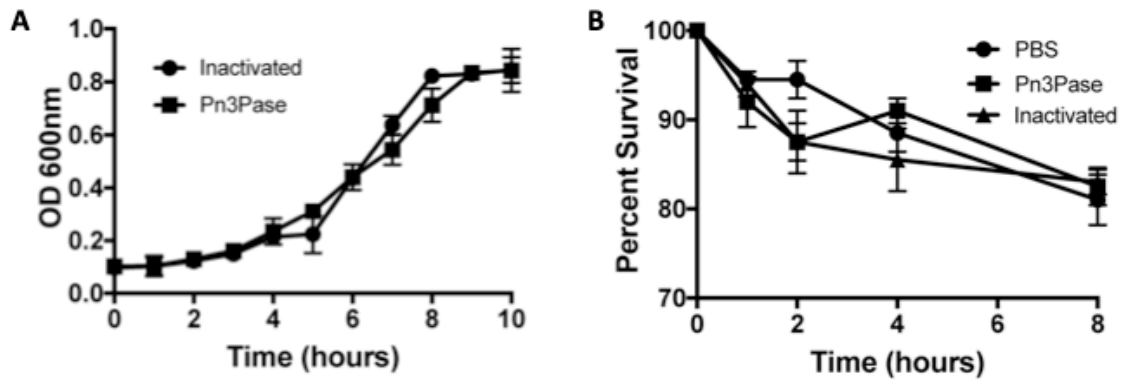


Fig 4.1. Effects of Pn3Pase treatment on type 3 *Spn* viability.

(A) Growth curve of WU2 in THY broth in the presence of 100mg/ml Pn3Pase following the OD at 600 nm. (B) WU2 survival in PBS in the presence of 100mg/ml active or heat inactivated Pn3Pase.

Figure 4.2

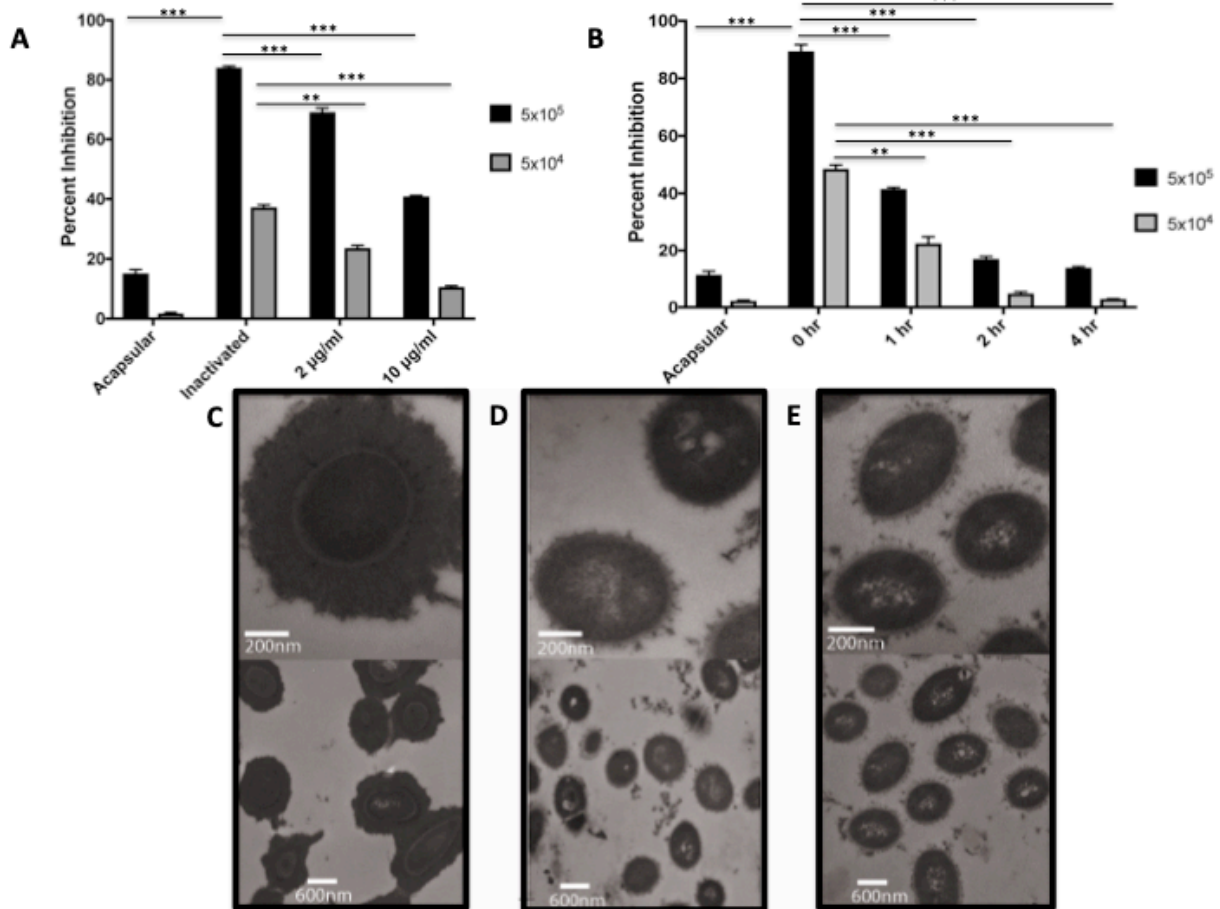


Fig 4.2. Depleting the capsule on live type 3 *Spn* by Pn3Pase treatment.

(A-B) Competition ELISA in which acapsular WU2, WU2 treated with heat-inactivated Pn3Pase, or WU2 treated with Pn3Pase at two different concentrations (2mg/ml or 10mg/ml) were used to compete for Pn3P specific antibody binding to Pn3P coated ELISA plate. Data is presented as percent inhibition of antibody binding. Statistical significance was determined with the two-tailed Student *t* test ** P<0.01, *** P<0.001. Transmission electron microscopy images of WU2 mock treated with 2mg/ml heat-inactivated Pn3Pase (C), acapsular WU2 strain (D) and 2mg/ml active-Pn3Pase treated WU2 (E). Bottom panels are imaged at 15000X direct magnification and top panels are imaged at 10000X direct magnification (C-E).

Figure 4.3

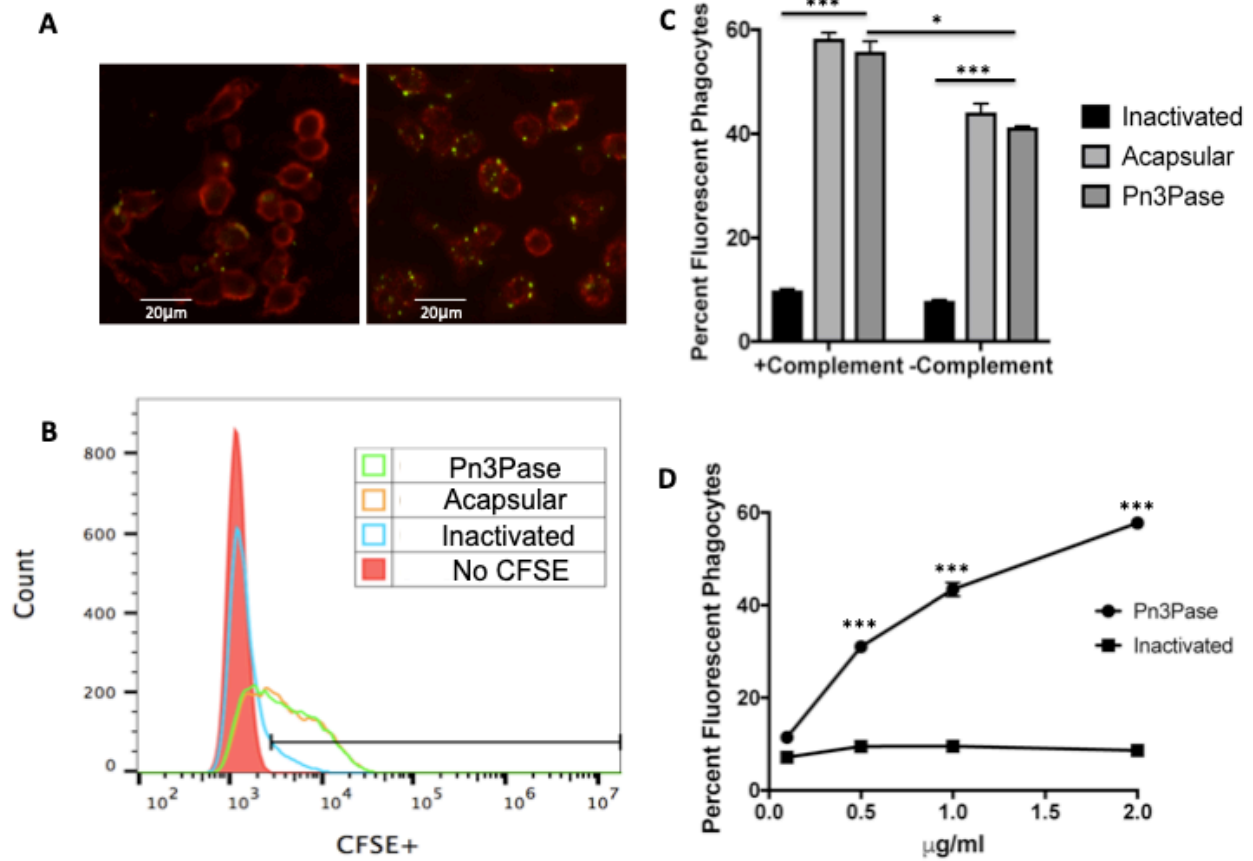


Fig 4.3. Macrophage uptake of type 3 *Spn* treated with Pn3Pase.

(A) A representative RAW 264.7 macrophage containing fluorescent streptococci following Pn3Pase treatment. Streptococci, CFSE, green. Macrophage, Biotinylated-WGA, Streptavidin-APC, red. (B) Histogram of the flow cytometry analysis of fluorescent phagocytes demonstrating increased fluorescence intensity for the acapsular control and Pn3Pase treated WU2 strain. (C) Influence of Pn3Pase treatment and complement on macrophage uptake of CFSE labeled *Spn* quantified by flow cytometry. (D) Pn3Pase dose dependent effect on the percent of fluorescent phagocytes. Statistical significance was determined with the two-tailed Student *t* test *** $P < 0.001$.

Figure 4.4

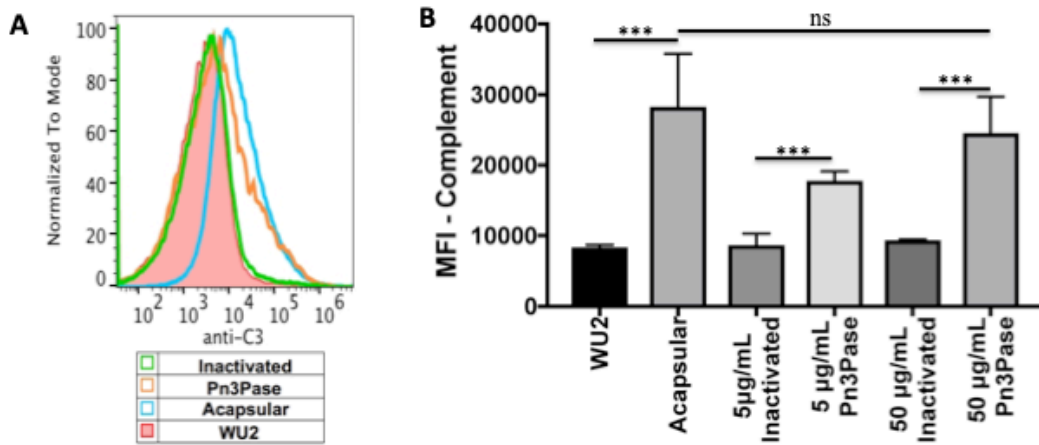


Fig 4.4. Effect of Pn3Pase treatment on complement deposition on *Spn* surface.

Analysis of mouse complement deposition on Pn3Pase treated or untreated type 3 *Spn* by flow cytometry. Mean fluorescent intensity (MFI) of FITC-A was calculated from gating of Hoechst-positive cells. Statistical significance was determined with the two-tailed Student *t* test ** $P < 0.01$, *** $P < 0.001$, ns= not significant

Figure 4.5

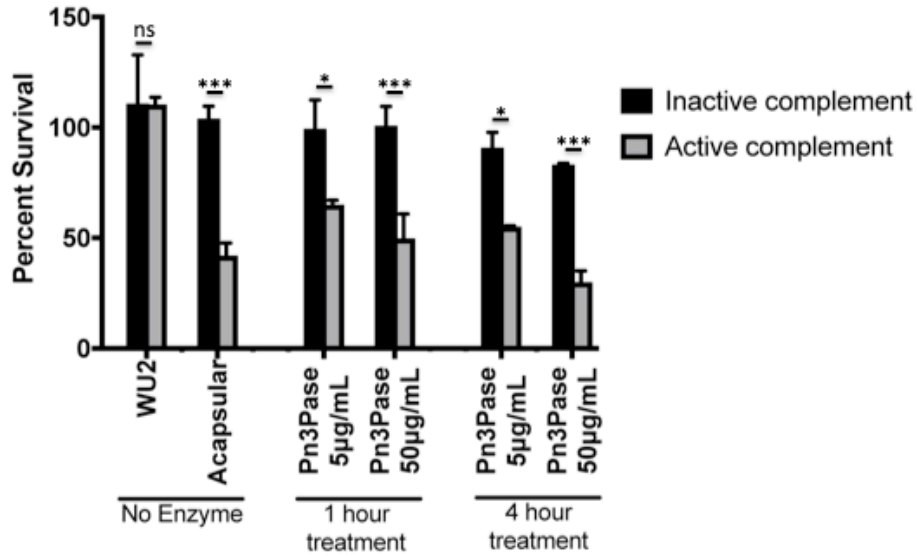


Fig 4.5. Effect of Pn3Pase treatment on complement mediated killing by neutrophils

Complement mediated killing capacity of differentiated HL-60 cells on Pn3Pase treated *Spn*. Percent survival was calculated as each duplicate reaction normalized to mean values obtained for control samples (reactions without HL60 cells, 100% survival). Statistical significance was determined with the two-tailed Student *t* test *** $P < 0.001$, ** $P < 0.01$, * $P < 0.05$, ns= not significant

Figure 4.6

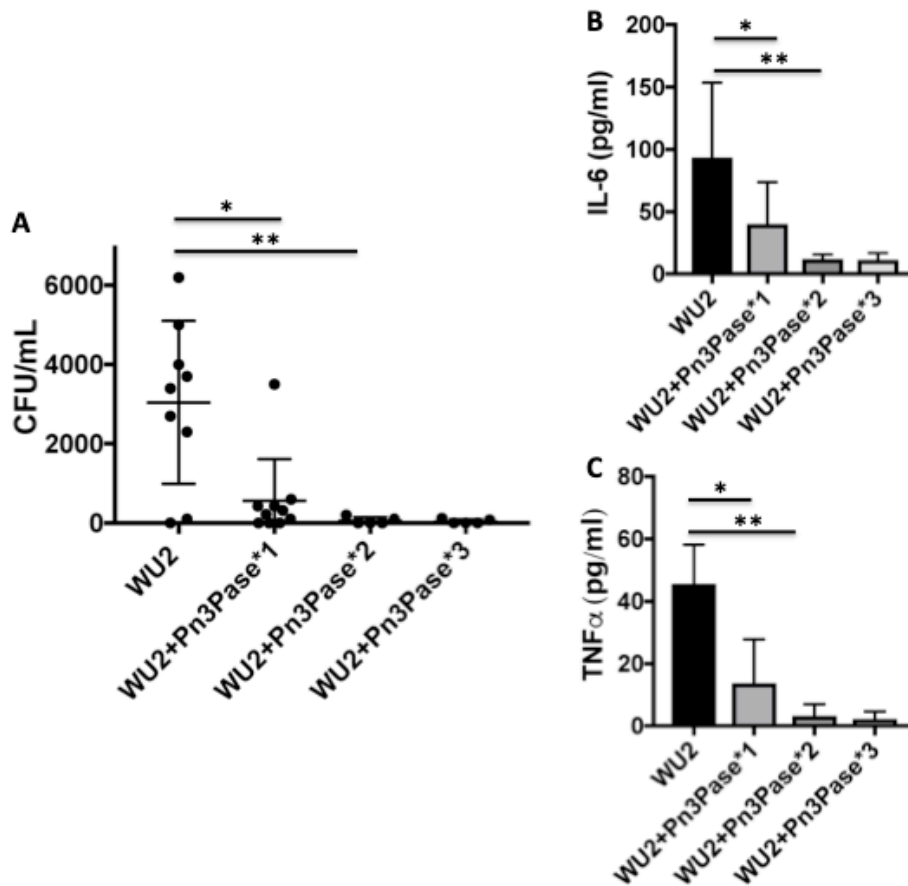


Fig 4.6. Intranasal colonization with type 3 *Spn*.

Ability of Pn3Pase treatment to reduce *Spn* colonization in nasopharynx of BALB/c mice. (A) Groups of mice were intranasally inoculated with 10^6 log-phase bacteria in 10 μ l PBS. All inocula were chased with either 50 μ g of Pn3Pase or buffer control (10 μ l). Groups were dosed with the enzyme at either day 0 (WU2+Pn3Pase*1), day 0 and 3 (WU2+Pn3Pase*2), or day 0, 3, and 7 (WU2+Pn3Pase*3). Serial dilutions of nasal lavage fluid were plated in duplicate to determine CFU values. (B) IL-6 and (C) TNF α concentrations in nasal lavage fluid was determined by ELISA. Statistical significance was determined with the two-tailed Student *t* test * $P < 0.05$, ** $P < 0.01$

Figure 4.7

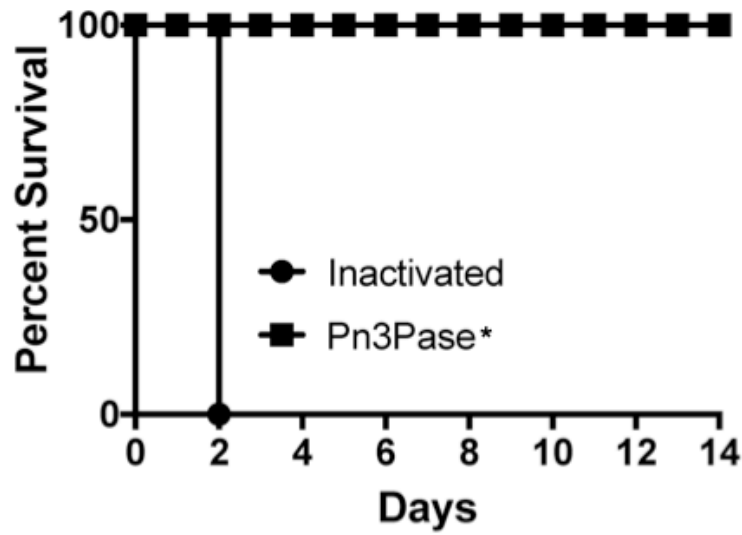


Fig 4.7. Protective ability of Pn3Pase

Assessment of ability of Pn3Pase to protect BALB/c mice from lethal challenge. Groups of mice were infected through intraperitoneal administration of 5×10^3 log-phase virulent type 3 *Spn*. *Shown are the effect of a single dose of $5 \mu\text{g}$ or $0.5 \mu\text{g}$, administered at time 0, 12, or 24 hours post infection.

CHAPTER 5

GLYCOSYLATION OF PNEUMOCOCCAL SERINE-RICH PROTEIN (PSRP) ENHANCES VIRULENCE AND HOST INFLAMMATORY RESPONSE

Dustin R Middleton, Javid Aceil, Seema Mustafa, Osman Sheikh, Jeremy A. Duke, Lance Wells
and Fikri Y. Avci

*To be submitted to *Molecular Microbiology*

Abstract

The Pneumococcal serine rich protein (PsrP) is a high-molecular weight, glycosylated adhesin that promotes bacterial attachment to host cells. PsrP, its associated glycosyltransferases, and dedicated secretion machinery, are encoded in a 37 kb genomic island that is present in ~50% of clinical isolates of *Streptococcus pneumoniae* (Spn). PsrP has been implicated in establishment of lung infection in murine models, although specific roles of the PsrP glycans in disease progression or bacterial physiology have yet to be uncovered. Moreover, enzymatic specificities of associated glycosyltransferases have not been well characterized. We hypothesize that many of the glycosyltransferases that modify PsrP are critical for the adhesion properties and infectivity of Spn. Here, we characterize the PsrP glycosylation and the putative Spn *psrP*-locus glycosyltransferases responsible for PsrP glycosylation. We also begin to elucidate their roles in Spn virulence. We show that the majority of putative glycosyltransferases within the *psrP* locus are indispensable for Spn biofilm formation, lung epithelial cell adherence, and establishment of lung infection in a mouse model of pneumococcal pneumonia.

Introduction

Streptococcus pneumoniae (Spn) is a Gram-positive bacterial pathogen that colonizes the host nasopharynx and upper respiratory tract. Although colonization in healthy individuals is asymptomatic, dissemination of the bacterium to otherwise sterile sites can prompt invasive pneumococcal diseases (IPDs) such as pneumonia (lungs), otitis media (middle ear), bacteremia (bloodstream), or meningitis (meninges)(1, 2). Spn is the leading cause of all community-acquired pneumonia cases(3). IPDs account for one million deaths in children less than 5 years of age each year(4). Despite vaccination programs and availability of antibiotic therapies, the

mortality rate for pneumococcal pneumonia remains as high as 40% in infants and the elderly(5, 6).

The pneumococcal serine-rich protein, or PsrP, is a putative adhesin protein that mediates bacterial attachment to host as well as other bacterial cells(7). This large glycoprotein is encoded in a 37-kb genomic island, *psrP-secY2A2* (**Figure 5.1A**). The *PsrP* island is present and conserved in many invasive clones of the pneumococcus(8). These loci carry all of the genes necessary to glycosylate and export the PsrP to the bacterial surface(9). PsrP consists of a signal peptide, a short, glycosylated serine rich repeat region, followed by a basic region composed mostly of lysine residues, a very long, glycosylated serine rich repeat region, and a domain to anchor the protein to the cell wall peptidoglycan.

Multiple reports have implicated PsrP in establishment of lung infection in murine models(7-11). As of yet, the specific roles of the PsrP glycans in disease progression or bacterial physiology are not completely understood. Moreover, enzymatic properties and specificities of these glycosyltransferases (**Figure 5.1B**) along with their potential role in bacterial virulence mechanisms have yet to be fully characterized. Here, we begin to characterize the putative *Spn psrP*-locus glycosyltransferases and elucidate their roles in *Spn* virulence. We hypothesize that many of the glycosyltransferases that modify PsrP are critical for the adhesion properties and infectivity of *Spn*.

Using recombinant enzymes we assess the sugar-nucleotide donor specificities of the glycosyltransferases within the *psrP* locus. We then create single gene mutant strains for each of the putative glycosyltransferases within this locus. We determine the enzymes necessary for *Spn* biofilm formation, lung epithelial cell adherence, and establishment of pneumococcal pneumonia in a mouse intratracheal infection.

Results

Glycosyltransferase sugar nucleotide specificities

Previous studies have reported that SP_1758 catalyzes the first step of PsrP glycosylation with the addition of an N-Acetyl Glucosamine (GlcNAc) residue(12, 13). The activities of the other glycosyltransferases in the psrP locus remain unknown. For preliminary characterization of the putative GTs of Spn, each enzyme was tested for its ability to hydrolyze UDP-sugars to determine sugar donor specificity in absence of acceptor substrate (**Figure 5.2A-E**). The reactions were assessed by detecting free UDP after hydrolysis using the UDP-Glo Glycosyltransferase assay kit (Promega) and six common available ultrapure UDP-sugars(14). While each enzyme showed some level of UDP-sugar hydrolysis, it is important to consider additional or preferred activities for other Spn sugar-nucleotide donors such as dTDP-Rha, UDP-ManNAc, UDP-FucNAc. The results confirmed the UDP-GlcNAc specificity of SP_1758 (**Figure 5.2A**). Furthermore, The only two donor sugars hydrolyzed by these GTs were UDP-Glucose and UDP-Galactose. While SP_1766, SP_1767, and SP_1771 preferentially utilize UDP-Galactose, SP_1768 shows specificity for UDP-Glucose. Surprisingly, SP_1765 hydrolyzed both UDP-Glucose and UDP-Galactose at very similar levels (**Figure 5.2B**).

PsrP is expressed in Δ GT mutant strains of Spn

Glycan modifications on proteins often can contribute to protein stability and solubility(15). To determine if deletion of PsrP-modifying glycosyltransferases influences PsrP stability or surface localization, we probed the WT or deletion strains with serum generated against the polybasic N-terminus of the protein, termed 72N. In a whole cell ELISA (**Figure 5.3A**) wild-type and GT mutant strains showed high 72N serum IgG binding, whereas the Omega (Δ psrP-SecY2A2) strain, Δ 1772(PsrP) strain, and Spn WU2 strain naturally lacking the

psrP locus were not recognized by the anti-sera indicating that the GT mutant strains display near equivalent quantities of PsrP. Furthermore, cell lysates from wild type and mutant strains were separated by SDS-PAGE and blotted with 72N serum. A high molecular weight protein band was reactive in all Δ GT strains, but not the Omega strain (**Figure 5.3B**). These results were confirmed by proteomics. This data indicates that PsrP is expressed on the surface of mutant strains, and defects in glycosylation do not drastically influence protein stability or secretion.

The *PsrP* locus glycosyltransferases are essential for biofilm formation

PsrP has been reported as a major adhesion that promotes bacterial aggregation and biofilm formation(7, 9, 16). We hypothesized that PsrP glycosylation could contribute to establishment of biofilms. We tested the capacity for the wild type and mutant strains to form a biofilm in a 24-hour assay on a polystyrene microtiter plate or glass cover slips for confocal microscopy. Biofilms were stained with crystal violet (**Figure 5.4A-C**) or Syto 9 (Figure 5A-B). The Ω strain that is missing PsrP and all associated glycosyltransferases failed to form a thick biofilm. Additionally, strains SP_1758, SP_1765, SP_1768, SP_1771, and SP_1772 were significantly impaired in the ability for form biofilms as shown by crystal violet staining of the biofilms grown on polystyrene plate or Syto 9 staining of biofilms grown on borosilicate glass coverslips (**Figure 5.4 and 5.5**). SP_1766 and SP_1767 strains formed biofilms of comparable intensities and thickness to the wild type strain, which grew to an average thickness of 27.2 μ m (**Figure 5.5B**).

Glycosylation mediates adherence to lung epithelial cells

A critical step in disease progression to pneumococcal pneumonia is adherence to lung epithelium(2). Because PsrP is a putative adhesin, we tested the wild type and GT mutant strains

to determine the role of PsrP glycosylation an *in vitro* lung epithelial cell adherence assay using A549 cells. We observed a significant reduction in A549 binding *in vitro* for all of the mutant strains tested, with the exception of SP_1766 and SP_1767 (**Figure 5.6**). Eighty-nine percent of the Wild-Type TIGR4 strain that was incubated on the confluent A549 monolayer bound, whereas only 52-56% of the most of the mutant strains bound. Again, SP_1766 and SP_1767 mutants had similar results to the wild-type at 86% and 93%, respectively. These results demonstrate a critical role for extended glycosylation of PsrP in binding to lung epithelium, and also show that SP_1766 and SP_1767 do not have critical activities that promote this binding.

Glycosyltransferases are indispensable for lung infection

It is known that the PsrP locus of the TIGR4 strain of Spn is required for lung infection in mice(17). However, the contribution of the PsrP-specific glycosyltransferases remains unclear. We performed an intratracheal infection of BALB/c mice with the wild-type and mutant strains to determine the roles of each GT in establishment of pneumococcal pneumonia. While one mouse from the PsrP locus deficient Ω strain, and one mouse from the Δ 1758 strain had measurable bacterial titers in the bronchoalveolar lavage fluid (BALF), only the wild-type strain was able to consistently infect the lung tissues of these mice (shown in **Figure 5.7A**), clearly demonstrating a role for the extended glycosylation of PsrP in establishing infection. No measurable bacterial loads were found in the blood of the mice in any groups. Pro-inflammatory IL-6 and TNF α levels were measured in the BALF (18). Wild-Type infected mice had significantly increased levels of both IL-6 and TNF α compared BALF of mice infected with mutant strains (**Figs 5.7B-C**) (18).

Discussion

Previous reports have implicated the pneumococcal serine rich protein in bacterial aggregation, biofilm formation, and virulence capacity of Spn. However, these studies have attributed their findings to the PsrP peptide backbone, specifically the N-terminal basic region of the protein(17, 19, 20). Specific roles of PsrP glycosylation, or contributions of PsrP-modifying glycosyltransferases have not been elucidated. Moreover, enzymatic properties and specificities of these glycosyltransferases have yet to be fully characterized. The majority of pneumococcal pneumonia clinical isolates contain the *psrP* locus in the genome, and the downstream glycosyltransferases are surprisingly well-conserved, suggesting their critical activities for Spn pathogenesis. We hypothesized that many of the glycosyltransferases that modify PsrP are critical for the adhesion properties and infectivity of Spn. Here, using single gene mutant strains for each of the putative glycosyltransferases within this locus we determined the enzymes necessary for Spn virulence properties *in vitro* and *in vivo*.

Previous reports have suggested that SP_1758 is important for PsrP stability, however the authors of the study recognize a lack of clear and convincing evidence for this(9). This is in contrast with our results here using anti-sera against PsrP to detect the protein in all of the Δ GT strains that we constructed. We can, therefore, consider that defects in bacterial aggregation, biofilm formation, cell adherence, and lung infection for strains lacking specific glycosyltransferases if an effect of missing glycan modifications on PsrP, although direct evidence for glycosylation changes is not presented in this work.

Interestingly, our results indicate that SP_1766 and SP_1767 are dispensable in *in vitro* virulence assays. This raises the possibility that these are redundant gene products and activities. Protein BLAST analysis reveals 38% identity across the length of the protein sequences and 58%

positive amino acid homology. Additionally, our preliminary UDP-sugar hydrolysis assays suggest that these enzymes can preferentially transfer galactose moieties. Future experiments will utilize a double knockout Spn strain to determine the effects of knocking out both genes in *in vitro* and *in vivo* experiments.

Based on reduction in lung epithelial cell binding by most Δ GT strains, we propose the existence of specific surface lectins on lung epithelium that recognize the mature PsrP glycoform. It has been proposed that Spn lung epithelium binding is mediated through the PsrP basic region binding to Keratin 10(20). While this may be one mechanism that contributes to binding, there is certainly a clear and demonstrable defect in binding of non-glycosylated PsrP Spn strains. Our results show that ~50% of Spn binds independent of PsrP glycosylation status. However, PsrP glycosylation remains critical for TIGR4 Spn pathogenesis in the murine pneumonia model.

There is very limited knowledge of PsrP glycosylation, biosynthetic pathways and potential role of PsrP glycans in Spn virulence and immunogenicity of PsrP (7, 9, 12, 17). However, there is an abundance of putative GTs with unknown function. Efforts to dissect the enzymatic pathway for PsrP glycosylation have begun to examine specificity and sequence of transfer to PsrP(13), but delineating the oligosaccharide structures on the natively expressed protein has remained out of reach. Furthermore, PsrP glycans may be a promising vaccine target as the immense size of the protein allows these epitopes to extend past the capsular polysaccharide shield. Therefore, we will evaluate the wild-type PsrP glycoform in vaccine constructs and assess protective capacities of these vaccines.

In conclusion, our results clearly demonstrate that the majority of putative glycosyltransferases within the psrP locus are indispensable for Spn biofilm formation, lung

epithelial cell adherence, and establishing lung infection in a murine model of pneumococcal pneumonia. Future studies will utilize the Δ GT strains constructed here to analyze changes in glycosylation profile and determine specific transfer activities of each glycosyltransferase within the PsrP glycosylation pathway.

Materials and Methods

Bacterial strains and mutant construction

Streptococcus pneumoniae type 4 (TIGR4 strain) and T4 Δ psrP-secY2A2 (Ω) generous gifts from Carlos Orihuela (University of Alabama at Birmingham), were cultured aerobically without shaking at 37 °C on Tryptic Soy Agar with 5% sheep blood (TSAB), or in Todd Hewitt Broth plus 0.5% yeast extract (THY) (BD Biosciences). Glycosyltransferase knock-out (Δ GT) strains were generated by allelic replacement with a “Sweet” janus cassette(21). Briefly, DNA fragments flanking each gene were amplified and assembled up and downstream of the cassette encoding SacB and Kanamycin resistance genes. Δ GT strains were selected and grown with kanamycin supplementation (200ug/ml). Primers used for mutant construction can be found in **table 5.1**.

Mice

Five-week-old female BALB/c mice were obtained from Taconic Biosciences (Hudson, NY) and housed in the Central Animal Facility at the University of Georgia. Mice were kept in microisolator cages and handled under BSL-2 hoods. All mouse experiments were in compliance with the University of Georgia Institutional Animal Care and Use Committee under the approved animal use protocol 2478 A2016 11-022-Y1-A0. Our animal use protocol adheres to the principles outlined in *U.S Government Principles for the Utilization and Care of Vertebrate*

Animals Used in Testing, Research and Training, the Animal Welfare Act, the Guide for the Care and Use of Laboratory Animals, and the AVMA Guidelines for the Euthanasia of Animals.

Recombinant glycosyltransferase production

Coding regions of GTs lacking a stop codon were obtained in Gateway clone sets from BEI Resources. An LR clonase(Thermo Scientific) reaction was performed to insert the gene into the pET-Dest42 destination vector for the expression of a C-terminal His-tagged fusion protein in BL21 cells. Glycosyltransferases were produced as described previously with minor modifications(22). Briefly, BL21(DE3) cells transformed with the pET-DEST42-GT plasmids were grown in Luria Broth supplemented with 100 µg/ml ampicillin at 37 °C, and cell density was monitored by absorbance at 600 nm. Once the OD 600 nm reached 0.6, the cells were transferred into 25 °C. Protein expression was induced by the addition of Isopropyl β-D-1-thiogalactopyranoside at a final concentration of 1 mM and the culture was incubated with shaking for 8 h. Cells were harvested by centrifugation, resuspended in phosphate-buffered saline (PBS, pH 7.2) and lysed by sonication. The lysate was clarified by centrifugation at 17,000 × g for 1 h at 4°C, and passed through a 0.45 µm syringe filter. Enzymes were purified by Ni²⁺-NTA resin at 4 °C, eluted with 300 mM imidazole and buffer exchanged into PBS pH 7.2. Protein concentration was determined by the bicinchoninic acid assay according to the instructions of the manufacturer. Purity was evaluated by coomassie staining.

UDP-Glc glycosyltransferase hydrolysis assays

Ultra Pure UDP-Glc, UDP-GlcNAc, UDP-Gal, UDP-GalNAc and UDP-GlcA were purchased from Promega Corporation. Ultra Pure UDP-Xyl was a generous gift from Dr. Osman Sheikh from the Wells laboratory at the University of Georgia. Specificity of each recombinant enzyme's sugar-nucleotide hydrolysis activity was performed by incubation of 3 µg of >90%

pure protein with 50 μ M of a single UDP-sugar in the absence of acceptor in 20 μ L reactions containing 20mM Tris pH 7.4, 10 mM MgCl₂ at 37°C for 16 h. Control samples were all reaction components, except enzymes. Hydrolysis reactions were stopped by the addition of the UDP-Glo Detection Reagent, and detection of free UDP was performed UDP-Glo Glycosyltransferase Assay Detection per manufacturers instructions. Each sugar-nucleotide hydrolysis reaction was combined in a ratio of 1:1 (20 μ L:20 μ L) with the UDP-Glo Detection Reagent. 10 μ L of each mixture was placed in independent wells of a white, flat bottom 384-well plate (Corning) and incubated at room temperature. After 1 h incubation, Relative Luminescence Units (RLU) was measured using a microplate reader (Synergy H1, Bio-Tek).

RNA Isolation and RT-PCR

Spn cultures were harvested at mid-log phase (OD 600 nm 0.6), RNA was purified using E.N.Z.A. Bacterial RNA Kit, followed by TRIzol (Thermo Fisher Scientific) extraction of RNA from contaminating genomic DNA as described previously (23). RNA purity was assessed with nanodrop, and 1 μ g of RNA was used for reverse transcription reaction using iscript CDNA synthesis kit (BioRad). RT-PCR was performed using primers designed to amplify a fragment within the glycosyltransferase gene and knockouts were confirmed by lack of amplification with this specific primer set. Results confirmed that recombination did not result in polar effects (**supplemental Figure 5.8**).

72N terminal serum production and whole cell ELISA

The coding region of the N-terminus of PsrP from signal peptide through two SRR2 repeats (amino acid 1-320) was amplified from TIGR4 genomic DNA using primers with adapter attB sites used in gateway cloning systems (Thermo Scientific). A BP clonase reaction was performed to insert the gene into the pDONR221 vector. After sequence confirmation, an LR

clonase reaction was performed to insert the gene into the pET-Dest42 destination vector for the expression of a C-terminal His-tagged fusion protein. The vector was transformed, expressed, and purified as described above for Spn glycosyltransferases. The purified protein was used to immunize 8-week-old BALB/c mice at 5ug/dose with alum as an adjuvant. 7 days after booster immunization, serum was taken by tail-vein bleeding.

ELISA plates (96 well, Nunc) were coated with 10^7 CFU of paraformaldehyde fixed Spn strains in phosphate buffered saline (pH 7.2) overnight at 4°C. Plates were washed 4-times with PBS +0.1% Tween (PBS-T) 20 using a Biotek 405/LS microplate washer. After 1 h blocking at room temperature with 1% BSA in PBS, microplate wells were incubated for 2 h with 1:2000 dilution of 72N serum in PBS-T. Plates were washed, and then incubated for 2 h at room temperature with 1:2000 dilution of goat anti-mouse IgG-AP (Southern Biotech #1030-04) in PBS-T. After washing, plates were incubated for ~30 min at 37 °C with 2 mg/ml phosphatase substrate (Sigma S0942) in 1 M Tris 0.3 mM MgCl₂. Absorbance at 405 nm was measured on a Biotek synergy H1 microplate reader.

Western blotting

Overnight cultures of WT and mutant Spn strains were pelleted by centrifugation at 5,000g for 15 minutes, and resuspended in PBS with 0.1% Sodium Dodecyl Sulfate + 0.1% Sodium Deoxycholate. After shaking at 200rpm at 37C for 30 minutes, the samples were centrifugation at 20,000g for 30 minutes. Cell lysates (supernatants) were mixed with loading dye and separated by SDS-PAGE on NuPage 3-8% Tris Acetate gel (Invitrogen) at 150V for 80 minutes. Proteins were transferred to a PVDF membrane at 100V for 50 minutes. Membrane was blocked with 3% BSA in TBS-T, and probed with 1:2000 dilution of 72N serum and 1:4000 dilution of goat anti-mouse IgG-HRP (Biolegend).

Biofilm formation assay with Crystal Violet staining

Equal CFU of mutant and WT *Spn* were inoculated individually into wells of 96-well polystyrene plates containing THY broth in quadruplicate. Cultures were incubated at 37°C and evaluated for biofilm formation at 24 hours. Supernatants containing non-adhered cells were discarded and attached biofilms were, stained with crystal violet, dried, suspended in 30% acetic acid, and quantified by measuring the absorbance at 550nm on a Biotek synergy H1 microplate reader (19, 24). For light microscopy, wells were visualized prior to suspension in 30% acetic acid on a Leica DMIL LED light microscope with the 20X objective lens.

Confocal microscopy of biofilms

Equal CFU of mutant and WT *Spn* were inoculated individually into wells of 24-well polystyrene plates with coverslips at the bottom of the wells containing THY broth in quadruplicate. Cultures were incubated at 37°C and evaluated for biofilm formation at 24 hours. Supernatants containing non-adhered cells were discarded and attached biofilms were stained with SYTO 9 (Thermo Scientific) per manufacturer's instructions. After gentle washing, coverslips were mounted on slides with Vectashield mounting medium (Vector Labs). Imaging was performed with an Olympus FV1200 microscope. Quantification of average biofilm thickness was performed using COMSTAT2 image analysis software in ImageJ(25).

A549 cell adherence assay

A549 cells were grown to confluence in 24-well plates, washed, and incubated with 10^7 CFU/ml of wild type and mutant *Spn* for 2 hours at 37C. After washing 3 times with sterile PBS, adhered bacterial counts were determined by lysis with 0.1% triton X-100, and plating dilutions(17).

Intratracheal Infection

Five-week old BALB/c mice were anesthetized with ketamine-acepromazine-xylazine mixture. After effective anesthesia, mice were hung by their incisors with their backs resting on a solid surface. Mice were inoculated intratracheally with 10^7 CFU of wild-type TIGR4, PsrP locus deficient, or GT mutant strains in 50ul of PBS using a gel loading tip to intubate the trachea. Bacterial burden in lungs was assessed 48 hours after infection by obtaining bronchoalveolar lavage fluid ~1.5mL and plating serial dilutions of BALF.

Cytokine ELISA

Cytokine production in BALF from the intratracheal experiment above was determined using enzyme-linked immunosorbent assay (ELISA). Briefly, 96-well plates (Costar) were coated overnight at 4C with anti-TNF α or anti-IL-6 antibodies (1:200 dilution; Biolegend) and blocked with 1% BSA in PBS. Plates were washed with PBS-T and incubated with BALF for 1 hour at room temperature. After washing, biotinylated anti-TNF α or anti-IL-6 detection antibodies (1:200 dilution; Biolegend) were added for 1 hour at room temperature followed by HRP-conjugated Avidin (1:1000 dilution; Biolegend) for 30 minutes at room temperature. Plates were developed using 3, 3', 5, 5' tetramethyl benzidine (TMB) substrate (Biolegend) and stopped with 2N H₂SO₄. The optical densities were determined at 450 nm using a microplate reader (Synergy H1, Bio-Tek).

Acknowledgements

We thank Dr. Carlos Orihuela (University of Alabama Birmingham) for providing us with the TIGR4 and TIGR4 Omega strains (PsrP-SecA2Y2) of *S. pneumoniae*. We thank Dr. Osman Sheikh for helpful protocols and reagents for the UDP-Glo assays.

References

1. Bogaert, D., R. De Groot, and P. W. Hermans. 2004. Streptococcus pneumoniae colonisation: the key to pneumococcal disease. *Lancet Infect Dis* 4: 144-154.
2. Kadioglu, A., J. N. Weiser, J. C. Paton, and P. W. Andrew. 2008. The role of Streptococcus pneumoniae virulence factors in host respiratory colonization and disease. *Nature Reviews Microbiology* 6: 288-301.
3. Verma, R., and P. Khanna. 2012. Pneumococcal conjugate vaccine: a newer vaccine available in India. *Hum Vaccin Immunother* 8: 1317-1320.
4. O'Brien, K. L., L. J. Wolfson, J. P. Watt, E. Henkle, M. Deloria-Knoll, N. McCall, E. Lee, K. Mulholland, O. S. Levine, T. Cherian, Hib, and T. Pneumococcal Global Burden of Disease Study. 2009. Burden of disease caused by Streptococcus pneumoniae in children younger than 5 years: global estimates. *Lancet* 374: 893-902.
5. Daniels, C. C., P. D. Rogers, and C. M. Shelton. 2016. A Review of Pneumococcal Vaccines: Current Polysaccharide Vaccine Recommendations and Future Protein Antigens. *J Pediatr Pharmacol Ther* 21: 27-35.
6. Geno, K. A., G. L. Gilbert, J. Y. Song, I. C. Skovsted, K. P. Klugman, C. Jones, H. B. Konradsen, and M. H. Nahm. 2015. Pneumococcal Capsules and Their Types: Past, Present, and Future. *Clin Microbiol Rev* 28: 871-899.
7. Sanchez, C., P. Shivshankar, K. Stol, S. Trakhtenbroit, and C. Orihuela. 2010. The Pneumococcal Serine-Rich Repeat Protein Is an IntraSpecies Bacterial Adhesin That Promotes Bacterial Aggregation In Vivo and in Biofilms. *PLOS Pathogens*.

8. Selva, L., P. Ciruela, K. Blanchette, E. del Amo, R. Pallares, C. J. Orihuela, and C. Muñoz-Almagro. 2012. Prevalence and clonal distribution of *pcpA*, *psrP* and Pilus-1 among pediatric isolates of *Streptococcus pneumoniae*. *PLoS One* 7: e41587.
9. Lizcano, A., R. Akula Suresh Babu, A. T. Shenoy, A. M. Saville, N. Kumar, A. D'Mello, C. A. Hinojosa, R. P. Gilley, J. Segovia, T. J. Mitchell, H. Tettelin, and C. J. Orihuela. 2017. Transcriptional organization of pneumococcal *psrP*-*secY2A2* and impact of *GtfA* and *GtfB* deletion on *PsrP*-associated virulence properties. *Microbes Infect* 19: 323-333.
10. Obert, C., J. Sublett, D. Kaushal, E. Hinojosa, T. Barton, E. I. Tuomanen, and C. J. Orihuela. 2006. Identification of a Candidate *Streptococcus pneumoniae* core genome and regions of diversity correlated with invasive pneumococcal disease. *Infect Immun* 74: 4766-4777.
11. Hava, D. L., and A. Camilli. 2002. Large-scale identification of serotype 4 *Streptococcus pneumoniae* virulence factors. *Mol Microbiol* 45: 1389-1406.
12. Shi, W. W., Y. L. Jiang, F. Zhu, Y. H. Yang, Q. Y. Shao, H. B. Yang, Y. M. Ren, H. Wu, Y. Chen, and C. Z. Zhou. 2014. Structure of a novel O-linked N-acetyl-D-glucosamine (O-GlcNAc) transferase, *GtfA*, reveals insights into the glycosylation of pneumococcal serine-rich repeat adhesins. *J Biol Chem* 289: 20898-20907.
13. Jiang, Y. L., H. Jin, H. B. Yang, R. L. Zhao, S. Wang, Y. Chen, and C. Z. Zhou. 2017. Defining the enzymatic pathway for polymorphic. *J Biol Chem* 292: 6213-6224.
14. Sheikh, M. O., S. M. Halmo, S. Patel, D. Middleton, H. Takeuchi, C. M. Schafer, C. M. West, R. S. Haltiwanger, F. Y. Avci, K. W. Moremen, and L. Wells. 2017. Rapid screening of sugar-nucleotide donor specificities of putative glycosyltransferases. *Glycobiology* 27: 206-212.

15. Varki, A., and P. Gagneux. 2015. Biological Functions of Glycans. In *Essentials of Glycobiology*. ed, A. Varki, R. D. Cummings, J. D. Esko, P. Stanley, G. W. Hart, M. Aebi, A. G. Darvill, T. Kinoshita, N. H. Packer, J. H. Prestegard, R. L. Schnaar, and P. H. Seeberger, eds, Cold Spring Harbor (NY). 77-88.
16. Lizcano, A., C. J. Sanchez, and C. J. Orihuela. 2012. A role for glycosylated serine-rich repeat proteins in gram-positive bacterial pathogenesis. *Mol Oral Microbiol* 27: 257-269.
17. Rose, L., P. Shivshankar, E. Hinojosa, A. Rodriguez, C. J. Sanchez, and C. J. Orihuela. 2008. Antibodies against PsrP, a novel *Streptococcus pneumoniae* adhesin, block adhesion and protect mice against pneumococcal challenge. *J Infect Dis* 198: 375-383.
18. Blanchette-Cain, K., C. A. Hinojosa, R. Akula Suresh Babu, A. Lizcano, N. Gonzalez-Juarbe, C. Munoz-Almagro, C. J. Sanchez, M. A. Bergman, and C. J. Orihuela. 2013. *Streptococcus pneumoniae* biofilm formation is strain dependent, multifactorial, and associated with reduced invasiveness and immunoreactivity during colonization. *MBio* 4: e00745-00713.
19. Sanchez, C. J., P. Shivshankar, K. Stol, S. Trakhtenbroit, P. M. Sullam, K. Sauer, P. W. Hermans, and C. J. Orihuela. 2010. The pneumococcal serine-rich repeat protein is an intra-species bacterial adhesin that promotes bacterial aggregation in vivo and in biofilms. *PLoS Pathog* 6: e1001044.
20. Shivshankar, P., C. Sanchez, L. F. Rose, and C. J. Orihuela. 2009. The *Streptococcus pneumoniae* adhesin PsrP binds to Keratin 10 on lung cells. *Mol Microbiol* 73: 663-679.
21. Li, Y., C. M. Thompson, and M. Lipsitch. 2014. A modified Janus cassette (Sweet Janus) to improve allelic replacement efficiency by high-stringency negative selection in *Streptococcus pneumoniae*. *PLoS One* 9: e100510.

22. Middleton, D. R., X. Zhang, P. L. Wantuch, A. Ozdilek, X. Liu, R. LoPilato, N. Gangasani, R. Bridger, L. Wells, R. J. Linhardt, and F. Y. Avci. 2018. Identification and characterization of the *Streptococcus pneumoniae* type 3 capsule-specific glycoside hydrolase of *Paenibacillus* species 32352. *Glycobiology* 28: 90-99.
23. Rio, D. C., M. Ares, G. J. Hannon, and T. W. Nilsen. 2010. Purification of RNA using TRIzol (TRI reagent). *Cold Spring Harb Protoc* 2010: pdb.prot5439.
24. O'Toole, G. A. 2011. Microtiter dish biofilm formation assay. *J Vis Exp*.
25. Heydorn, A., A. T. Nielsen, M. Hentzer, C. Sternberg, M. Givskov, B. K. Ersboll, and S. Molin. 2000. Quantification of biofilm structures by the novel computer program COMSTAT. *Microbiology* 146 (Pt 10): 2395-2407.

Figure 5.1

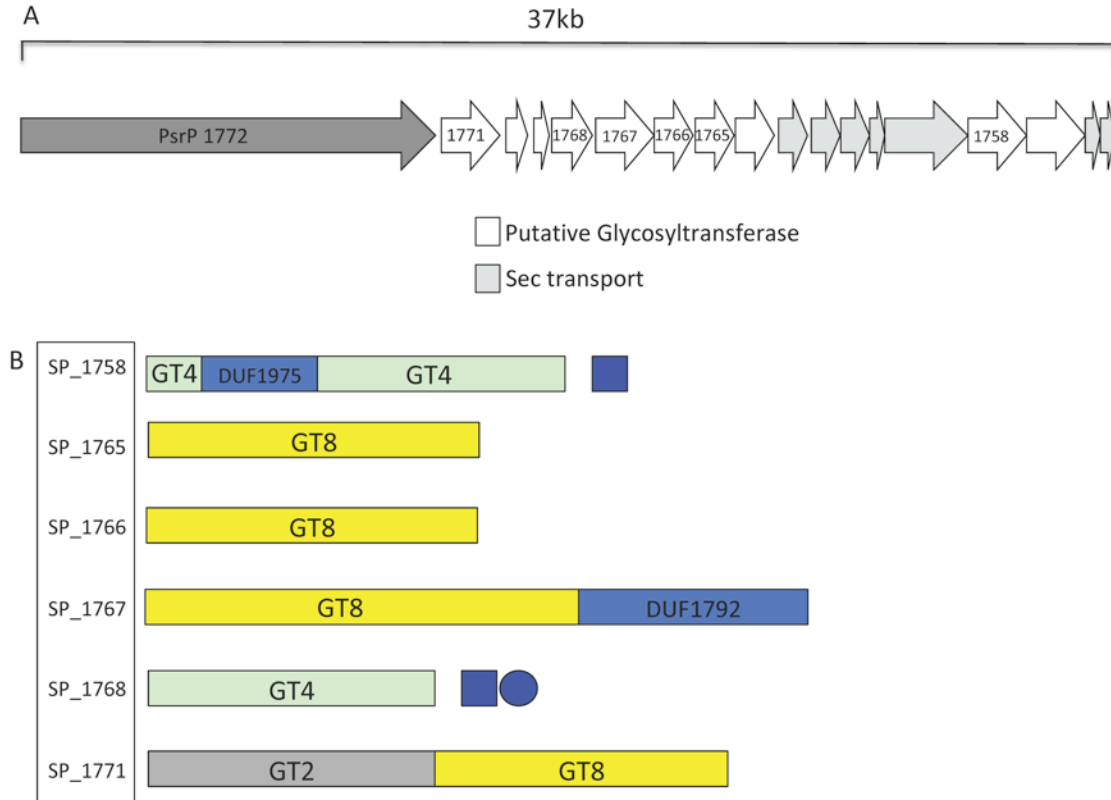


Figure 5.1

A.) Genomic organization of *PsrP-secY2A2* locus. Lightly shaded arrows are putative transport genes, whereas white arrows indicate putative or experimentally determined glycosyltransferases. Uniprot TIGR4 gene products SP_1772(*PsrP*) to SP_1755. B.) Domain organizations of the glycosyltransferases encoded by the *psrP* locus with their CAZY(carbohydrate active enzymes) Glycosyltransferase family predictions, along with proposed functions for SP_1758, and SP_1768. There are Domains of Unknown Function (DUF) in SP_1758, and SP_1767.

Figure 5.2

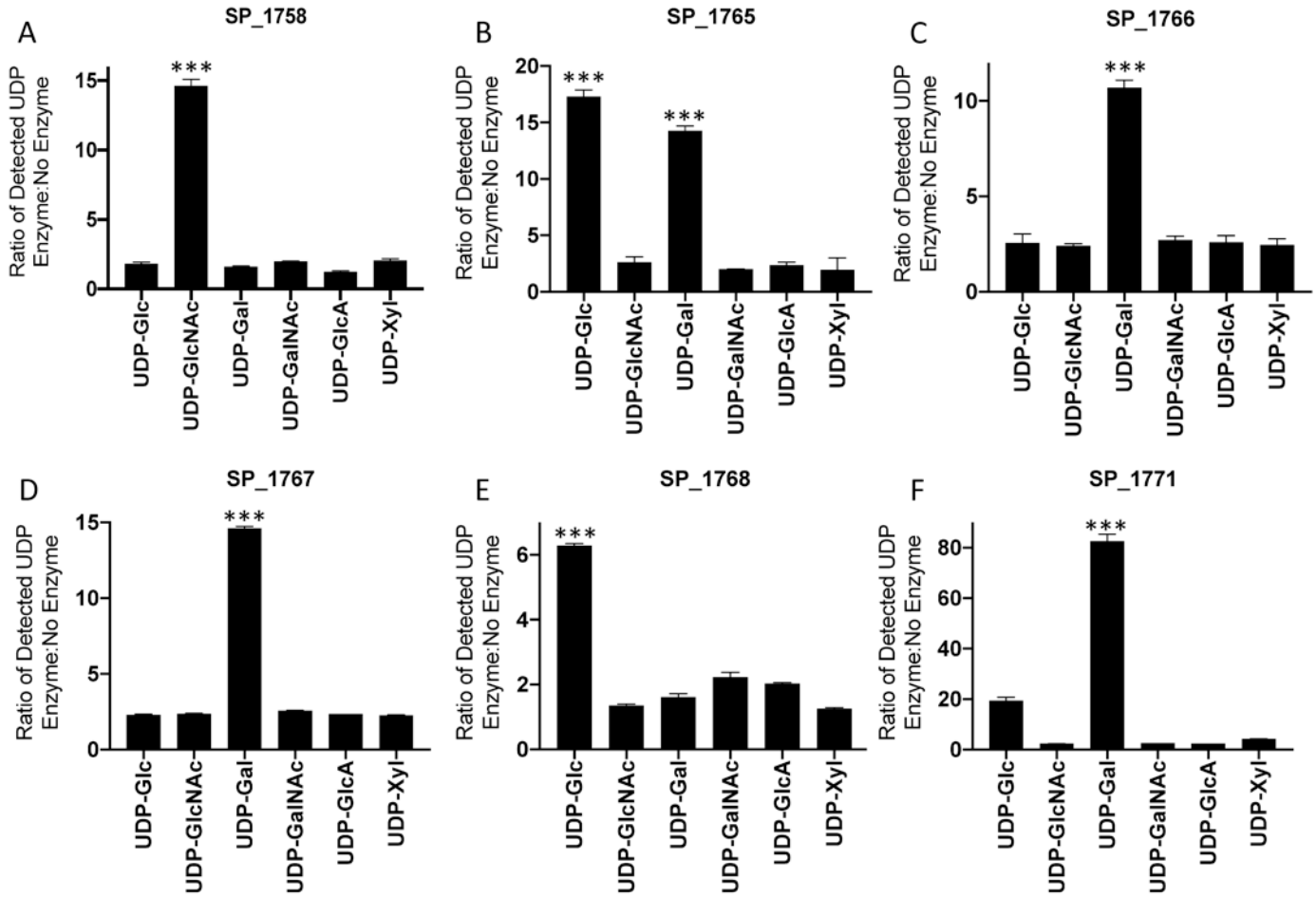


Figure 5.2

Comparison of UDP-sugar donor specificities of *psrP* locus glycosyltransferases. Each enzyme was incubated with 50 μ M of each UDP-sugar for 16 h at 37°C, and UDP release was detected by the UDPGlo (Promega) assay. Data are represented as the ratio of the UDP detected from the reactions with enzyme to the reactions without enzyme.

Figure 5.3

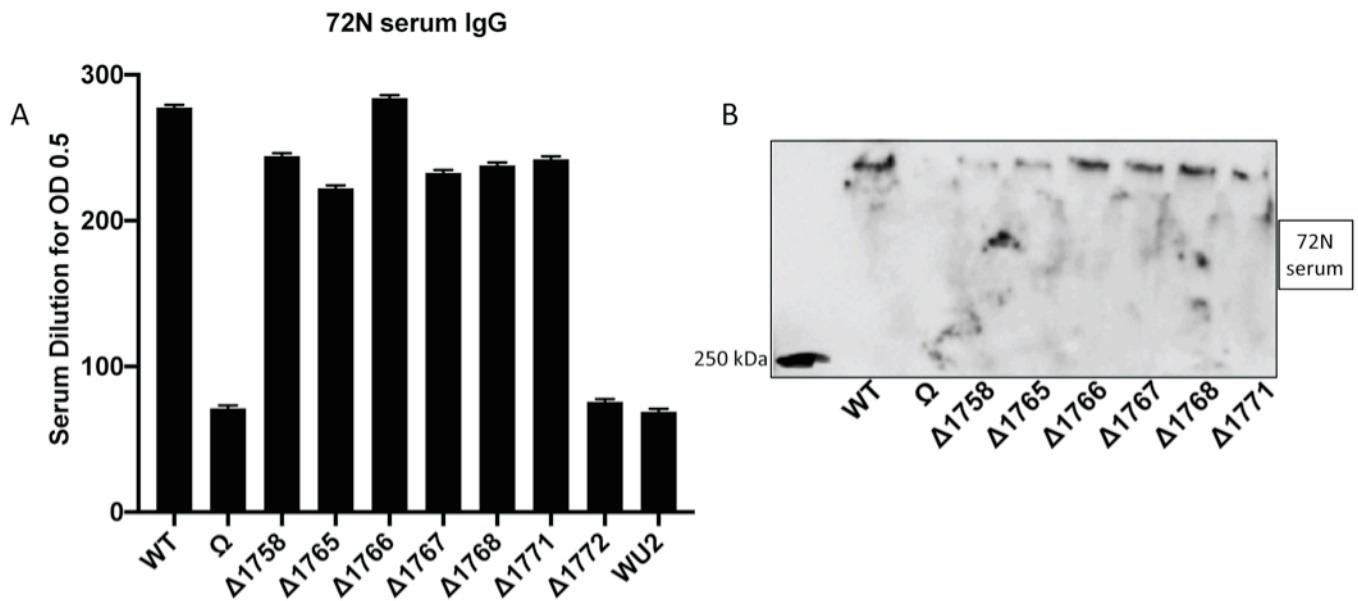


Figure 5.3

Whole cell ELISA (A), and Western blot (B) showing expression of PsrP in Δ GT strains. Wild-type and mutant strains were probed with anti-sera raised against the N-terminal basic region of PsrP.

Figure 5.4

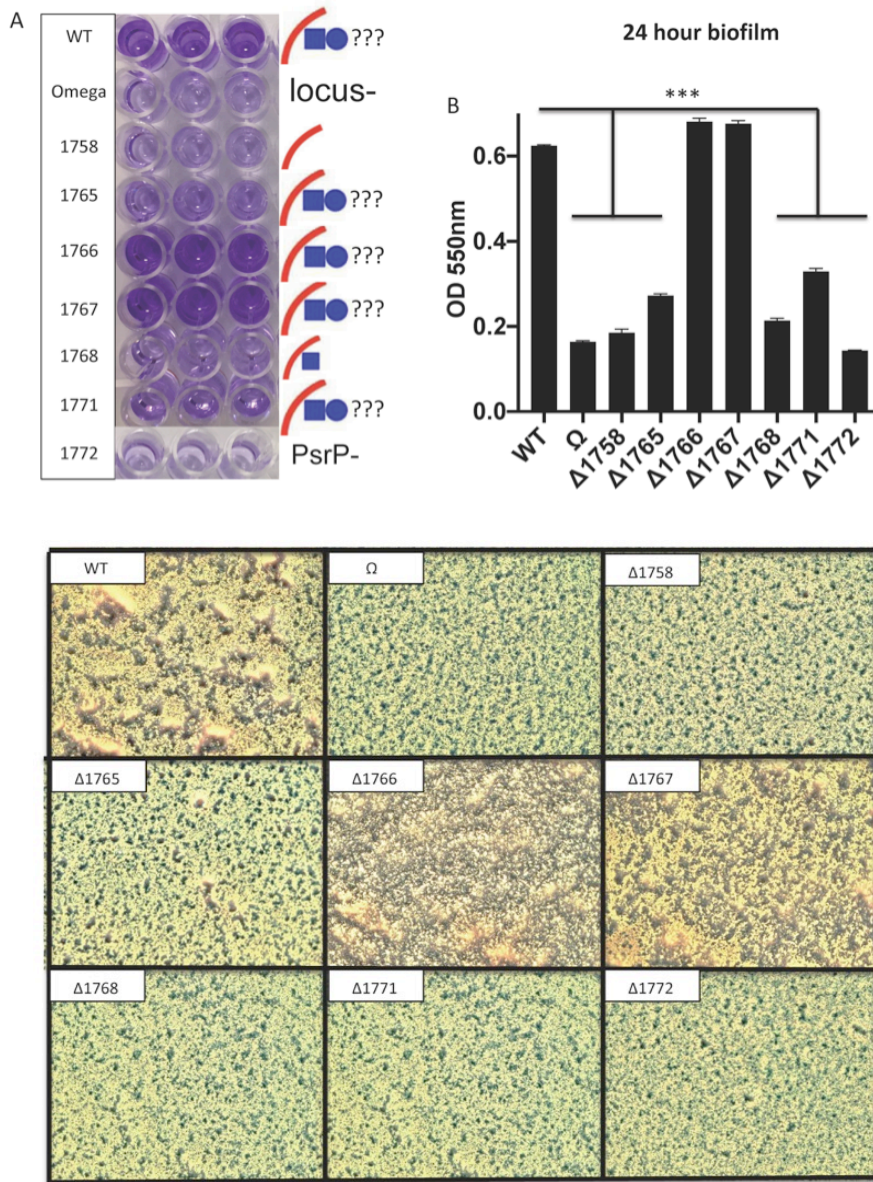


Figure 5.4

Biofilm formation assay with crystal violet staining. Attachment of Wild-Type and mutant strains to the bottom of 96-well polystyrene plate after 24 hours. A.) Biofilm was stained using crystal violet and B.) absorbance was read at 550nm. C.) Before dissolving crystal violet, stained bacteria were viewed on a Leica light microscope with a 20X objective. All experiments were performed in quadruplicate. Statistical analysis was performed using a two-tailed Student's t-test.

Figure 5.5

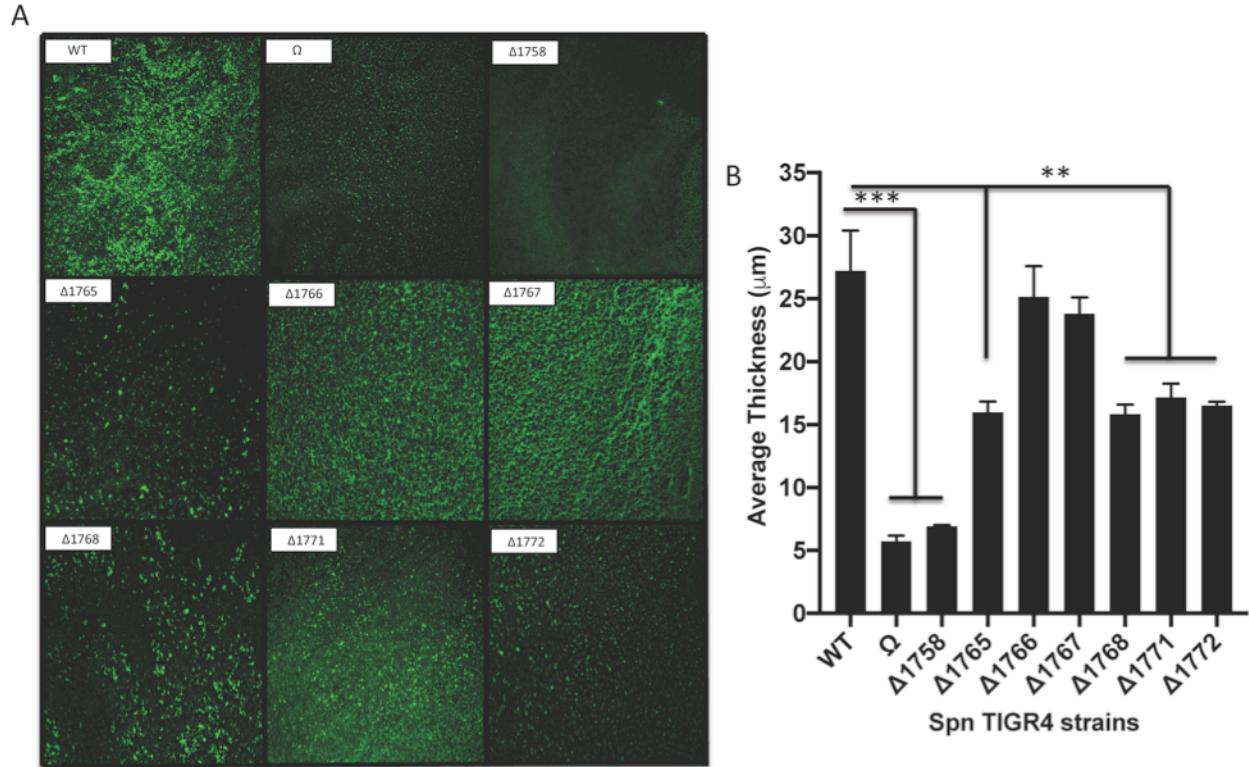


Figure 5.5

Biofilm formation assay with Syto 9 staining. Attachment of TIGR4 (WT) and mutant strains to borosilicate glass coverslip after 24 hours. A.) Biofilm was stained using Syto 9 and imaged by confocal microscopy on an Olympus FV1200 microscope. B. Average thickness of the biofilms was calculated using COMSTAT image analysis software plugin on ImageJ. All experiments were performed in quadruplicate. Statistical analysis was performed using a two-tailed Student's t-test.

Figure 5.6

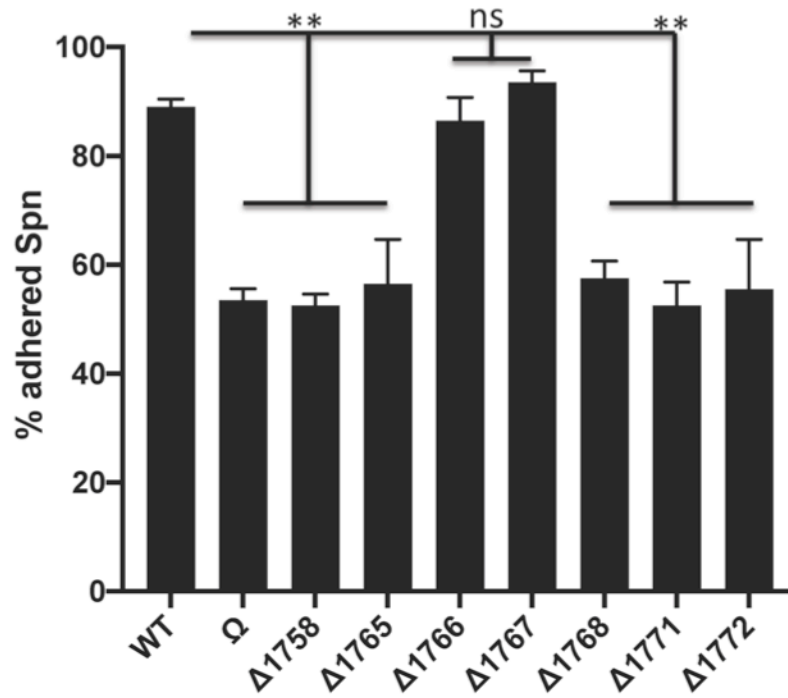


Figure 5.6

A549 adherence of Wild-type and mutant strains of Spn. The ability of Wild-type and mutant Spn to bind to a confluent monolayer of A549 cells. Results displayed as percent of total input. Assay performed in duplicate, Statistical analysis was performed using a two-tailed Student's t-test.

Figure 5.8

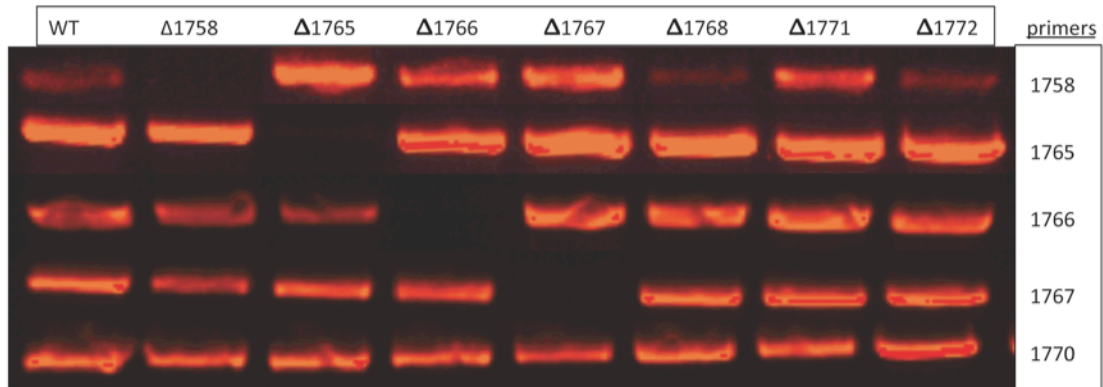


Figure 5.8

RT-PCR of adjacent genes in *psrP* locus of mutant strains to confirm knock-out and demonstrate no polar affects from knock-out procedure. RNA was isolated from mutant strains, and cDNA was prepared by reverse transcriptase. No RT was used as control to ensure no genomic DNA contamination in reactions (data not shown).

Table 5.1. Oligonucleotides used in this study

Oligonucleotide	Sequence (5' to 3')
1758downfor	ttatatttactggatgaattgtttagactttatgatagttacagtcagaagtc
1758downrev	cccagcaaagtaaagagcaaacc
1758upfor	gctcataagctcttactaaagataagg
1758uprev	ttaaaaatcaaacggatcgatccttaaattttctctttatggaaaatgagtcac
1765downfor	ttatatttactggatgaattgtttagtgagtgaattaattagtggtggtac
1765downrev	cctgaggaatatttaaaccatactgg
1765upfor	ttgattttatgtatgcttgacactac
1765uprev	ttaaaaatcaaacggatcgatccttaaactgttctctacctcatgtaagtc
1766 upfor	gagattgcatccacaaattgttc
1766 uprev	ttaaaaatcaaacggatcgatccttaacattttaaatccttatcatttttaaatagtctag
1766 downfor	ttatatttactggatgaattgtttagagaacagtatgagaaaatcaatagattagc
1766 downrev	ggacttgctgataaagagtccaac
1767 upfor	tgaaacacgctatgtgtatgac
1767 uprev	ttaaaaatcaaacggatcgatccttaattcattcccttaacaaattccaag
1767 downfor	ttatatttactggatgaattgtttagactatttaaataaatgataaggattaaatgag
1767 downrev	ctgtcgcaaaaaatctaaagtaagaag
1768downfor	ttatatttactggatgaattgtttaggggaatgaaatgaacaaaacaattg
1768downrev	atttctgcaacgatatcggatg
1768upfor	aatcataaatggtatgagatttctgagttg
1768uprev	ttaaaaatcaaacggatcgatccttaaacgctatctcatttttactatctacg
1771downfor	ttatatttactggatgaattgtttagagaaaaatcatttagtaggagatgctc
1771downrev	ctaccattttgttggttcgg
1771upfor	caagtgcgctcggttcag
1771uprev	ttaaaaatcaaacggatcgatccttaattctgaaaattctttacaaattcacctg
1772 upfor	cgtctatcttgatggcaaac
1772 uprev	ttaaaaatcaaacggatcgatccttaagacctgagtagtatcaacaccac
1772 downfor	ttatatttactggatgaattgtttaggacaacctgtaaagttaggctaaac
1772 downrev	gtccaattccaaccatttatgttc
sweetjanfor	ttaaggatcgatccggttgatttttaattg
sweetjanrev	ctaaaacaattcatccagtaaaatataatattttatttc

CHAPTER 6

IMMUNOLOGICAL CHARACTERIZATION OF PNEUMOCOCCAL SURFACE PROTEIN

A (PSPA) GLYCOSYLATION

Dustin R Middleton, Ahmet Ozdilek, Osman Sheikh, Robert Bridger, Lance Wells and Fikri Y.

Avcı

*To be submitted to *mBio*

Abstract

Since the introduction of the 13-valent (PCV13) glycoconjugate vaccine the incidence rates of invasive pneumococcal diseases (IPDs) in children and the elderly have been greatly reduced. However, *Streptococcus pneumoniae* (Spn) remains the leading cause of community acquired pneumonia and otitis media with high mortality rates. A global serotype distribution shift and a rise of nonencapsulated Spn, highlight the need for urgent investigation of serotype-independent, conserved, protective subunit vaccine targets. Currently Spn surface proteins are being examined as vaccine candidates, without considering potential post-translational modifications. Reports on glycosylation of Spn surface proteins, and how such modifications impact virulence and immunogenicity are limited. Here, we describe for the first time, the glycosylation of highly immunogenic, conserved Pneumococcal surface protein A (PspA), and show that PspA glycans are antigenic and they enhance the immunogenicity of the protein. Our results indicate that pneumococcal surface glycans on glycoproteins are ideal and promising targets for next generation pneumococcal vaccine design.

Introduction

A global serotype distribution shift has highlighted the importance of generating improved pneumococcal vaccines to include a wider range of serotypes(1, 2). Moreover, increasing numbers of clinical isolates from IPD patients are nonencapsulated Spn (NESpn), indicating the emergence of pathogenic NESpn strains(3-5). The serotype distribution shift and increasing NESpn in the clinical isolates necessitate the urgent investigation of serotype-independent, conserved, protective subunit vaccine targets. Spn surface proteins are major virulence factors and conserved immunogens and, therefore, Spn proteins have been examined as

vaccine candidates, without considering potential post-translational modifications(6, 7). Current knowledge on the potential glycosylation of Spn surface proteins, such as Pneumococcal surface protein A, and how this modification impacts virulence and immunogenicity is surprisingly very limited.

PspA has been shown to inhibit complement-mediated opsonization by interfering with the C3 complement component(8, 9). PspA also helps to protect Spn from bactericidal activity by binding lactoferrin (10, 11). This surface-exposed virulence determinant is also antigenic and is therefore an attractive vaccine target. PspA has been characterized as a protective antigen in multiple reports(7, 12-15). It was demonstrated that mice immunized with native PspA isolated from Spn were protected from fatal sepsis in challenge experiments, whereas PspA expressed in *E. coli* recombinantly was significantly less immunogenic and protective in comparison to native PspA (15). This observation suggests potential roles for posttranslational modifications in immunogenicity of PspA.

We hypothesized that PspA glycosylation is essential for Spn virulence and carbohydrate epitopes from PspA can induce protective adaptive immune responses. In this study PspA is investigated due to its possession of three important features: surface localization, critical roles in Spn virulence, and high immunogenicity. We have collected evidence for the glycosylation of PspA. Moreover, we show that PspA glycans are antigenic and contribute to the immunogenicity of the protein. Here, we characterize PspA glycosylation, develop a glycan dependent monoclonal antibody, and identify PspA glycosylation as a target for vaccine design.

Results

PspA is a periodate-reactive glycoprotein

Choline Binding Proteins (CBPs) are a family of surface proteins that contain multiple conserved 20-amino-acid repeats through which they attach to the choline units of the lipoteichoic acids and teichoic acids on the cell wall (16, 17). We first isolated (CBPs) from Spn TIGR4 as described previously(16, 18) by stripping them from the bacterial cell surface in a suspension of 2% choline chloride. The crude CBP mixture was visualized using the Pro-Q 488 Glycoprotein Gel kit from Invitrogen (**Figure 6.1A**). This revealed a predominant reactive band that we identified as Pneumococcal surface protein A. This fluorescent reagent reacts with oxidized vicinal diols on glycan moieties on proteins to selectively stain glycoproteins. PspA is a major component of the CBP mixture. PspA was further purified by flowing the choline chloride released protein mixture over a Sepharose Q column utilizing the choline-like, quaternary amine resin (19). PspA was then purified from the total CBP mixture by size exclusion chromatography (SEC) using a Superdex 200 column. Purity of PspA was confirmed by SEC and SDS-PAGE (**Figure 6.1B**). Proteomic analysis of trypsin digested PspA confirmed the identity of isolated PspA (data not shown here).

PspA is modified by O-linked di-hexose-glycerol moiety

After isolation of pure PspA, we identified its monosaccharide composition by methanolysis-trimethylsilyl (TMS) derivatization GC-MS(20, 21) Monosaccharides were run along with standard monosaccharides. Peaks identified in the PspA sample were galactose, and glucose, shown in **Figure 6.2**. O-linked oligosaccharides from PspA were released by in-gel beta-elimination after separation by SDS-PAGE, permethylated, and analyzed by electrospray

ionization direct infusion MS for MS1 and ion trap MS for MS2. Peaks were assigned manually. Further fragmentation of the 565.278 m/z peak aided in structural assignment. The results confirmed the presence of an O-linked di-hexose-glycerol glycan with a permethylated mass/charge of 565.278(**Figure 6.3A-B**).

Native PspA is more immunogenic than recombinant PspA

To determine how glycosylation affects the humoral immune responses to native PspA, we performed an immunization experiment in which glycosylated, Spn-expressed PspA was compared to non-glycosylated *E.coli* expressed recombinant PspA. In an ELISA, the plate was coated with paraformaldehyde-fixed TIGR4 Spn. Serum generated against native or recombinant PspA was used as the primary antibody. The results in **Figure 6.4A-B** strongly suggest that serum IgGs/IgMs generated from native PspA immunization recognize PspA on the fixed Spn at a significantly higher degree than serum IgGs/IgMs from recombinant PspA immunizations (immunization schemes and antigen concentrations are identical for both groups). These results as well as results from others (15) suggest that the native form of PspA has different antigenic and immunogenic epitopes with contributions from glycan modifications.

Glycan dependent monoclonal antibodies are generated upon immunization with native PspA

With such a robust response against the native protein, we were interested to see if there are glycan specific antibodies generated upon native PspA immunization. B cell hybridomas were generated and, after limiting dilution of cells, we screened out and purified antibodies from wells that responded to native PspA and not recombinant PspA, which would infer their glycan dependence (**Figure 6.5A**). The monoclonal antibody 2.83 was analyzed further by coating an ELISA plate with native or recombinant PspA, treating with increasing concentrations of periodate for 20 minutes, disrupting the glycan structure, and using either 2.83 mAb or

recombinant PspA serum as primary antibody. 2.83 mAb binding decreases as periodate concentration increases, whereas recombinant PspA serum reactivity stays the same (**Figure 6.5B**). This indicates glycan specificity or dependence of the 2.83 monoclonal antibody.

In vitro T cell response to native PspA.

To compare T cell responses to native and recombinant PspA, groups of Balb/c mice were immunized intranasally with ethanol killed TIGR4 Spn whole cell antigen (WCA) with Cholera toxin (CT) as adjuvant or CT alone. Lymphocytes were isolated 3 weeks after final immunization and stimulated *in vitro* with native or recombinant PspA, and type 4 capsular polysaccharide (Pn4P), as a negative control. CD4⁺ T cells from WCA immunized mice showed higher proliferation upon stimulation with native PspA than with recombinant PspA as shown by the reduction in CFSE division in **Figure 6.7A**. Cytokine levels, after *in vitro* stimulation, were measured by ELISA. Native PspA stimulated the secretion of significantly more IL-2 (**Figure 6.7B**) and IL-17 (**Figure 6.7C**) than recombinant PspA. Measured IL-4 and IFN- γ levels were not significantly different upon stimulation with these different antigens (data not shown). These results suggest a major contribution from the glycan component of native PspA in the generation of robust T cell responses.

Discussion

This study investigates and uncovers novel glycosylation of pneumococcal surface protein A (PspA). We demonstrate that PspA glycans are antigenic and contribute to the immunogenicity of the protein. While these results are important and exciting to the pneumococcal field, several questions remain unanswered. Future efforts will determine the amino acid(s) of PspA that receives the glycan modification, specific enzymes that catalyze the glycosylation reactions, conservation of the modification between strains, and contribution of the

glycan in pathogenicity of Spn.

PspA is present in essentially all clinical isolates, but has variable primary amino acid sequence amongst strains (22, 23). Based on its sequence, PspA can be organized into three families, or 6 clades. It has been reported that up to 99% of pneumococcal isolates belong to families 1 and 2 (clades 1-5)(24, 25). Although PspA is divided into these distinct groups, it is exceptionally cross-reactive with anti-sera and monoclonal antibodies(26, 27). Immunization with a single PspA can protect mice against strains expressing other clades of PspA. This cross-protection was observed when mice were challenged with 14 Spn strains after immunization with individual PspAs from different clades(22). Monoclonal antibodies to PspA have been shown to protect mice from fatal pneumococcal sepsis(28, 29). How the glycan structures on PspA influence or contribute to this cross-reactivity remains to be investigated. In future experiments we will utilize the glycan dependent 2.83 monoclonal antibody in passive immunization experiments to assess the protective ability of this antibody. Furthermore, we will determine if the specific mAb epitope is conserved among a variety of Spn strains and serotypes.

We previously demonstrated a novel mechanism through which uptake of a glycoconjugate vaccine by antigen presenting cells (APCs) results in the presentation of a carbohydrate epitope by the major histocompatibility class II complex (MHCII), thus stimulating carbohydrate-specific CD4⁺ T-cell clones (*i.e.*, Tcarbs) (30, 31). These findings led us to postulate that it is highly unlikely that T cells have evolved to only recognize carbohydrate epitopes derived from artificially synthesized protein-polysaccharide conjugates. Thus, we hypothesized that carbohydrate epitopes from native PspA are presented by antigen presenting cells for recognition by T cells, and that carbohydrate-induced, adaptive immune responses can contribute to the clearance of pathogen in an infection. CD4⁺ T cells play a key role in mediating

antibody-independent protective immunity to pneumococcal colonization(32). Specifically, IL-17A-secreting CD4⁺ T cells (TH17) are found to be critical for protection offered by ethanol killed whole cell pneumococcal antigen (33). Humans lacking TH17 cells are highly susceptible to Spn infections (34). A number of pneumococcal antigens were identified in whole cell-immunized mice and shown to induce TH17 response to protect mice from colonization by Spn (35, 36). Our results indicate that the PspA glycopeptides may be T cell epitopes, as native PspA promotes the production of both IL-2 and IL-17 significantly more than nonglycosylated recombinant PspA.

In conclusion, we have collected evidence for the first time that PspA is glycosylated, and we showed that PspA glycans are antigenic and enhance the immunogenicity of the protein. We developed a glycan dependent monoclonal antibody, and identified PspA glycosylation as a target for vaccine design to be used in future studies. Identification and immunological characterization of PspA glycosylation may lay the foundation for a new field of study within pneumococcal research, which may contribute to our understanding of Spn infectivity. Using glycan-based novel and conserved immunogens as new-generation pneumococcal vaccine targets may enable us to combat this major human pathogen and overcome IPDs caused by Spn.

Materials and Methods

Bacterial strains and mutant construction

Streptococcus pneumoniae type 4 (TIGR4 strain) was obtained from ATCC and cultured aerobically without shaking at 37 °C on Tryptic Soy Agar with 5% sheep blood (TSAB), or in Todd Hewitt Broth plus 0.5% yeast extract (THY) (BD Biosciences). PspA knock-out (Δ PspA) strains were generated by allelic replacement with a “Sweet” janus cassette(37). Briefly, DNA fragments flanking each gene were amplified and assembled up and downstream of the cassette

encoding SacB and Kanamycin resistance genes. Δ GT strains were selected and grown with kanamycin supplementation (200ug/ml).

Mice

8-week-old female BALB/c mice were obtained from Taconic Biosciences (Hudson, NY) and housed in the Coverdell Rodent Vivarium at the University of Georgia. Mice were kept in microisolator. All mouse experiments were in compliance with the University of Georgia Institutional Animal Care and Use Committee under the approved animal use protocol 2478 A2016 11-022-Y1-A0. Our animal use protocol adheres to the principles outlined in *U.S. Government Principles for the Utilization and Care of Vertebrate Animals Used in Testing, Research and Training, the Animal Welfare Act, the Guide for the Care and Use of Laboratory Animals, and the AVMA Guidelines for the Euthanasia of Animals*.

Proteomic Identification of PspA

An in-gel trypsin digestion was performed as described previously (38). Briefly, after SDS-PAGE, the gel was stained with coomassie blue. The stained protein band extracted with a razor blade and gel slice was destained with 25mM ammonium bicarbonate in 50% acetonitrile. After gel was shrunk with acetonitrile, dried, and rehydrated, the protein was digested with 100 ng of sequencing grade trypsin (Promega) in 40 mM ammonium bicarbonate overnight at 37 °C. Trypsin digest was stopped with 1% trifluoroacetic acid and incubation on ice for 30 min. The resulting peptides were obtained from digestion buffer, dried down, and reconstituted in 0.1% formic acid. The peptides were analyzed on a Orbitrap Fusion Tribrid mass spectrometer (Thermo Fisher Scientific) interfaced with an UltiMate 3000 RSLCnano HPLC system (Thermo Fisher Scientific). Peptides were resolved on an Acclaim™ PepMap™ RSLC C18 column (75 μ m ID x 15 cm; 2 μ m particle size) at a flow rate of 200 nL/min using a linear gradient of 1-100% solvent B (0.1% formic acid in 80% acetonitrile) over 60 min and a total run time of 90 min. Data-dependent acquisition was carried out using the Orbitrap mass analyzer collecting full scans

of 200-2000 m/z range at 60,000 mass resolution. Most intense precursor ions were selected using top speed mode with a maximum cycle time of 3 s. Precursor ions with charge state 2-5 were selected with dynamic exclusion set to exclude precursors for 20 s following a third selection within 10 s. Selected precursors were fragmented using collision-induced dissociation (CID) set to 38%, and resulting MS/MS ions were scanned out in the ion trap. The raw MS/MS spectra were searched against the Rapid Annotation Server(39) (RAST) annotated genome database for TIGR4 Spn using SEQUEST HT in Proteome Discoverer 1.4 (Thermo Fisher Scientific) with precursor mass tolerance of 10 ppm and fragment tolerance of 0.3 Da. Dynamic modification of +15.995 Da (oxidation of methionine residues) was allowed in the search parameters. Results were filtered at a 1% false discovery rate for peptide assignments.

Recombinant PspA production

Coding regions of PspA without stop codon was amplified from TIGR4 genomic DNA using primers with adapter attB sites used in gateway cloning systems (Thermo Scientific). A BP clonase reaction was performed to insert the gene into the pDONR221 vector. After sequence confirmation, an LR clonase(Thermo Scientific) reaction was performed to insert the gene into the pET-Dest42 destination vector for the expression of a C-terminal His-tagged fusion protein in BL21 cells. PspA were produced as described previously with minor modifications(40). Briefly, BL21(DE3) cells transformed with the pET-DEST42-PspA plasmids were grown in Luria Broth supplemented with 100 µg/ml ampicillin at 37 °C, and cell density was monitored by absorbance at 600 nm. Once the OD 600 nm reached 0.6, the cells were transferred into 25 °C. Protein expression was induced by the addition of Isopropyl β-D-1-thiogalactopyranoside at a final concentration of 1 mM and the culture was incubated with shaking for 8 h. Cells were harvested by centrifugation, resuspended in phosphate-buffered saline (PBS, pH 7.2) and lysed by sonication. The lysate was clarified by centrifugation at 17,000 × g for 1 h at 4°C, and passed

through a 0.45 μm syringe filter. PspA was purified by Ni^{2+} -NTA resin at 4 $^{\circ}\text{C}$, eluted with 300 mM imidazole and buffer exchanged into PBS pH 7.2. Protein concentration was determined by the bicinchoninic acid assay according to the instructions of the manufacturer. Purity was evaluated by coomassie staining.

Pro-Q 488 glycoprotein staining

The choline binding protein mixture was separated by SDS-PAGE along side the CandyCane molecular weight standards (Invitrogen) and the gel was stained with the Pro-Q Emerald 488 glycoprotein stain kit (Invitrogen) according to the manufacturer's protocol. Briefly, after staining, the gel was fixed with 50% methanol and 5% acetic acid. After washing with 3% acetic acid, the gel was incubated with oxidizing solution for 20 minutes in the dark to oxidize the carbohydrates. After extensive washing, the gel was incubated with the Pro-Q Emerald 488 staining solution for 2 hours at room temperature. After extensive and prolonged washing, the gels were imaged on a typhoon scanner with 510nm excitation.

Trimethylsilane Derivatization Gas Chromatography- Mass Spectrometry

100 μg of native PspA was added to 20 μg of inositol (internal standard) and the sample was lyophilized. 800 μl of 1M methanolic HCL was added to the tube, and the sample was heated at 80 $^{\circ}\text{C}$ for 16 hours. The sample was dried down with a stream of nitrogen gas. 200 μl of anhydrous methanol was added, and sample was dried down once more. 200 μl of methanol, 100 μl of pyridine, and 100 μl of acetic anhydride was added and incubated at room temperature for 30 minutes. After the sample was dried down, 1ml of Trimethylsilane was added, and the sample was incubated at 80 $^{\circ}\text{C}$ for 20 minutes. After incubation, the sample was dried down incompletely, and 1 ml of hexanes was added. This sample was passed over a glass wool filter,

dried down to ~100µl and GC-MS was performed on an Agilent 7890A GC-MS.

In-gel Beta elimination

In-gel Beta elimination was performed as described previously(41). Briefly, after separation of proteins by SDS-PAGE the gel was stained with coomassie blue. The PspA protein band was excised and destained by alternating acetonitrile and ammonium bicarbonate incubations. After the gel was destained, the gel slice was washed with ethyl acetate overnight at 4°C followed by a 10 minute wash with ammonium bicarbonate. The gel slide was then washed with water, and then acetonitrile and dried under a stream of nitrogen. The washed gel was swelled with 100mM sodium hydroxide and sodium borohydride was added at a final concentration of 1M. The sample was incubated for 18 hours at 45°C. After incubation, 10% acetic acid was added to the tube on ice to neutralize the base. The supernatant was passed through a glass wool filter and lyophilized to dryness overnight. To remove excess borate salts 300µl of 10% acetic acid in methanol was added and dried under a stream of nitrogen gas three times. Sample was dissolved in 5% acetic acid and passed through a C18 sepak column (waters), and flow through was lyophilized overnight. Sample was permethylated by traditional methods as previously described(41), and analyzed by electrospray ionization direct infusion MS for MS1 and ion trap MS for MS2. Peaks were assigned manually using ChemDraw software.

Immunizations

Groups of BALB/c mice were immunized intraperitoneally on days 0 and 14 with 5µg of Native PspA or recombinant PspA per dose with alum as adjuvant. Mice were bled from the tail vein 14 days after prime and 7 days after boost to obtain serum used in whole cell ELISA.

Whole cell ELISAs

ELISA plates (96 well, Nunc) were coated with 10^7 CFU of paraformaldehyde fixed Spn strains in phosphate buffered saline (pH 7.2) overnight at 4°C. Plates were washed 4-times with PBS +0.1% Tween (PBS-T) 20 using a Biotek 405/LS microplate washer. After 1 h blocking at room temperature with 1% BSA in PBS, microplate wells were incubated for 2 h with 1:2000 dilution of Native or recombinant PspA serum in PBS-T. Plates were washed, and then incubated for 2 h at room temperature with 1:2000 dilution of goat anti-mouse IgG-AP (Southern Biotech #1030-04) in PBS-T. After washing, plates were incubated for ~30 min at 37 °C with 2 mg/ml phosphatase substrate (Sigma S0942) in 1 M Tris 0.3 mM MgCl₂. Absorbance at 405 nm was measured on a Biotek synergy H1 microplate reader.

Generation of monoclonal antibodies

A mouse was immunized with native PspA and its splenocytes were harvested three days after a secondary immunization. After filtering through 40um cell strainers red blood cells were lysed by ACK lysis buffer. 10^8 splenocytes were mixed with 2×10^7 Sp2/0 myeloma cells and washed with DME. Cells were pelleted at 300G for five minutes, supernatant was removed. 700 ul of Polyethylene glycol (PEG) was added. Then, 15ml DMEM was slowly added. Cells were pelleted again, and media was removed. Cells were resuspended in 60 ml complete media with 20% FBS and plated in six 96 well plates. On the following day complete media with 2X HAT supplement was added to the plates to select fused hybridoma cells. Once colonies were established, the presence of PspA specific antibodies in hybridomas supernatant was tested by ELISA. Colonies with positive results underwent limited dilutions to obtain monoclones in complete media with 10% FBS and 1X HT supplement. After confirming the presence of anti PspA antibodies, colonies were grown in regular complete media with 10% FBS.

T-cell proliferation and cytokine ELISAs

Groups of Balb/c mice were immunized intranasally with 10^7 ethanol killed TIGR4 Spn whole cell antigen (WCA) with 1ug Cholera toxin (CT) as adjuvant or CT alone. $CD4^+$ T cells were isolated from lymph nodes of mice 3 weeks after boost immunization using mouse $CD4$ T lymphocyte enrichment set (BD Biosciences) following manufacturer's protocol. $CD4^+$ T cells were stimulated *in vitro* in the presence of irradiated splenic mononuclear cells pulsed with 10ug/ml of indicated antigens for 5 days. For CFSE labeling, $CD4^+$ T cells were incubated with 2uM CFSE solution (Sigma) at 37°C for 8 minutes before stimulation. CFSE dilution was measured by flow cytometry as an indication of T cell proliferation.

Cytokine release upon *in vitro* T-cell stimulation with native and recombinant PspA was determined using ELISA. Briefly, 96-well plates (Costar) were coated overnight at 4C with anti-IL-2 or anti-IL-17 antibodies (1:200 dilution; Biolegend) and blocked with 1% BSA in PBS. Plates were washed with PBS-T and incubated with culture supernatants for 1 hour at room temperature. After washing, biotinylated anti-IL-2 or anti-IL-17 detection antibodies (1:200 dilution; Biolegend) were added for 1 hour at room temperature followed by HRP-conjugated Avidin (1:1000 dilution; Biolegend) for 30 minutes at room temperature. Plates were developed using 3, 3', 5, 5' tetramethyl benzidine (TMB) substrate (Biolegend) and stopped with 2N H_2SO_4 . The optical densities were determined at 450 nm using a microplate reader (Synergy H1, Bio-Tek).

References

1. Richter, S. S., K. P. Heilmann, C. L. Dohrn, F. Riahi, D. J. Diekema, and G. V. Doern. 2013. Pneumococcal serotypes before and after introduction of conjugate vaccines, United States, 1999-2011(1.). *Emerg Infect Dis* 19: 1074-1083.
2. Wantuch, P. L., and F. Y. Avci. 2018. Current status and future directions of invasive pneumococcal diseases and prophylactic approaches to control them. *Hum Vaccin Immunother*: 1-19.
3. Keller, L. E., D. A. Robinson, and L. S. McDaniel. 2016. Nonencapsulated *Streptococcus pneumoniae*: Emergence and Pathogenesis. *MBio* 7.
4. Nunes, S., R. Sá-Leão, J. Carriço, C. R. Alves, R. Mato, A. B. Avô, J. Saldanha, J. S. Almeida, I. S. Sanches, and H. de Lencastre. 2005. Trends in drug resistance, serotypes, and molecular types of *Streptococcus pneumoniae* colonizing preschool-age children attending day care centers in Lisbon, Portugal: a summary of 4 years of annual surveillance. *J Clin Microbiol* 43: 1285-1293.
5. Andrade, A. L., C. M. Franco, J. Lamaro-Cardoso, M. C. André, L. L. Oliveira, A. Kipnis, C. G. Rocha, J. G. Andrade, S. L. Alves, I. H. Park, M. H. Nahm, S. G. Almeida, and M. C. Brandileone. 2010. Non-typeable *Streptococcus pneumoniae* carriage isolates genetically similar to invasive and carriage isolates expressing capsular type 14 in Brazilian infants. *J Infect* 61: 314-322.
6. Darrieux, M., C. Goulart, D. Briles, and L. C. Leite. 2015. Current status and perspectives on protein-based pneumococcal vaccines. *Crit Rev Microbiol* 41: 190-200.

7. Goulart, C., T. R. da Silva, D. Rodriguez, W. R. Politano, L. C. Leite, and M. Darrieux. 2013. Characterization of protective immune responses induced by pneumococcal surface protein A in fusion with pneumolysin derivatives. *PLoS One* 8: e59605.
8. Ren, B., J. Li, K. Genschmer, S. K. Hollingshead, and D. E. Briles. 2012. The absence of PspA or presence of antibody to PspA facilitates the complement-dependent phagocytosis of pneumococci in vitro. *Clin Vaccine Immunol* 19: 1574-1582.
9. Ren, B., A. J. Szalai, S. K. Hollingshead, and D. E. Briles. 2004. Effects of PspA and antibodies to PspA on activation and deposition of complement on the pneumococcal surface. *Infect Immun* 72: 114-122.
10. Kadioglu, A., J. N. Weiser, J. C. Paton, and P. W. Andrew. 2008. The role of *Streptococcus pneumoniae* virulence factors in host respiratory colonization and disease. *Nature Reviews Microbiology* 6: 288-301.
11. Shaper, M., S. K. Hollingshead, W. H. Benjamin, and D. E. Briles. 2004. PspA protects *Streptococcus pneumoniae* from killing by apolactoferrin, and antibody to PspA enhances killing of pneumococci by apolactoferrin [corrected]. *Infect Immun* 72: 5031-5040.
12. Ogunniyi, A. D., M. Grabowicz, D. E. Briles, J. Cook, and J. C. Paton. 2007. Development of a vaccine against invasive pneumococcal disease based on combinations of virulence proteins of *Streptococcus pneumoniae*. *Infect Immun* 75: 350-357.
13. Briles, D. E., E. Ades, J. C. Paton, J. S. Sampson, G. M. Carlone, R. C. Huebner, A. Virolainen, E. Swiatlo, and S. K. Hollingshead. 2000. Intranasal immunization of mice with a mixture of the pneumococcal proteins PsaA and PspA is highly protective against nasopharyngeal carriage of *Streptococcus pneumoniae*. *Infect Immun* 68: 796-800.

14. Briles, D. E., S. K. Hollingshead, J. C. Paton, E. W. Ades, L. Novak, F. W. van Ginkel, and W. H. Benjamin. 2003. Immunizations with pneumococcal surface protein A and pneumolysin are protective against pneumonia in a murine model of pulmonary infection with *Streptococcus pneumoniae*. *J Infect Dis* 188: 339-348.
15. Briles, D. E., J. D. King, M. A. Gray, L. S. McDaniel, E. Swiatlo, and K. A. Benton. 1996. PspA, a protection-eliciting pneumococcal protein: immunogenicity of isolated native PspA in mice. *Vaccine* 14: 858-867.
16. Yother, J., and J. M. White. 1994. Novel surface attachment mechanism of the *Streptococcus pneumoniae* protein PspA. *J Bacteriol* 176: 2976-2985.
17. Gosink, K. K., E. R. Mann, C. Guglielmo, E. I. Tuomanen, and H. R. Masure. 2000. Role of novel choline binding proteins in virulence of *Streptococcus pneumoniae*. *Infect Immun* 68: 5690-5695.
18. Rosenow, C., P. Ryan, J. N. Weiser, S. Johnson, P. Fontan, A. Ortqvist, and H. R. Masure. 1997. Contribution of novel choline-binding proteins to adherence, colonization and immunogenicity of *Streptococcus pneumoniae*. *Mol Microbiol* 25: 819-829.
19. Paterson, N. G., A. Riboldi-Tunicliffe, T. J. Mitchell, and N. W. Isaacs. 2006. Overexpression, purification and crystallization of a choline-binding protein CbpI from *Streptococcus pneumoniae*. *Acta Crystallogr Sect F Struct Biol Cryst Commun* 62: 672-675.
20. Santander, J., T. Martin, A. Loh, C. Pohlenz, D. M. Gatlin, and R. Curtiss. 2013. Mechanisms of intrinsic resistance to antimicrobial peptides of *Edwardsiella ictaluri* and its influence on fish gut inflammation and virulence. *Microbiology* 159: 1471-1486.

21. Hardy, M. R., and R. R. Townsend. 1994. High-pH anion-exchange chromatography of glycoprotein-derived carbohydrates. *Methods Enzymol* 230: 208-225.
22. Briles, D. E., R. C. Tart, E. Swiatlo, J. P. Dillard, P. Smith, K. A. Benton, B. A. Ralph, A. Brooks-Walter, M. J. Crain, S. K. Hollingshead, and L. S. McDaniel. 1998. Pneumococcal diversity: considerations for new vaccine strategies with emphasis on pneumococcal surface protein A (PspA). *Clin Microbiol Rev* 11: 645-657.
23. Khan, N., R. A. Qadri, and D. Sehgal. 2015. Correlation between in vitro complement deposition and passive mouse protection of anti-pneumococcal surface protein A monoclonal antibodies. *Clin Vaccine Immunol* 22: 99-107.
24. Hotomi, M., A. Togawa, M. Kono, Y. Ikeda, S. Takei, S. K. Hollingshead, D. E. Briles, K. Suzuki, and N. Yamanaka. 2013. PspA family distribution, antimicrobial resistance and serotype of *Streptococcus pneumoniae* isolated from upper respiratory tract infections in Japan. *PLoS One* 8: e58124.
25. Hollingshead, S. K., L. Baril, S. Ferro, J. King, P. Coan, D. E. Briles, and P. P. E. S. Group. 2006. Pneumococcal surface protein A (PspA) family distribution among clinical isolates from adults over 50 years of age collected in seven countries. *J Med Microbiol* 55: 215-221.
26. Crain, M. J., W. D. Waltman, J. S. Turner, J. Yother, D. F. Talkington, L. S. McDaniel, B. M. Gray, and D. E. Briles. 1990. Pneumococcal surface protein A (PspA) is serologically highly variable and is expressed by all clinically important capsular serotypes of *Streptococcus pneumoniae*. *Infect Immun* 58: 3293-3299.

27. McDaniel, L. S., J. S. Sheffield, P. Delucchi, and D. E. Briles. 1991. PspA, a surface protein of *Streptococcus pneumoniae*, is capable of eliciting protection against pneumococci of more than one capsular type. *Infect Immun* 59: 222-228.
28. McDaniel, L. S., G. Scott, J. F. Kearney, and D. E. Briles. 1984. Monoclonal antibodies against protease-sensitive pneumococcal antigens can protect mice from fatal infection with *Streptococcus pneumoniae*. *J Exp Med* 160: 386-397.
29. Briles, D. E., C. Forman, J. C. Horowitz, J. E. Volanakis, W. H. Benjamin, L. S. McDaniel, J. Eldridge, and J. Brooks. 1989. Antipneumococcal effects of C-reactive protein and monoclonal antibodies to pneumococcal cell wall and capsular antigens. *Infect Immun* 57: 1457-1464.
30. Avci, F., X. Li, M. Tsuji, and D. Kasper. 2011. A mechanism for glycoconjugate vaccine activation of the adaptive immune system and its implications for vaccine design. *Nat Med* 17: 1602-U1115.
31. Avci, F., X. Li, M. Tsuji, and D. Kasper. 2012. Isolation of carbohydrate-specific CD4(+) T cell clones from mice after stimulation by two model glycoconjugate vaccines. *Nat Protoc* 7: 2180-2192.
32. Malley, R., K. Trzcinski, A. Srivastava, C. M. Thompson, P. W. Anderson, and M. Lipsitch. 2005. CD4+ T cells mediate antibody-independent acquired immunity to pneumococcal colonization. *Proceedings of the National Academy of Sciences of the United States of America* 102: 4848-4853.
33. Moffitt, K. L., P. Yadav, D. M. Weinberger, P. W. Anderson, and R. Malley. 2012. Broad antibody and T cell reactivity induced by a pneumococcal whole-cell vaccine. *Vaccine* 30: 4316-4322.

34. Milner, J. D., J. M. Brenchley, A. Laurence, A. F. Freeman, B. J. Hill, K. M. Elias, Y. Kanno, C. Spalding, H. Z. Elloumi, M. L. Paulson, J. Davis, A. Hsu, A. I. Asher, J. O'Shea, S. M. Holland, W. E. Paul, and D. C. Douek. 2008. Impaired T(H)17 cell differentiation in subjects with autosomal dominant hyper-IgE syndrome. *Nature* 452: 773-776.
35. Li, Y., T. Gierahn, C. M. Thompson, K. Trzcinski, C. B. Ford, N. Croucher, P. Gouveia, J. B. Flechtner, R. Malley, and M. Lipsitch. 2012. Distinct effects on diversifying selection by two mechanisms of immunity against *Streptococcus pneumoniae*. *PLoS pathogens* 8: e1002989.
36. Moffitt, K. L., T. M. Gierahn, Y. J. Lu, P. Gouveia, M. Alderson, J. B. Flechtner, D. E. Higgins, and R. Malley. 2011. T(H)17-based vaccine design for prevention of *Streptococcus pneumoniae* colonization. *Cell host & microbe* 9: 158-165.
37. Li, Y., C. M. Thompson, and M. Lipsitch. 2014. A modified Janus cassette (Sweet Janus) to improve allelic replacement efficiency by high-stringency negative selection in *Streptococcus pneumoniae*. *PLoS One* 9: e100510.
38. Lim, J. M., D. Sherling, C. F. Teo, D. B. Hausman, D. Lin, and L. Wells. 2008. Defining the regulated secreted proteome of rodent adipocytes upon the induction of insulin resistance. *J Proteome Res* 7: 1251-1263.
39. Aziz, R. K., D. Bartels, A. A. Best, M. DeJongh, T. Disz, R. A. Edwards, K. Formsma, S. Gerdes, E. M. Glass, M. Kubal, F. Meyer, G. J. Olsen, R. Olson, A. L. Osterman, R. A. Overbeek, L. K. McNeil, D. Paarmann, T. Paczian, B. Parrello, G. D. Pusch, C. Reich, R. Stevens, O. Vassieva, V. Vonstein, A. Wilke, and O. Zagnitko. 2008. The RAST Server: rapid annotations using subsystems technology. *BMC Genomics* 9: 75.

40. Middleton, D. R., X. Zhang, P. L. Wantuch, A. Ozdilek, X. Liu, R. LoPilato, N. Gangasani, R. Bridger, L. Wells, R. J. Linhardt, and F. Y. Avci. 2018. Identification and characterization of the *Streptococcus pneumoniae* type 3 capsule-specific glycoside hydrolase of *Paenibacillus* species 32352. *Glycobiology* 28: 90-99.
41. Nix, D. B., T. Kumagai, T. Katoh, M. Tiemeyer, and K. Aoki. 2014. Improved in-gel reductive beta-elimination for comprehensive O-linked and sulfo-glycomics by mass spectrometry. *J Vis Exp*: e51840.

Figure 6.1

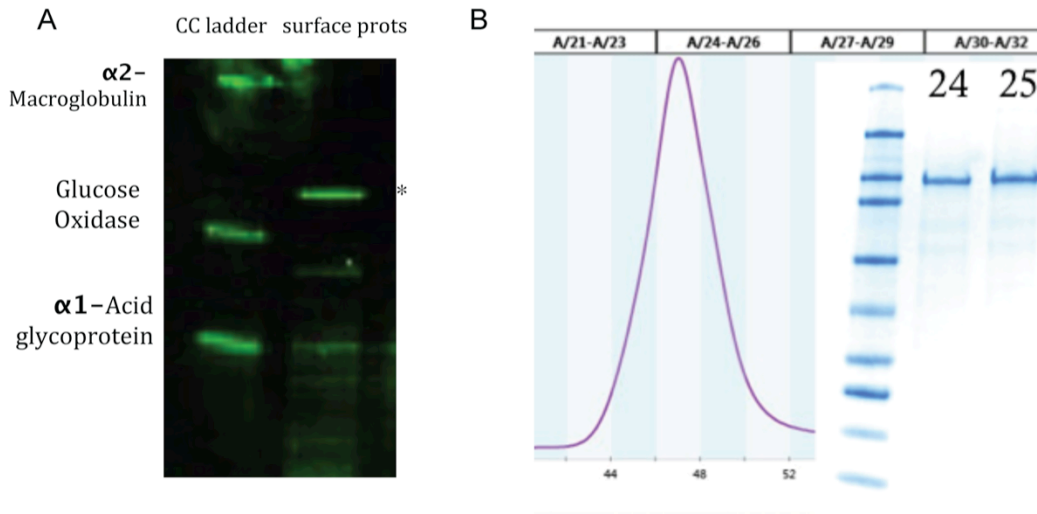


Figure 6.1

A.) Pro-Q Emerald 488 Glycoprotein Gel of crude choline binding protein mixture (lane 2) along with CandyCane ladder with positive and negative controls. B.) Purification of native PspA from TIGR4 Spn. Size exclusion chromatography and Coomassie blue stain (lane 1: ladder) indicates purity protein.

Figure 6.2

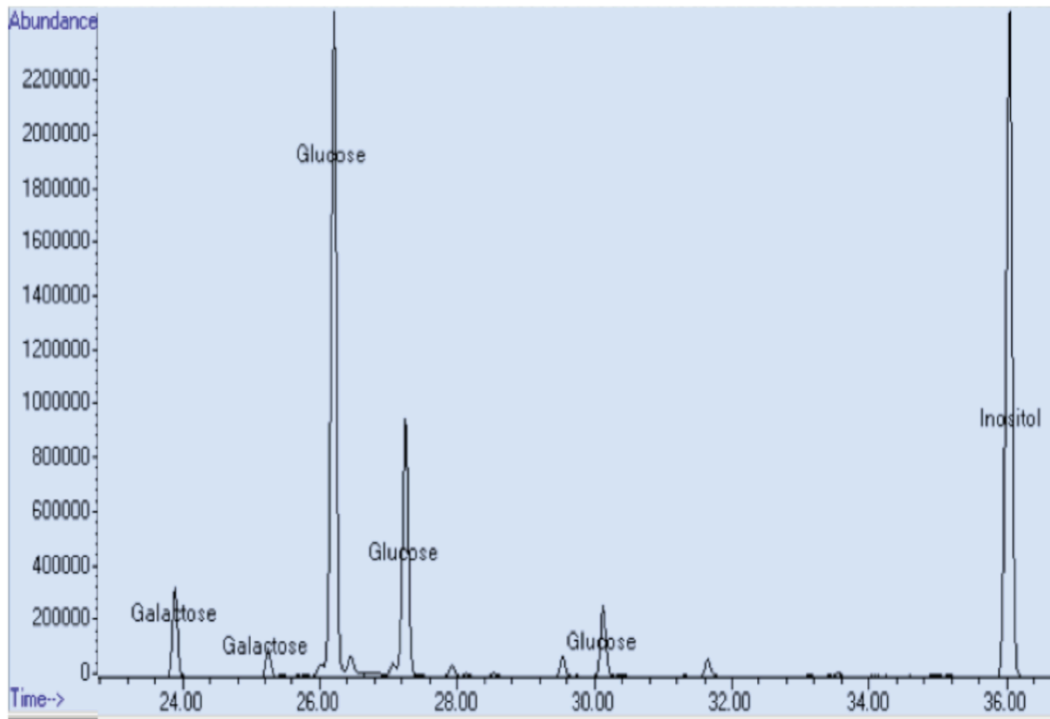


Figure 6.2

Tri-methyl silyl-derivatized GC-MS monosaccharide analysis of purified native PspA. Inositol served as an internal standard for all samples.

Figure 6.3

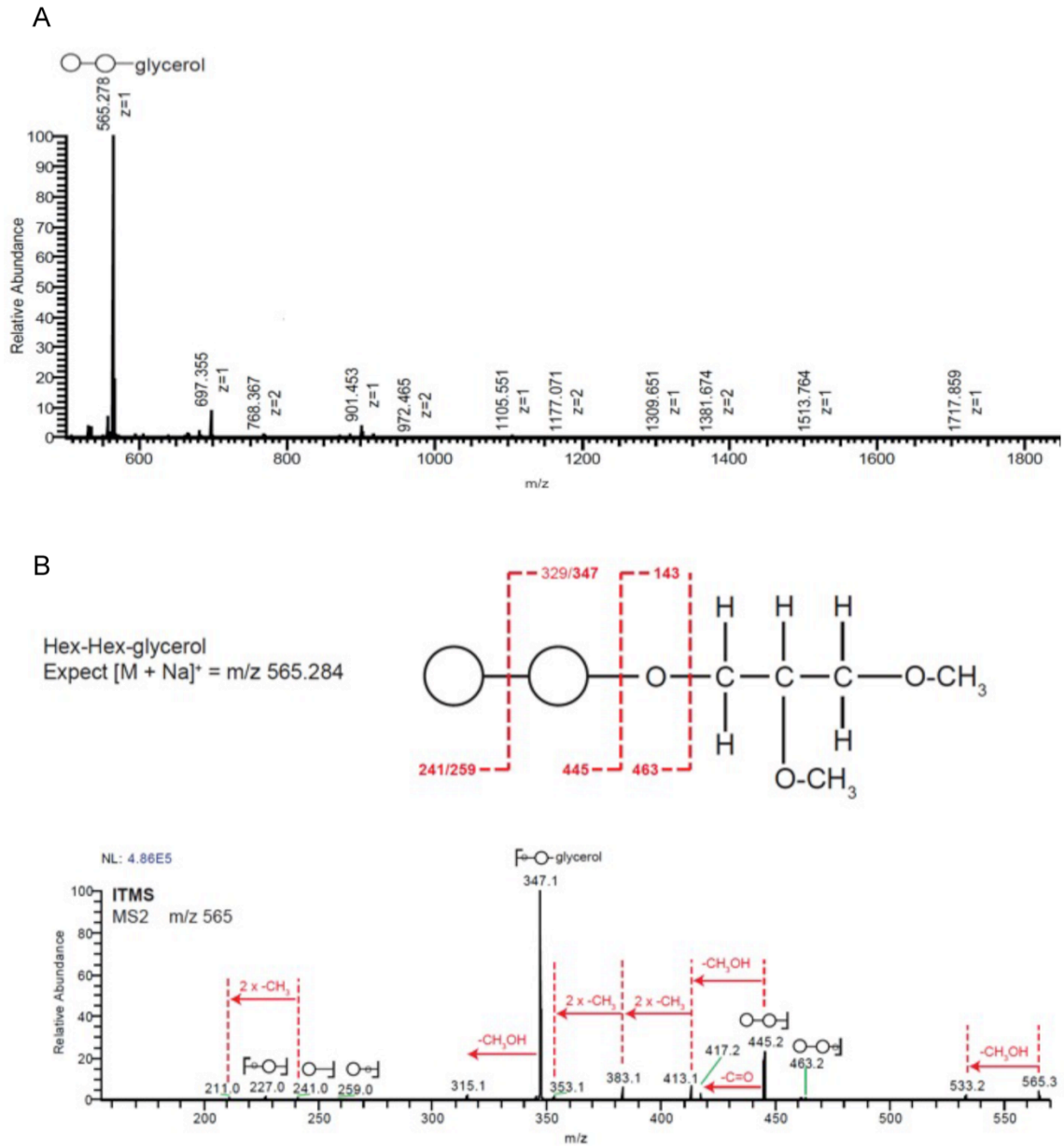


Figure 6.3

ESI-MS/MS of in-gel Beta-eliminated, permethylated PspA oligosaccharide. A) Full FTMS of PspA oligosaccharide. B) ITMS showing fragmentation of parent ion confirming oligosaccharide species.

Figure 6.4

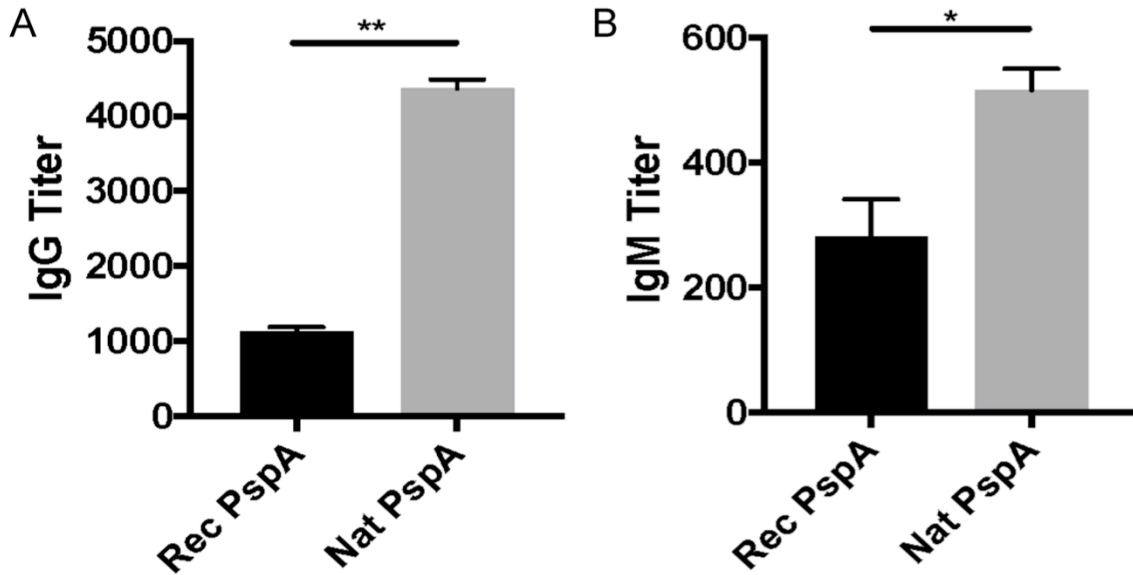


Figure 6.4

Fixed Spn cells reacted against serum from mice immunized with either native (black) or recombinant (grey) PspA in a whole cell ELISA. Antibody titers are reported as the reciprocal dilution that resulted in an A405 of 0.5.

Figure 6.5

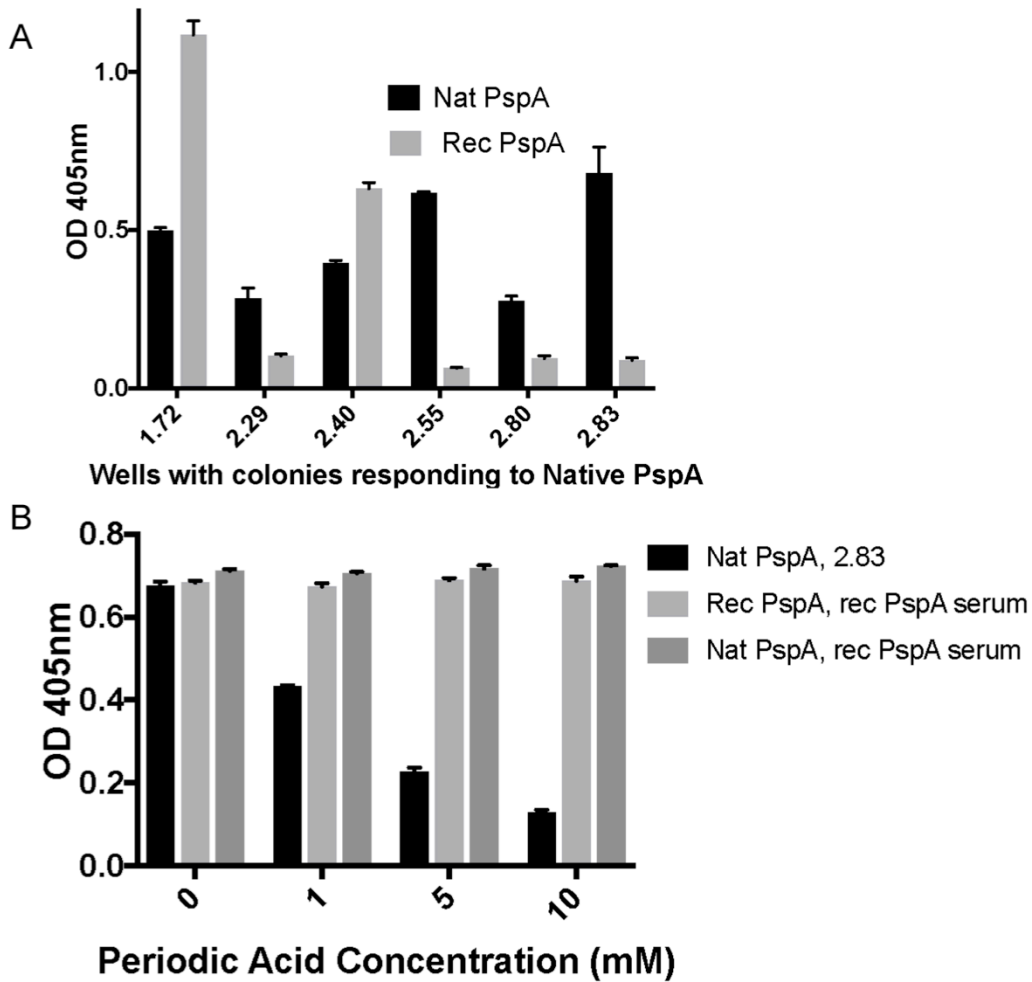


Figure 6.5

A.) B cell hybridomas generated upon immunization of Balb/c mice with native PspA were screened for differential recognition of native (glycosylated) PspA and *E. coli* recombinant PspA in an ELISA. B.) Glycan dependence of mAb 2.83 was examined by treatment of native PspA with increasing concentrations of periodate to disrupt glycan structures, while not interfering with protein specific recognition.

Figure 6.6

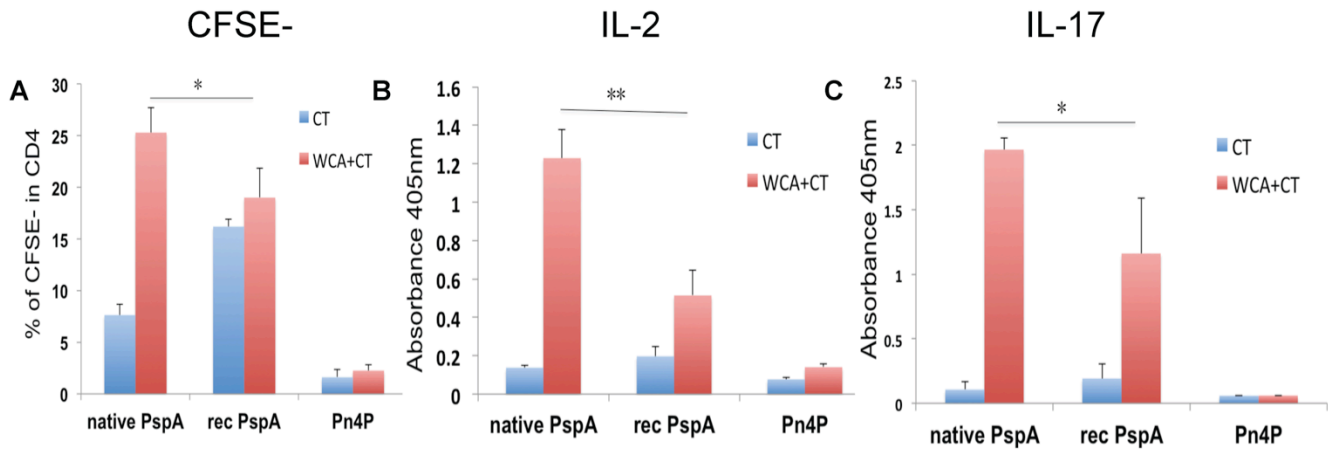


Figure 6.6

In vitro stimulation of T cells after immunization with whole cell (Spn) antigen. A.) CD4+ T cell proliferation measured by flow cytometry reduction in CFSE staining, B.) IL-2 and C.) IL-17 secretion measured by ELISA upon stimulation

CHAPTER 7

CONCLUSIONS AND FUTURE DIRECTIONS

In this dissertation, we employ glycoconjugates of type 3 *Streptococcus pneumoniae* (*Spn*) Capsular polysaccharide (CPS) to assess whether the carbohydrate-specific adaptive immune responses can be applied to type 3 *Spn* (Pn3P) conjugates. We provide evidence for the functional roles of Pn3P-specific CD4⁺ T cells utilizing mouse immunization schemes that induce Pn3P-specific immunoglobulin G (IgG) responses in a Tcarb-dependent manner. These T cell responses are consistent with our previous findings (6,7) This work contributes to the universalization of Tcarb (carbohydrate-specific T cell) mediated immune responses and generalizable vaccine development strategies against encapsulated bacterial pathogens. Future studies on cloning these T cell populations will shed light on functional properties of Tcarb populations and structural requirements for their T cell receptor engagement with carbohydrate epitopes and MHCII complexes. Further identification of Tcarb epitopes generated through processing and presentation of pneumococcal glycoconjugate vaccines by the antigen presenting cells will have direct implications in producing future knowledge-based vaccines that are target-specific, structurally designed, highly immunogenic and protective, and produced at much lower cost, thus allowing a much wider use on a global scale than current vaccines to control or eliminate invasive pneumococcal diseases (IPDs) (1).

Despite the availability of a glycoconjugate vaccine against *Spn*, it remains one of the world's most deadly pathogens. The current 13-valent vaccine induces variable immune responses to each serotype and is not as effective against serotype 3, an exceptionally virulent

serotype (2, 3). Studies have shown that multivalent glycoconjugate vaccines encompassing serotype 3 CPS have impaired booster responses, and fail to protect from otitis media infections from serotype 3 (4). In addition, individuals vaccinated with PCV13 require higher opsonophagocytosis assay serum titers for serotype 3 in comparison with other serotypes(5)

In this dissertation, we identify and evaluate the protective role of a glycoside hydrolase, Pn3Pase, targeting the CPS of serotype 3 *Spn*. IPDs caused by *Spn*, specifically serotype 3, have been a major threat to human health. Widespread use of antibiotics against IPD led to spread of drug resistance pneumococcal strains. We hypothesized that enzymatic removal of the major pneumococcal virulence factor, the CPS, would allow the host immune system to clear the infection. Through *in vitro* assays we observe that Pn3Pase treatment increases the bacterium's susceptibility to phagocytosis by macrophages and complement-mediated killing by neutrophils. We further demonstrate that *in vivo* Pn3Pase treatment reduces nasopharyngeal colonization, and protects mice from sepsis caused by type 3 *Spn*. This study offers an alternative targeted therapeutic approach to the shortcomings of the incumbent vaccine and antibiotic solutions to IPD. The results presented here indicate that enzymatic hydrolysis of the CPS may be a valid alternative or complementary therapeutic approach for diseases caused by *Spn* and other important encapsulated pathogens such as *Neisseria meningitidis* and Methicillin-Resistant *Staphylococcus aureus* (MRSA).

In addition to the high potential of Pn3Pase as a therapeutic enzyme, this glycoside hydrolase has unique properties from a structure/function point of view in that it does not fall into a currently established glycoside hydrolase Carbohydrate Active enZYme (CAZY) family (6). Further examination of structural properties of this protein may lead to the discovery of structurally similar enzymes with activities toward other unique bacterial CPSs. Future

investigations will explore the existence of enzymes for use against other prevalent pneumococcal serotypes and other encapsulated pathogenic bacteria. Based on earlier studies, the native species expressing Pn3Pase has the capacity to degrade two additional pneumococcal CPSs (7, 8). While this Pn3Pase expressing *Paenibacillus* species was isolated from the soil (8-10), it is befitting to question why this species would evolve to possess such enzymes that are capable of degrading capsules of a human pathogen. Whether these are the natural substrates for the enzymes, indicating co-evolutionary relationship, or whether other soil-dwelling microbes or plants express similar glycan residues and linkages remains to be explored.

Additional work presented here investigates the glycosylation of the pneumococcal serine-rich protein, or PsrP, a putative adhesin protein that mediates bacterial attachment to host as well as other bacterial cells(11). Previous reports implicate the pneumococcal serine rich protein in bacterial aggregation, biofilm formation, and virulence capacity of *Spn*. However, these studies have attributed their findings to the PsrP peptide backbone, specifically the N-terminal basic region of the protein(12-14). Specific roles of PsrP glycosylation, or contributions of PsrP-modifying glycosyltransferases have not been elucidated. Moreover, enzymatic properties and specificities of these glycosyltransferases have yet to be fully characterized. The majority of pneumococcal pneumonia clinical isolates contain the *psrP* locus in the genome, and the downstream glycosyltransferases are surprisingly well-conserved, suggesting their critical activities for *Spn* pathogenesis. We hypothesized that many of the glycosyltransferases that modify PsrP are critical for the adhesion properties and infectivity of *Spn*. We use single gene mutant strains for each of the putative glycosyltransferases within this locus to determine the enzymes necessary for *Spn* virulence properties *in vitro* and *in vivo*.

Based on reduction in lung epithelial cell binding by Δ GT strains, we propose the

existence of specific surface lectins on lung epithelium that recognize the mature PsrP glycoform. It has been proposed that Spn lung epithelium binding is mediated through the PsrP basic region binding to Keratin 10(14). While this may be one mechanism that contributes to binding, there is certainly a clear and demonstrable defect in binding of non-glycosylated PsrP Spn strains. Our results show that ~50% of Spn binds independent of PsrP glycosylation status. However, PsrP glycosylation remains critical for TIGR4 Spn pathogenesis in the murine pneumonia model.

There is very limited knowledge of PsrP glycosylation, biosynthetic pathways and potential role of PsrP glycans in Spn virulence and immunogenicity of PsrP (11, 12, 15, 16). Efforts to dissect the enzymatic pathway for PsrP glycosylation have begun to examine specificity and sequence of transfer to PsrP(17), but delineating the oligosaccharide structures on the natively expressed protein has remained out of reach. Furthermore, PsrP glycans may be a promising vaccine target as the immense size of the protein allows these epitopes to extend past the capsular polysaccharide shield. Therefore, in future studies we will evaluate the wild-type PsrP glycoform in vaccine constructs and assess protective capacities of these vaccines.

Finally, we uncover novel glycosylation of pneumococcal surface protein A (PspA). We demonstrate that the PspA glycan is antigenic and contributes to the immunogenicity of the protein. While these results are important and exciting to the pneumococcal field, several questions remain unanswered. Future efforts will determine the amino acid(s) of PspA that receives the glycan modification, specific enzymes that catalyze the glycosylation reactions, conservation of the modification between strains, and contribution of the glycan in pathogenicity of *Spn*.

PspA is present in essentially all clinical isolates, but has variable primary amino acid

sequence amongst strains (18, 19). Based on its sequence, PspA can be organized into three families, or 6 clades. It has been reported that up to 99% of pneumococcal isolates belong to families 1 and 2 (clades 1-5)(20, 21). Although PspA is divided into these distinct groups, it is exceptionally cross-reactive with anti-sera and monoclonal antibodies(22, 23). How the glycan structures on PspA influence or contribute to this cross-reactivity remains to be investigated. In future experiments we will utilize the glycan dependent 2.83 monoclonal antibody in passive immunization experiments to assess the protective ability of this antibody. Furthermore, we will determine if the specific mAb epitope is conserved among a variety of Spn strains and serotypes.

We previously demonstrated a novel mechanism through which uptake of a glycoconjugate vaccine by antigen presenting cells (APCs) results in the presentation of a carbohydrate epitope by the major histocompatibility class II complex (MHCII), thus stimulating carbohydrate-specific CD4⁺ T-cell clones (*i.e.*, Tcarbs) (24, 25). These findings led us to postulate that it is highly unlikely that T cells have evolved to only recognize carbohydrate epitopes derived from artificially synthesized protein-polysaccharide conjugates. Thus, we hypothesized that carbohydrate epitopes from native PspA are presented by antigen presenting cells for recognition by T cells, and that carbohydrate-induced, adaptive immune responses can contribute to the clearance of pathogen in an infection. CD4⁺ T cells play a key role in mediating antibody-independent protective immunity to pneumococcal colonization(26). Specifically, IL-17-secreting CD4⁺ T cells (TH17) are found to be critical for protection offered by ethanol killed whole cell pneumococcal antigen (27). Our results indicate that the PspA glycopeptides may be T cell epitopes, as native PspA promotes the production of both IL-2 and IL-17 significantly more than non-glycosylated recombinant PspA. Future efforts will try to identify T cell clones that recognize the PspA glycan.

In summary, we identify PspA glycosylation as a target for vaccine design to be used in future studies. Identification and immunological characterization of PspA glycosylation may lay the foundation for a new field of study within pneumococcal research, which may contribute to our understanding of *Spn* infectivity. Using glycan-based novel and conserved immunogens as new-generation pneumococcal vaccine targets may enable us to combat this major human pathogen and overcome IPDs caused by *Spn*.

Overall, the efforts and results of this dissertation increase our understanding of the interactions of pneumococcal surface glycans with the host and may lead to new treatments and vaccines against this highly virulent human pathogen to reduce the burden of invasive pneumococcal diseases.

References

1. Huang, S. S., K. M. Johnson, G. T. Ray, P. Wroe, T. A. Lieu, M. R. Moore, E. R. Zell, J. A. Linder, C. G. Grijalva, J. P. Metlay, and J. A. Finkelstein. 2011. Healthcare utilization and cost of pneumococcal disease in the United States. *Vaccine* 29: 3398-3412.
2. Dagan, R., S. Patterson, C. Juergens, D. Greenberg, N. Givon-Lavi, N. Porat, A. Gurtman, W. C. Gruber, and D. A. Scott. 2013. Comparative immunogenicity and efficacy of 13-valent and 7-valent pneumococcal conjugate vaccines in reducing nasopharyngeal colonization: a randomized double-blind trial. *Clin Infect Dis* 57: 952-962.
3. Gruber, W. C., D. A. Scott, and E. A. Emini. 2012. Development and clinical evaluation of Prevnar 13, a 13-valent pneumococcal CRM197 conjugate vaccine. *Ann N Y Acad Sci* 1263: 15-26.
4. Hausdorff, W. P., R. Dagan, F. Beckers, and L. Schuerman. 2009. Estimating the direct impact of new conjugate vaccines against invasive pneumococcal disease. *Vaccine* 27: 7257-7269.
5. Kieninger, D. M., K. Kueper, K. Steul, C. Juergens, N. Ahlers, S. Baker, K. U. Jansen, C. Devlin, W. C. Gruber, E. A. Emini, D. A. Scott, and s. group. 2010. Safety, tolerability, and immunologic noninferiority of a 13-valent pneumococcal conjugate vaccine compared to a 7-valent pneumococcal conjugate vaccine given with routine pediatric vaccinations in Germany. *Vaccine* 28: 4192-4203.

6. Henrissat, B., and A. Bairoch. 1996. Updating the sequence-based classification of glycosyl hydrolases. *Biochem J* 316 (Pt 2): 695-696.
7. Shaw, M., and G. M. Sickles. 1950. Production of specific pneumococcus carbohydrate-splitting enzymes in media to which the specific substrate was not added. *J Immunol* 64: 27-32.
8. Sickles, G. M., and M. Shaw. 1934. A Systematic Study of Microorganisms Which Decompose the Specific Carbohydrates of the Pneumococcus. *J Bacteriol* 28: 415-431.
9. Middleton, D. R., W. Lorenz, and F. Y. Avci. 2017. Complete Genome Sequence of the Bacterium *Bacillus circulans* Jordan Strain 32352. *Genome Announcements* (In press).
10. Middleton, D. R., X. Zhang, P. L. Wantuch, A. Ozdilek, X. Liu, R. LoPilato, N. Gangasani, R. Bridger, L. Wells, R. J. Linhardt, and F. Y. Avci. 2018. Identification and characterization of the *Streptococcus pneumoniae* type 3 capsule-specific glycoside hydrolase of *Paenibacillus* species 32352. *Glycobiology* 28: 90-99.
11. Sanchez, C., P. Shivshankar, K. Stol, S. Trakhtenbroit, and C. Orihuela. 2010. The Pneumococcal Serine-Rich Repeat Protein Is an IntraSpecies Bacterial Adhesin That Promotes Bacterial Aggregation In Vivo and in Biofilms. *PLOS Pathogens*.
12. Rose, L., P. Shivshankar, E. Hinojosa, A. Rodriguez, C. J. Sanchez, and C. J. Orihuela. 2008. Antibodies against PsrP, a novel *Streptococcus pneumoniae* adhesin, block adhesion and protect mice against pneumococcal challenge. *J Infect Dis* 198: 375-383.
13. Sanchez, C. J., P. Shivshankar, K. Stol, S. Trakhtenbroit, P. M. Sullam, K. Sauer, P. W. Hermans, and C. J. Orihuela. 2010. The pneumococcal serine-rich repeat protein is an intra-species bacterial adhesin that promotes bacterial aggregation in vivo and in biofilms. *PLoS Pathog* 6: e1001044.

14. Shivshankar, P., C. Sanchez, L. F. Rose, and C. J. Orihuela. 2009. The Streptococcus pneumoniae adhesin PsrP binds to Keratin 10 on lung cells. *Mol Microbiol* 73: 663-679.
15. Shi, W. W., Y. L. Jiang, F. Zhu, Y. H. Yang, Q. Y. Shao, H. B. Yang, Y. M. Ren, H. Wu, Y. Chen, and C. Z. Zhou. 2014. Structure of a novel O-linked N-acetyl-D-glucosamine (O-GlcNAc) transferase, GtfA, reveals insights into the glycosylation of pneumococcal serine-rich repeat adhesins. *J Biol Chem* 289: 20898-20907.
16. Lizcano, A., R. Akula Suresh Babu, A. T. Shenoy, A. M. Saville, N. Kumar, A. D'Mello, C. A. Hinojosa, R. P. Gilley, J. Segovia, T. J. Mitchell, H. Tettelin, and C. J. Orihuela. 2017. Transcriptional organization of pneumococcal psrP-secY2A2 and impact of GtfA and GtfB deletion on PsrP-associated virulence properties. *Microbes Infect* 19: 323-333.
17. Jiang, Y. L., H. Jin, H. B. Yang, R. L. Zhao, S. Wang, Y. Chen, and C. Z. Zhou. 2017. Defining the enzymatic pathway for polymorphic. *J Biol Chem* 292: 6213-6224.
18. Briles, D. E., R. C. Tart, E. Swiatlo, J. P. Dillard, P. Smith, K. A. Benton, B. A. Ralph, A. Brooks-Walter, M. J. Crain, S. K. Hollingshead, and L. S. McDaniel. 1998. Pneumococcal diversity: considerations for new vaccine strategies with emphasis on pneumococcal surface protein A (PspA). *Clin Microbiol Rev* 11: 645-657.
19. Khan, N., R. A. Qadri, and D. Sehgal. 2015. Correlation between in vitro complement deposition and passive mouse protection of anti-pneumococcal surface protein A monoclonal antibodies. *Clin Vaccine Immunol* 22: 99-107.
20. Hotomi, M., A. Togawa, M. Kono, Y. Ikeda, S. Takei, S. K. Hollingshead, D. E. Briles, K. Suzuki, and N. Yamanaka. 2013. PspA family distribution, antimicrobial resistance and serotype of Streptococcus pneumoniae isolated from upper respiratory tract infections in Japan. *PLoS One* 8: e58124.

21. Hollingshead, S. K., L. Baril, S. Ferro, J. King, P. Coan, D. E. Briles, and P. P. E. S. Group. 2006. Pneumococcal surface protein A (PspA) family distribution among clinical isolates from adults over 50 years of age collected in seven countries. *J Med Microbiol* 55: 215-221.
22. Crain, M. J., W. D. Waltman, J. S. Turner, J. Yother, D. F. Talkington, L. S. McDaniel, B. M. Gray, and D. E. Briles. 1990. Pneumococcal surface protein A (PspA) is serologically highly variable and is expressed by all clinically important capsular serotypes of *Streptococcus pneumoniae*. *Infect Immun* 58: 3293-3299.
23. McDaniel, L. S., J. S. Sheffield, P. Delucchi, and D. E. Briles. 1991. PspA, a surface protein of *Streptococcus pneumoniae*, is capable of eliciting protection against pneumococci of more than one capsular type. *Infect Immun* 59: 222-228.
24. Avci, F., X. Li, M. Tsuji, and D. Kasper. 2011. A mechanism for glycoconjugate vaccine activation of the adaptive immune system and its implications for vaccine design. *Nat Med* 17: 1602-U1115.
25. Avci, F., X. Li, M. Tsuji, and D. Kasper. 2012. Isolation of carbohydrate-specific CD4(+) T cell clones from mice after stimulation by two model glycoconjugate vaccines. *Nat Protoc* 7: 2180-2192.
26. Malley, R., K. Trzcinski, A. Srivastava, C. M. Thompson, P. W. Anderson, and M. Lipsitch. 2005. CD4+ T cells mediate antibody-independent acquired immunity to pneumococcal colonization. *Proceedings of the National Academy of Sciences of the United States of America* 102: 4848-4853.

27. Moffitt, K. L., P. Yadav, D. M. Weinberger, P. W. Anderson, and R. Malley. 2012. Broad antibody and T cell reactivity induced by a pneumococcal whole-cell vaccine. *Vaccine* 30: 4316-4322.

APPENDIX A
COMPLETE GENOME SEQUENCE OF THE BACTERIUM *BACILLUS CIRCULANS*
JORDAN STRAIN 32352

Dustin R. Middleton, Walter Lorenz, and Fikri Y. Avcı

Accepted by *Genome Announcements*. Reprinted here with permission of publisher.

Abstract

Here, we report the complete genome sequence for the *Bacillus circulans* Jordan strain 32352. This species is a soil dwelling bacterium that expresses glycoside hydrolase enzymes degrading pneumococcal capsular polysaccharides.

Introduction

The soil microbiome is a tremendously diverse microbial community of bacteria and fungi that produce a variety of enzymes and small molecules relevant to human biology(1, 2). In 1930, Avery and Dubos described a soil-dwelling *Bacillus* produced an enzyme capable of degrading the type III capsular polysaccharide (Pn3P) of *Streptococcus pneumoniae*(3). A few years later, Sickles and Shaw were able to isolate a similar enzyme producing, *Bacillus palustris* (renamed later *Bacillus circulans*) strain from decaying organic matter in soil. They described this bacterium as a sporulating, gram-negative, aerobic bacillus with peritrichous flagella(4). In several studies since, researchers have utilized culture filtrate preparations of this Pn3P degrading enzyme (Pn3Pd) while investigating Pn3P biosynthesis and its antigenic and immunological properties(5-7). We set out to sequence this bacterium in order to identify the enzyme responsible for Pn3P depolymerization and other potential carbohydrate active enzymes produced in this strain.

Bacillus circulans Jordan strain 32352 was acquired from American Type Culture Collection (ATCC[®]14175). Genomic DNA was isolated using DNeasy Blood & Tissue Kit (Qiagen, USA). Genomic DNA was submitted to the Georgia Genomics Facility (University of Georgia) for DNA library synthesis using a KAPA Hyper Kit (Kapa Biosystems, Ina

Wilmington, MA) and TrueSeq LT adapters. Paired-end (PE) 150-base reads were sequenced on an Illumina (Illumina Inc. San Diego, CA) NextSeq 500 system run with NextSeq v2 reagents.

Genome assembly and analysis was performed by the Quantitative Biology Consulting Group (University of Georgia). Raw and trimmed reads were assessed using FastQC (8) and quality trimming was done using Trimmomatic (9) with the following settings (ILLUMINACLIP:TruSeq3-PE-2.fa:2:30:10 LEADING:20 TRAILING:15 SLIDINGWINDOW:4:25 MINLEN:50). Genome assembly was performed using SPAdes (ver.3.9) software (10) with both paired and unpaired reads as input. Assembly metrics were determined using QUAST (11) and genome annotation was performed on the RAST server (12). Identification of putative prophage elements was done with PHAST (13).

Trimmed reads (ca. 2.4 million paired and 1.54 million unpaired) representing 150 X base coverage were assembled. The genome assembly of *Bacillus circulans* Jordan strain 32352 contained 494 contigs of which 40 were ≥ 500 bp. The largest scaffold was 1.36 Mb in length and total assembly length was 7.92 Mb with an N50 = 433 kb and an L50 = 6. GC content was 49.3%. RAST annotation predicted 7,269 coding sequences and PHAST analysis detected two regions containing questionable and incomplete prophage elements, respectively.

Accession number. The whole-genome shotgun project has been deposited at DDBJ/ENA/GenBank under the accession number MZNT00000000. The version described in this paper is the first version, MZNT01000000.

Funding Information

This work was supported by the grant from the National Institute of Health: R01AI123383

References

1. Traxler, M. F., and R. Kolter. 2015. Natural products in soil microbe interactions and evolution. *Nat Prod Rep* 32: 956-970.
2. Mendes, L. W., S. M. Tsai, A. A. Navarrete, M. de Hollander, J. A. van Veen, and E. E. Kuramae. 2015. Soil-borne microbiome: linking diversity to function. *Microb Ecol* 70: 255-265.
3. Avery, O. T., and R. Dubos. 1930. The specific action of a bacterial enzyme on pneumococci of type III. *Science* 72: 151-152.
4. Sickles, G. M., and M. Shaw. 1934. A Systematic Study of Microorganisms Which Decompose the Specific Carbohydrates of the Pneumococcus. *J Bacteriol* 28: 415-431.
5. Shaw, M., and G. M. Sickles. 1950. Production of specific pneumococcus carbohydrate-splitting enzymes in media to which the specific substrate was not added. *J Immunol* 64: 27-32.
6. Torriani, A., and A. M. Pappenheimer. 1962. Inducible polysaccharide depolymerases of *Bacillus palustris*. *J Biol Chem* 237: 3-13.
7. Cartee, R. T., W. T. Forsee, J. S. Schutzbach, and J. Yother. 2000. Mechanism of type 3 capsular polysaccharide synthesis in *Streptococcus pneumoniae*. *J Biol Chem* 275: 3907-3914.
8. FastQC. Babraham Bioinformatics.
9. Bolger, A. M., M. Lohse, and B. Usadel. 2014. Trimmomatic: A flexible trimmer for Illumina Sequence Data. *Bioinformatics*.

10. Bankevich, A., S. Nurk, D. Antipov, A. A. Gurevich, M. Dvorkin, A. S. Kulikov, V. M. Lesin, S. I. Nikolenko, S. Pham, A. D. Prjibelski, A. V. Pyshkin, A. V. Sirotkin, N. Vyahhi, G. Tesler, M. A. Alekseyev, and P. A. Pevzner. 2012. SPAdes: a new genome assembly algorithm and its applications to single-cell sequencing. *Journal of computational biology : a journal of computational molecular cell biology* 19: 455-477.
11. Gurevich, A., V. Saveliev, N. Vyahhi, and G. Tesler. 2013. QUAST: quality assessment tool for genome assemblies. *Bioinformatics* 29: 1072-1075.
12. Aziz, R. K., D. Bartels, A. A. Best, M. DeJongh, T. Disz, R. A. Edwards, K. Formsma, S. Gerdes, E. M. Glass, M. Kubal, F. Meyer, G. J. Olsen, R. Olson, A. L. Osterman, R. A. Overbeek, L. K. McNeil, D. Paarmann, T. Paczian, B. Parrello, G. D. Pusch, C. Reich, R. Stevens, O. Vassieva, V. Vonstein, A. Wilke, and O. Zagnitko. 2008. The RAST Server: Rapid Annotations using Subsystems Technology. *BMC Genomics* 9: 75-75.
13. Zhou, Y., Y. Liang, K. H. Lynch, J. J. Dennis, and D. S. Wishart. 2011. PHAST: A Fast Phage Search Tool. *Nucleic Acids Research*.